Nickel-Catalyzed Reductive Couplings of Aldehydes and Alkynes: Controlling Stereochemistry and Regioselectivity using N-Heterocyclic Carbene Ligands

by

Grant Jari Sormunen

A dissertation submitted in partial fulfillment
of the requirements for the degree of
Doctor of Philosophy
(Chemistry)
in the University of Michigan
2011

Doctoral Committee:

Professor John Montgomery, Chair
Professor Melanie S. Sanford
Associate Professor John P. Wolfe
Assistant Professor Garry Dean Dotson

I dedicate this work to Aileen, Seppo and Anita Sormunen.

Acknowledgements

I'd like to thank my advisor John Montgomery for his guidance and support during my time at the University of Michigan. Through you I have learned how to be both an independent and a diligent scientist.

Thank you to my colleagues in the Montgomery lab. Those of the past have taught me a great deal, while those present still have provided support, interesting insights and the opportunity to act as a mentor. I'd like to specifically thank both Mani and Hasnain for the collaborations we have had. Thank you Ben, for feedback regarding this thesis as well the countless other documents over the last four years.

Thank you to all the friends I've had during graduate school for their support, both within the department and outside the department. A special thanks to Beverly, for being such a great friend and roommate.

Finally, I'd like thank my family for their continuous love and support.

Table of Contents

List of Schemes

List of Tables

List of Figures

Abbreviations

n-Bu	butyl
t-Bu	*tert*-butyl
COD	1, 5-cyclooctadiene
^{o}C	temperature in degrees centigrade
Cy	cyclohexyl
d	day(s)
dr	diastereomeric ratio
DEMS	diethoxymethylsilane
Et	ethyl
equiv	equivalent
ee	enantiomeric excess
er	enantiomeric ratio
GCMS	gas chromatography mass spectrometry
h	hour(s)
n-Hept	heptyl
n-Hex	hexyl
Hex	hexanes/hexyl
IMes	1, 3-bis-(1, 3, 5-trimethylphenyl)imidazol-2-ylidene
IPr	1, 3-bis-(2, 6-diisopropylphenyl)imidazol-2-ylidene
Me	methyl
min	minute(s)
NHC	*N*-heterocyclic carbene
Nu	Nucleophile
PCC	pyridinium chlorochromate
Pent	pentyl
Ph	phenyl

i-Pr	isopropyl
n-Pr	propyl
rt	room temperature
TBAF	tetrabutylammonium fluoride
TBS	*tert*-butyldimethylsilyl
THF	tetrahydrofuran
TLC	thin layer chromatography
Tol	toluene

ABSTRACT

Nickel-Catalyzed Reductive Couplings of Aldehydes and Alkynes: Controlling Stereochemistry and Regioselectivity using N-Heterocyclic Carbene Ligands

by

Grant Jari Sormunen

Chair: John Montgomery

Allylic alcohols are a common substructure in natural products and useful intermediates for a variety of organic transformations. One of the most direct synthetic approaches for the synthesis of allylic alcohols is the reductive coupling of an aldehyde and an alkyne. While many different methods have been developed, the use of N-heterocyclic carbenes as ligands in nickel-catalyzed aldehyde-alkyne reductive couplings has allowed the reaction to be synthetically useful for a broad range of substrates. In this body of work, strategies for both enantioselectivity and regioselectivity using N-heterocyclic carbenes as ligands will be discussed.

A new N-heterocyclic carbene ligand, analogous to ligands used in asymmetric ring-closing metathesis, was developed that exhibited high enantioselectivities in the asymmetric reductive coupling of aldehydes and alkynes. Its scope was examined for a wide variety of intermolecular couplings as well as a macrocyclization.

Advances in the control of alkyne regioselectivity have been made, with the ability to produce either regioisomer, with the complementary use of small cyclopropenylidene carbene ligands or highly hindered *N*-heterocyclic carbene ligands. Regioselectivities were typically quite high in cases where the standard conditions were unselective. In some cases with strong substrate biases for a single regioisomer, the opposite regioisomer was achievable using our highly hindered *N*-heterocyclic carbene ligands.

Finally, studies to combine these two concepts, regiocontrol and enantiocontrol, were executed, exploring *N*-heterocyclic carbene ligands which allowed for the both high regiocontrol and enantiocontrol within aldehyde-alkyne reductive coupling. Advances were made in the understanding of the impacts of different *N*-aryl substitutions and backbone structures on both regiocontrol and enantiocontrol.

Chapter 1

Introduction to the Nickel-Catalyzed Aldehyde-Alkyne Coupling Reaction

1.1 Allylic Alcohols

1.1.1 Importance of Allylic Alcohols in Organic Synthesis

Allylic alcohols are a common substructure in a variety of natural products (Figure 1.1)[1,2] and a useful functional group for a variety of organic transformations. The range of applications for allylic alcohols in organic transformations includes metal π-allyl chemistry[3], directed epoxidations[4], directed cyclopropanations[5,6], cationic cyclization processes[7], S_N2' allylic displacement processes[8], and sigmatropic rearrangements, most notably Claisen rearrangements (Scheme 1.1). [9]

Figure 1.1. Selected Natural Products Containing Allylic Alcohols

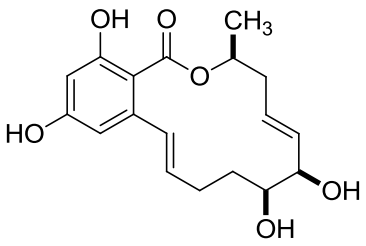

aigialomycin D

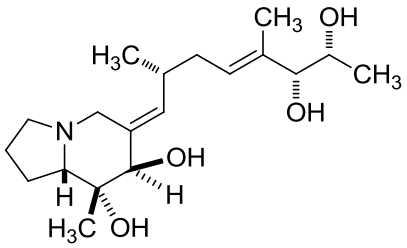

(+)-allopumiliotoxin-339A

Scheme 1.1. Applications of Allylic Alcohols in Organic Synthesis

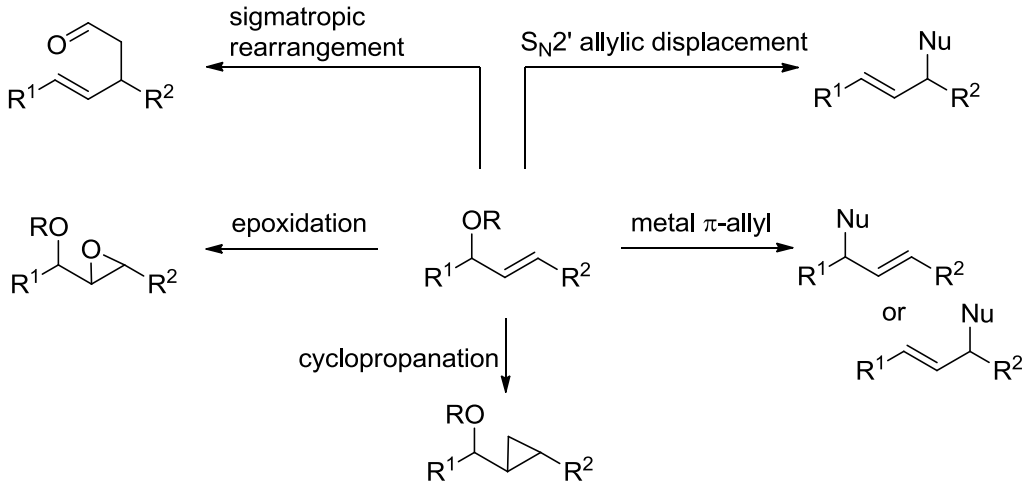

1.1.2 Methods of Forming Allylic Alcohols

Two classical methods of formation of allylic alcohols are the 1,2-reduction of enones and the addition of vinyl organometallics to aldehydes and ketones (Scheme 1.2). A more recent development is the Nozaki-Hiyama- Kishi (NHK) coupling, which utilizes nickel as a catalyst and chromium as a reductant to add a vinyl halide to an aldehyde (Scheme 1.3).[10,11] The NHK reaction is considered to be the benchmark for allylic alcohol synthesis, and has been expanded in utility to include enantioselective processes.[12] While initially the methodology required stoichiometric chromium, the Fürstner modification[13] has allowed from the use of catalytic quantities of chromium.

Scheme 1.2. Classical Allylic Alcohol Synthesis

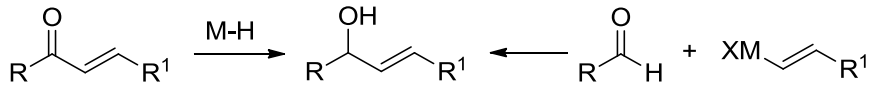

Scheme 1.3. Nozaki-Hiyama-Kishi Coupling

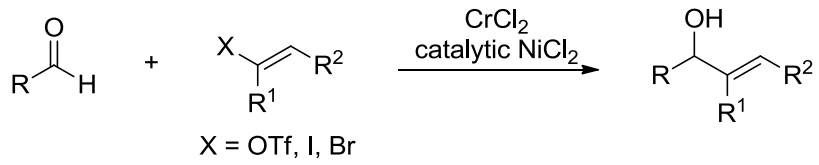

1.2 Reductive Couplings

1.2.1 Aldehyde-Alkyne Reductive Couplings

A variety of different methods have been developed for the reductive couplings of aldehydes and alkynes to produce allylic alcohols.[14] Two related processes were developed by Oppolzer[15,16] and Wipf,[17,18] where the reductive coupling begins with either hydroboration or hydrozirconation of the alkyne followed by transmetallation to an organozinc species. This alkenyl-zinc species can then undergo addition to an aldehyde to produce the reductive coupling product. The enantioselectivities for these reactions can be impressively high (up to 98% intermolecular, 92% macrocyclizations). The only product is the trans alkene, as the methodology is limited to couplings of terminal alkynes (Scheme 1.4).

Scheme 1.4. Hydrometallation-Transmetalation Pathways for Reductive Couplings of Aldehydes and Alkynes

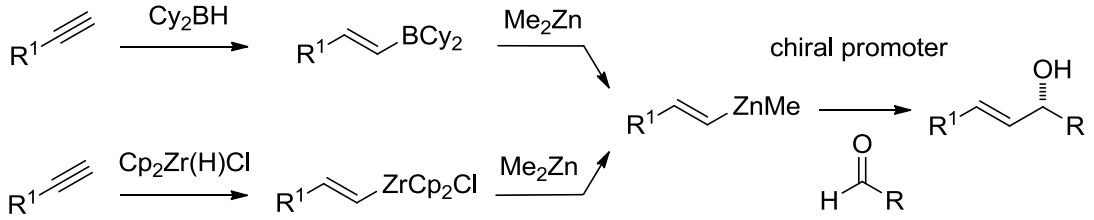

Alkylative couplings by Negishi utilized catalytic zirconium to facilitate the addition of trialkyl aluminum reagents to terminal alkynes.[19] These alkenyl-aluminum species could then undergo in-situ additions to aldehydes, though the scope is limited (Scheme 1.5). The use of such a strong Lewis acid limits the functionality tolerated in this methodology.

Scheme 1.5. Carboalumination Pathway for Alkylative Couplings of Aldehydes and Alkynes

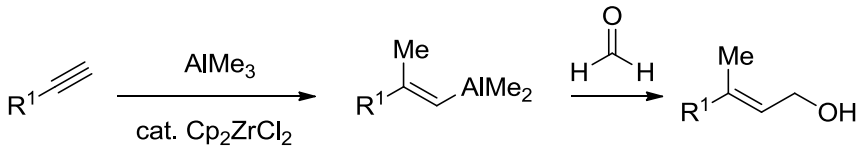

While these methods do accomplish the reductive/alkylative couplings of aldehydes and alkynes, all are limited to terminal alkynes and go through a very different mechanistic pathway than the mechanism for the nickel-catalyzed couplings, where the carbon-carbon bond-forming step is metallacycle formation. Metallacycle formation for the reductive couplings of aldehydes and alkynes was observed using stoichiometric amounts of titanium alkoxides (Scheme 1.6) as well as zirconium.[20-22] Because titanium alkoxides are generally low cost, the use of stoichiometric amounts does not prevent this from being an economically viable methodology.

Scheme 1.6. Stoichiometric Titanium Pathway for Reductive Couplings of Aldehydes and Alkynes

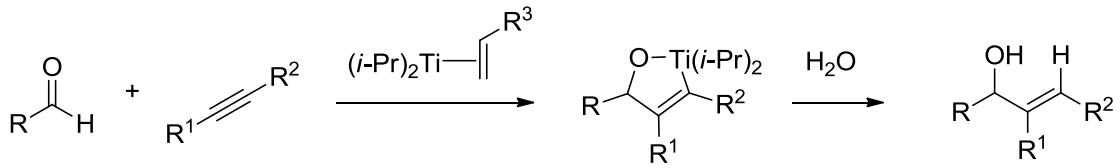

Titanium-mediated reductive couplings of ynals were made catalytic with the use of trialkoxysilanes and titanocene catalysts. This report represented the first use of silane reducing agents in aldehyde-alkyne reductive couplings (Scheme 1.7).[23,24] In this case, the metallacycle is formed catalytically, followed by the reaction with the trialkoxysilane to reform the active catalyst.

Scheme 1.7. Catalytic Titanium Pathway for Reductive Couplings of Aldehydes and Alkynes

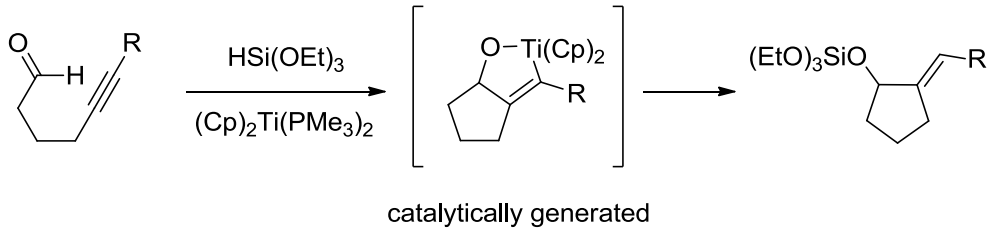

Rhodium catalysts have been shown to be very powerful in the coupling of aldehydes and alkynes under hydrogenation conditions (Scheme 1.8).[25,26] Rhodium catalysts are also thought to proceed through a metallacycle intermediate. This methodology proceeds exceptionally well when conjugated alkynes are coupled to α-ketoaldehydes, α-ketoesters or heterocyclic aromatic aldehydes. This reaction is also

capable of producing very high levels of enantioselectivity. However, the scope is currently limited to these classes of aldehydes and alkynes.

Scheme 1.8. Rhodium-Catalyzed Hydrogenative Coupling of Aldehydes and Alkynes

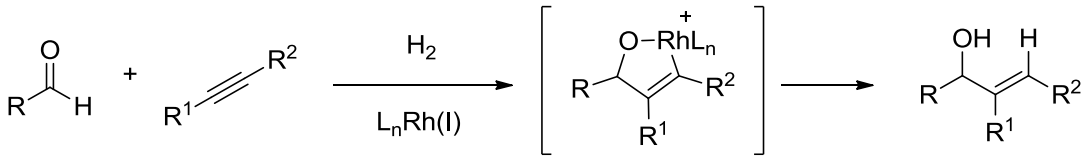

1.2.2 Nickel-Catalyzed Reductive Couplings

Our group first reported the direct reductive coupling of aldehydes and alkynes using a nickel catalyst.[27] Utilizing different organozinc reagents, either alkylative or reductive coupling may be observed in cyclization reactions, based on whether the alkyl group undergoing transmetallation from the zinc to the nickel contains a β-hydrogen (Scheme 1.9). Because these products result from an oxidative cyclization, the alkene stereochemistry is a single stereoisomer. Within this original report, the intermolecular alkylative coupling was also initially developed, though the scope of the reaction was limited, as aldehydes with epimerizable centers gave considerably lower yields (Scheme 1.10).

Scheme 1.9. Nickel-Catalyzed Reductive and Alkylative Cyclizations using Organozincs

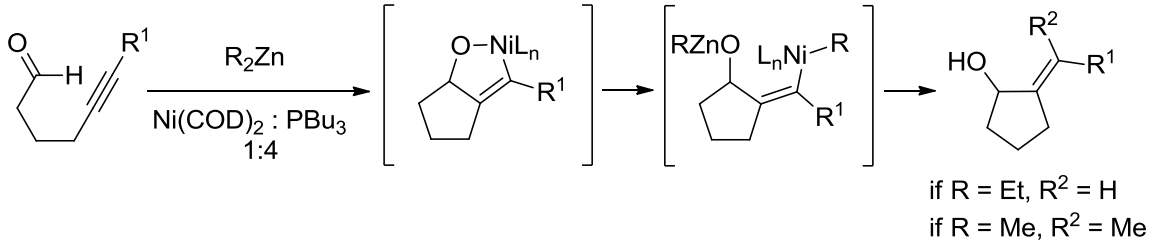

Scheme 1.10. Intermolecular Nickel-Catalyzed Alkylative Coupling using Organozincs

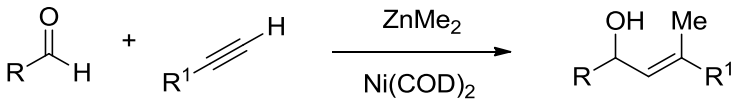

The nickel-catalyzed aldehyde-alkyne coupling was then advanced by Jamison and coworkers, through a change in reducing agents to trialkylboranes (Scheme 1.11).[28]

When trialkylboranes are used as the reducing agent, the reductive coupling product forms exclusively over alkylative coupling. Typically, yields in this reaction are best using internal aromatic alkynes, though there are some examples of good yields for both aliphatic internal and terminal alkynes. This methodology was utilized in the synthesis of (-)-terpestacin, where the key reductive coupling step proceeded with 2.6:1 regioselectivity and 2:1 diastereoselectivity.[29,30]

Scheme 1.11. Nickel-Catalyzed Alkylative Coupling using Trialkylborane Reducing Agents

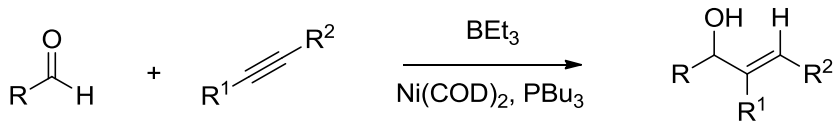

In cyclization reactions, it was found that silane reducing agents could be used to produce silyl ethers using a nickel catalyst.[31] The silane reducing agents afford high yielding couplings using a nickel-phosphine complex in intermolecular cases, which then allowed for the efficient synthesis of (+)-allopumiliotoxin 339A (Scheme 1).[2]

By using chromium(II) as a reducing agent, very different nickel reactivity was observed relative to these metallacycle mechanisms for the coupling of terminal alkynes to aldehydes. Takai and coworkers observed that in the presence of water and chromium(II), nickel-phosphine complexes could undergo some form of a hydronickelation process, followed by transmetallation to chromium.[32,33] The alkenyl-chromium species is then sufficiently nucleophilic to undergo addition into aldehydes (Scheme 1.12). Interestingly, the hydronickelation step of terminal alkynes provides the opposite stereochemistry of that observed when the aldehyde-alkyne union occurs via a metallacycle. Unfortunately, this procedure requires the use of at least two equivalents of chromium(II) chloride, greatly reducing its potential for larger scale use, though it is possible that the Fürstner modification[13] or a similar process may be developed for this reductive coupling.

Scheme 1.12. Nickel-Catalyzed Reductive Couplings using Chromium Reducing Agents

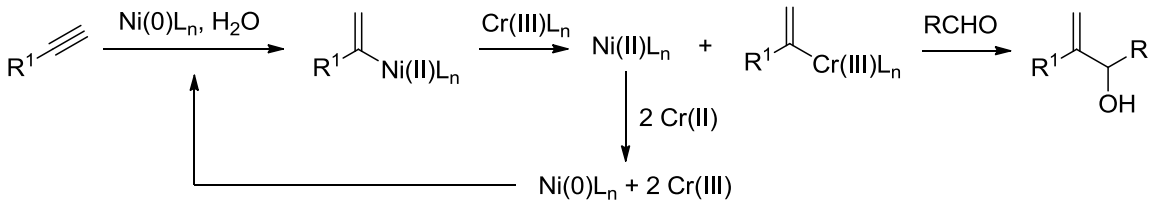

In 2004, our lab reported the NHC variant of the nickel-catalyzed aldehyde-alkyne coupling reaction (Scheme 1.13).[34] Due to the differences in NHC reactivity, which will be discussed in the next section, the successful intermolecular coupling of aldehydes and alkynes was accomplished using simple, mild silane reducing agents. The scope of this reaction using IMes as a ligand was broader than previously reported procedures, allowing for the efficient coupling of a variety of aldehydes (aliphatic, aromatic) and alkynes (aliphatic, aromatic, internal, terminal, alkynyl silane).

Scheme 1.13. NHC Nickel-Catalyzed Aldehyde-Alkyne Coupling Reaction

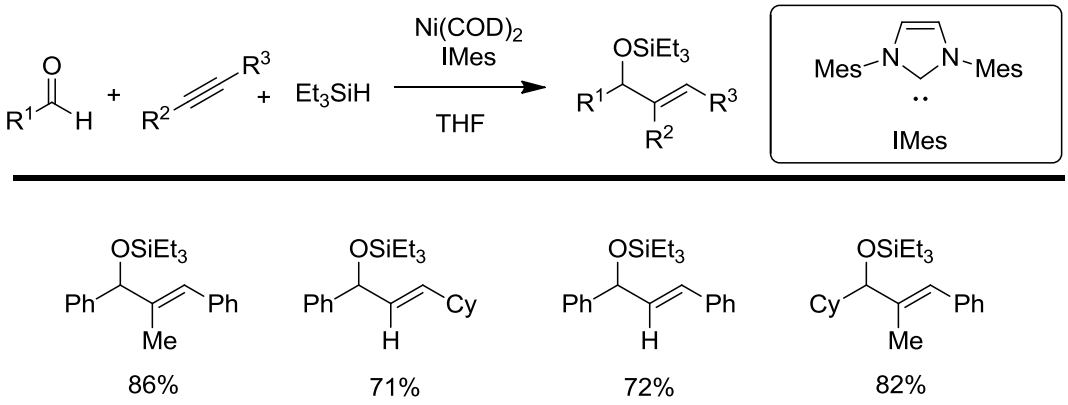

1.3 *N*-Heterocyclic Carbenes

1.3.1 Stability and Reactivity

There are two primary classes of carbenes, which are neutral compounds containing six electrons with a divalent carbon atom.[38] These are differentiated by their ground state spin multiplicity: singlet or triplet (Scheme 1.14). A triplet carbene contains one electron in each of its two non-bonding degenerate orbitals, creating an sp-hybridization, which prefers a linear geometry. A triplet carbene can also refer to a bent geometry where one electron is located in each non-bonding orbital. A singlet carbene

prefers an sp^2-type hybridization where both electrons reside in the in-plane sp^2 orbital, while the p orbital is vacant.

Scheme 1.14. Singlet and Triplet Carbenes

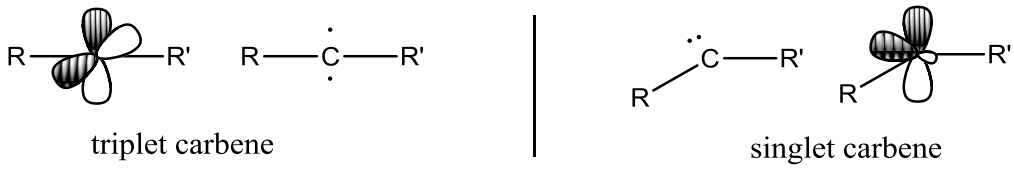

The geometry and electronic nature of the carbene is based on the groups surrounding it. In general, groups that are able to donate heavily into a carbocation are also able to donate into a carbene. In order for this donation to occur, the carbene must adopt the singlet state so there is an available orbital for this interaction. Because triplet carbenes have little electronic stabilization they are typically highly reactive; the few triplet carbenes that have been stable enough to characterize have used bulky aromatic substituents to abate reactivity.[39] The imidazol-2-ylidene ligands we have utilized in nickel-catalyzed reductive couplings have been characterized as singlet carbenes (Scheme 1.15).[38] With both nitrogens able to donate into the carbene, the most accurate form of this class of ligands is one where there is a delocalized positive charge within the ring, with a strong negative charge of the carbene lone pair. When you add in the physical constraints of carbenes in a ring structure, forcing a bent configuration over a linear configuration, the relative stability of the singlet over the triplet becomes amplified.[40,41]

Scheme 1.15. Stable Carbenes: Imidazol-2-ylidenes

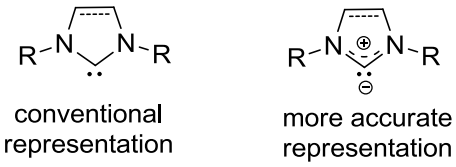

1.3.2 *N*-Heterocyclic Carbenes as Ligands in Catalysis

When a carbene is bound to a metal, different terminology is typically used.[42] Fischer carbenes refer to carbenes that contain an electron-withdrawing group, causing them to be electrophilic. Schrock carbenes are carbenes that contain an electron-donating

group, causing them to be nucleophilic. The third class is persistent carbenes; these carbenes act as ligands instead of having direct reactivity at the carbene site. The trademark carbenes of this class are the NHCs, originally discovered by Wanzlick,[43] but not make widely available until Arduengo isolated an NHC as the free carbene nearly 20 years later.[44]

Phosphines and NHC's vary greatly in reactivity as ligands for nickel. Nolan and Hoff conducted a physical and computational study of the properties of nickel-NHC complexes with CO, in order to examine the differences between NHC's and phosphines as ligands for nickel.[45] Based on DFT studies, the BDE of typical NHC-nickel bonds in $Ni(CO)_3(L)$ was 10-13 kcal/mol higher than that of phosphine ligands (Table 1.1). Not only does the bond strength vary, but the electron donation of the ligands does as well. Measured IR values of the stretching frequency of CO in $Ni(CO)_3(L)$ indicate that NHCs also have a greater donation than phosphines. Because of the higher electron donation of the NHC ligands, this allows for great stabilizing of cationic complexes, which should also enhance the rates of metal oxidation in steps such as oxidative addition and oxidative cyclization. To quantify differences in sterics, % V_{bur} has been developed as a measurement of how much of a sphere centered at the metal center would overlap with a ligand. Though this calculated value has some validity, it is a simple approximation that does not take into account the location of the ligand sterics with respect to the binding of the substrates in reaction transition states.

Table 1.1. BDE Energies, CO Stretching Frequencies and % V_{bur} for NHCs and Phosphines

complex	ligand-nickel BDE (kcal/mol)	υ_{CO}	% V_{bur}
$Ni(CO)_3(IMes)$	41.1	2050.7	26
$Ni(CO)_3(SIMes)$	40.2	2051.5	27
$Ni(CO)_3(IPr)$	38.5	2051.5	29
$Ni(CO)_3(SIPr)$	38.0	2052.2	30
$Ni(CO)_3(P^tBu_3)$	28.0	2056.1	30
$Ni(CO)_3(PCy_3)$	-	2056.4	26
$Ni(CO)_3(PPh_3)$	26.7	2068.0	22

Between different NHCs, there are fundamental reactivity differences as well. Some NHCs tend to homodimerize, which, depending on the NHC, may or may not be reversible (Scheme 26).[46] In general, the unsaturation of the backbone of imidazolylidenes favors monomer over dimer, while saturation of the backbone of imidazolinylidenes tends to favor dimer formation. As the *N*-substituents become larger, dimer formation becomes less favorable. Dimerization arises as an issue when the formation of the ligand-metal complex involves formation of the free carbene, followed by complexation. The most common method to circumvent dimerization pathways is the use of silver as a metal transfer agent. While silver methods have been shown to work widely on cationic metal systems such as Au(I), Cu(I), Cu(II), Ni(II), Pd(II), Pt(II), Rh(I), Rh(III), Ir(I), Ir(III), Ru(II), Ru(III) and Ru(IV),[47] their use on neutral metals has not yet been demonstrated, likely due to being energetically disfavorable. A second issue is the ability for two NHCs to bind the same metal center,[48] producing either an inactive complex or a complex capable of producing side reactions. The core factor in ligand propensity to form a 2:1 NHC:metal adduct over a 1:1 NHC:metal adduct is ligand sterics, where ligands with large amounts of sterics prevent the binding of a second ligand.

Scheme 1.16. Dimerization of NHCs and NHC-Metal Stoichiometry

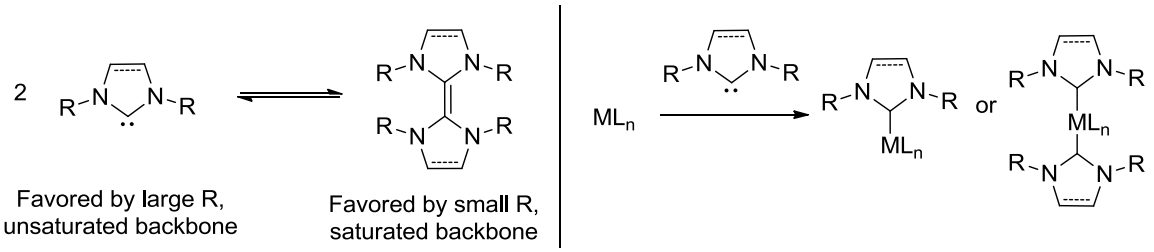

1.4 Advancement of Nickel Catalyzed Aldehyde-Alkyne Reductive Couplings using *N*-Heterocyclic Carbene Ligands

1.4.1 Mechanism

As stated previously in this chapter, the use of NHCs in the nickel-catalyzed aldehyde-alkyne reductive couplings allowed for intramolecular coupling of aldehydes and alkynes using very mild silane reducing agents. A crossover experiment from the initial communication indicated that it is likely that NHC ligands are undergoing a different mechanism than their phosphine counterparts. Cyclizing an enal, with either IMes or Bu_3P as the ligand and using a mixture of Et_3SiD and Pr_3SiH gave minimal crossover for IMes, while giving complete crossover for Bu_3P (Table 1.17). This experiment clearly demonstrates that there is a difference in mechanisms between these systems.

Table 1.2. Crossover Study Contrasting NHCs and Phosphines

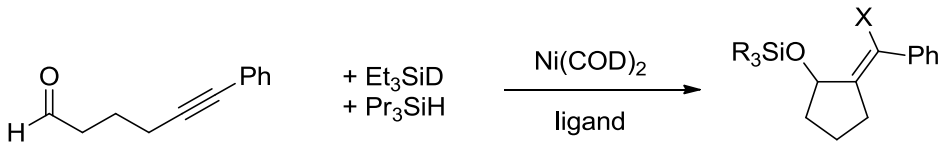

R	X	relative %	
		from IMes	from PBu_3
Et	H	<2	25
Et	D	55	34
Pr	H	41	23
Pr	D	<2	18

The proposed mechanism for the nickel-catalyzed aldehyde-alkyne coupling[34] begins with the *in situ* deprotonation of the NHC-HX salt followed by complexation to nickel to form the catalytically active NHC-nickel(0) complex (Scheme 1.17). This catalyst then reversibly coordinates both an aldehyde and an alkyne. The complex then undergoes oxidative cyclization, to produce the metallacycle. In our studies, this is the most important step since it is considered to be irreversible, and it dictates both the stereochemistry and regiochemistry for the reaction. The nickel-oxygen bond then undergoes σ-bond metathesis with the silane-hydride bond, to produce a silyl ether and a nickel-hydride species. The nickel-hydride then reductively eliminates to produce the allylic silyl ether and reform the NHC-nickel(0) complex.

Scheme 1.17. Mechanism of NHC-mediated Nickel-Catalyzed Aldehyde Alkyne Couplings

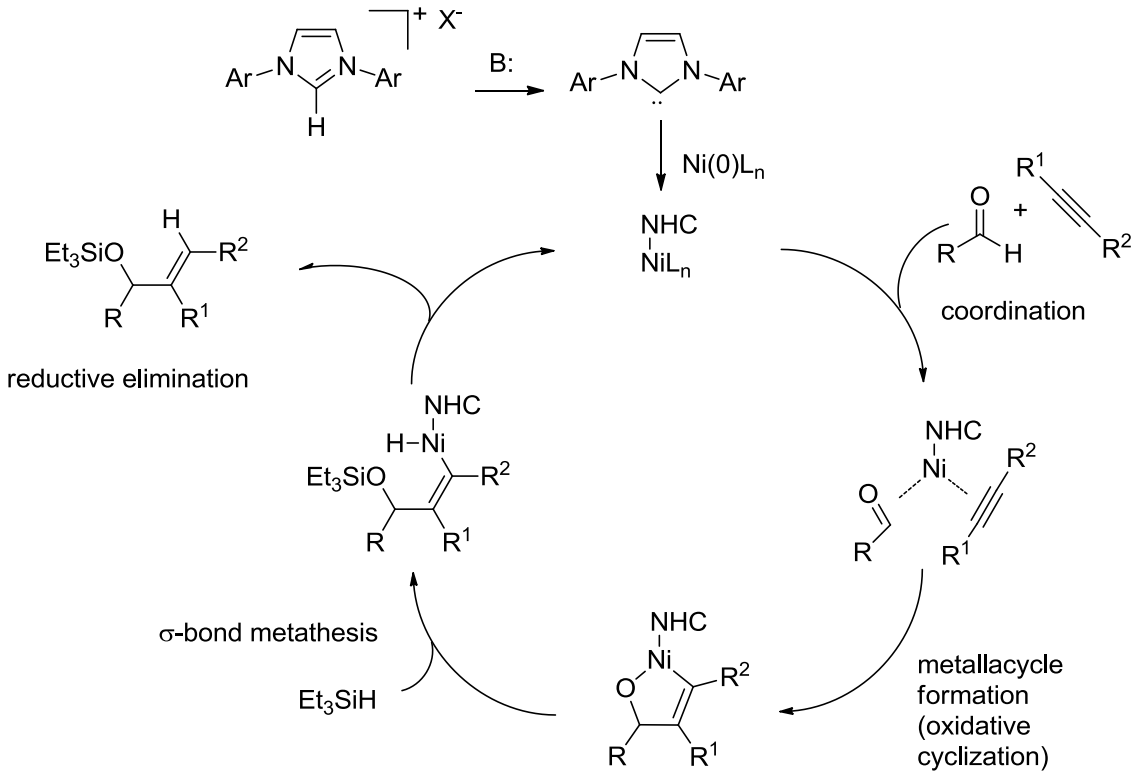

1.4.2 Competing Reactions in Nickel-Catalyzed Aldehyde-Alkyne Couplings

There are a variety of other reactions involving some or all of the components of the aldehyde-alkyne coupling reaction. Homo-dimerization, and trimerization of the alkyne can compete with the cross-coupling, leading to consumption of the alkyne (Scheme 1.18). The primary solution to this issue has been the switch from phosphines to NHCs as nickel-ligands, though slow addition of the alkyne can also greatly reduce the amount of alkyne that undergoes these side reactions by keeping the alkyne in low concentration.

Scheme 1.18. Dimerization-Hydrosylation and Trimerization of Alkynes

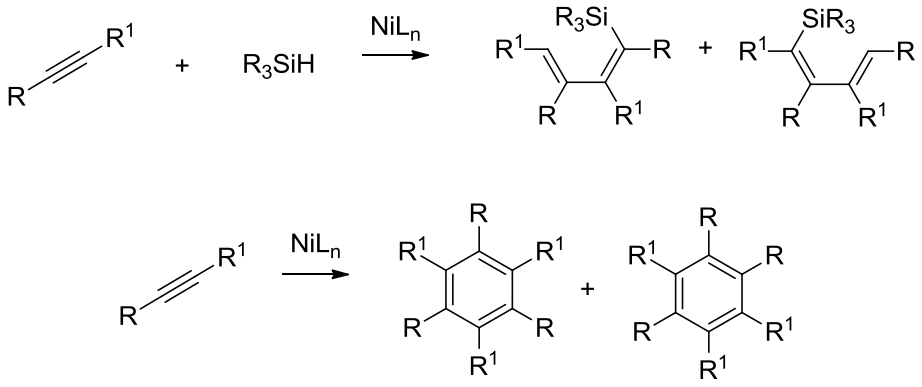

Carbonyl hydrosilylation and alkyne hydrosilylation have been demonstrated as productive reactions (Scheme 1.19).[35-37] If these pathways are too fast, they can lead to lower yields in cross-coupling reactions. Thankfully, silane choice can be used to greatly reduce the rates of these hydrosilylation reactions, likely because they occur via nickel undergoing an oxidative addition into the silane-hydrogen bond, while in the aldehyde-alkyne cross coupling the hydrosilane reacts via σ-bond metathesis after the rate-determining step.

Scheme 1.19. Hydrosilylation of Aldehydes and Alkynes

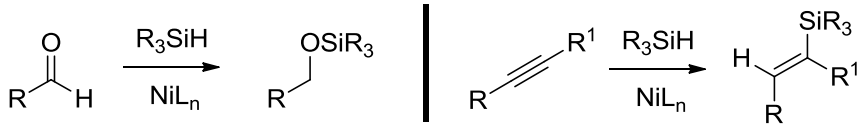

1.4.3 Macrocyclizations

Expanding the substrate scope from intermolecular couplings to macrocyclizations was an important demonstration of the power of this coupling procedure. Jamison and coworkers had shown an example of a macrocyclization using an internal aromatic alkyne in the synthesis of amphidinolide T1, where the aromatic group directed the regiochemistry. To develop a general method for both internal and terminal alkynes, both nickel-phosphine and nickel-NHC complexes were studied in macrocyclizations.[50] Our lab found that, for the macrocyclizations of terminal alkynes and aldehydes, IMes performed well as a ligand, producing 62-70% yield for 14- to 22-membered rings (Scheme 1.20). For the study of an internal alkyne, where the end group was methyl, a ligand screen of both phosphines and NHCs was conducted. It was found that using Me_3P as a ligand and Et_3B as a reducing agent resulted in the exocyclic product in a 4.5:1 ratio (Scheme 1.21). When IPr was used as a ligand, the endocyclic product became the major product with a 1:5 ratio.

Scheme 1.20. Nickel-Catalyzed Macrocyclizations of Terminal Alkynes

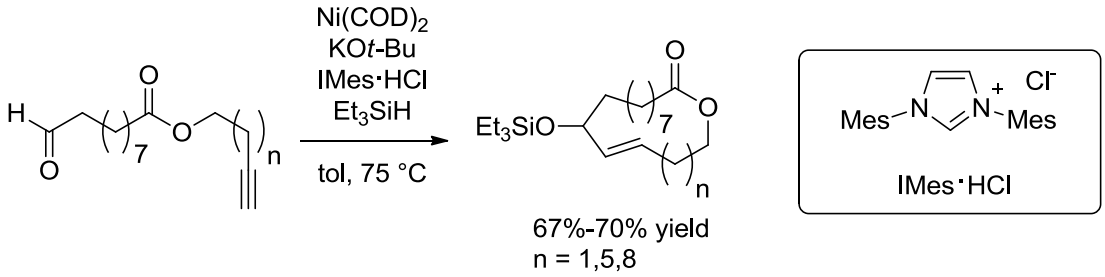

Scheme 1.21. Nickel-Catalyzed Macrocyclization of Internal Alkynes

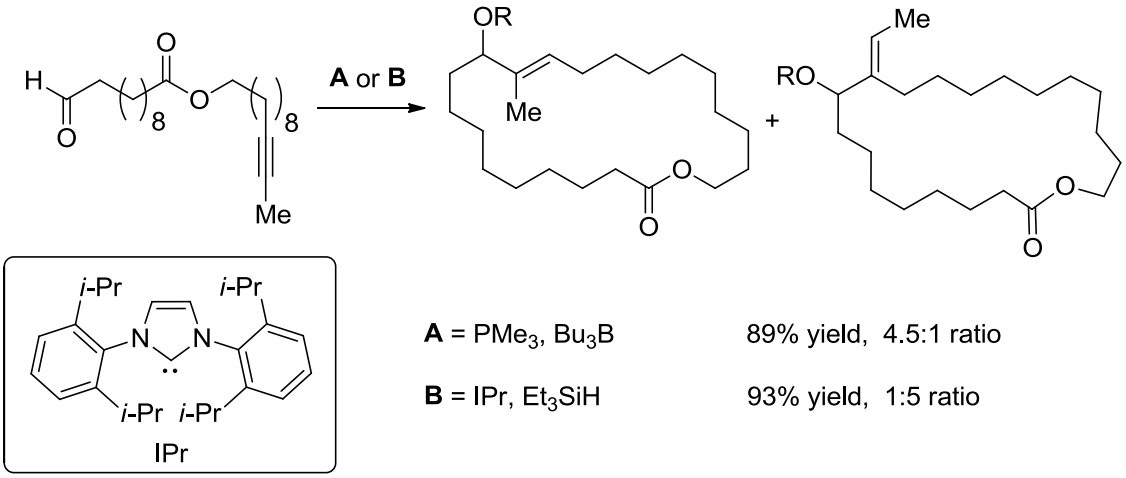

Based on the dependence of regioselectivity on ligand size, a general model for ligand-based regioselectivity in aldehyde-alkyne couplings was developed (Scheme 1.22). With small ligands, the larger alkyne substituent prefers to face away from the aldehyde, to avoid the steric interaction with the aldehyde. With large ligands the steric interaction between the alkyne and the ligand becomes more significant than the aldehyde-alkyne interaction, causing the larger group of the alkyne to be placed near the aldehyde.

Scheme 1.22. Model for Regioselectivity

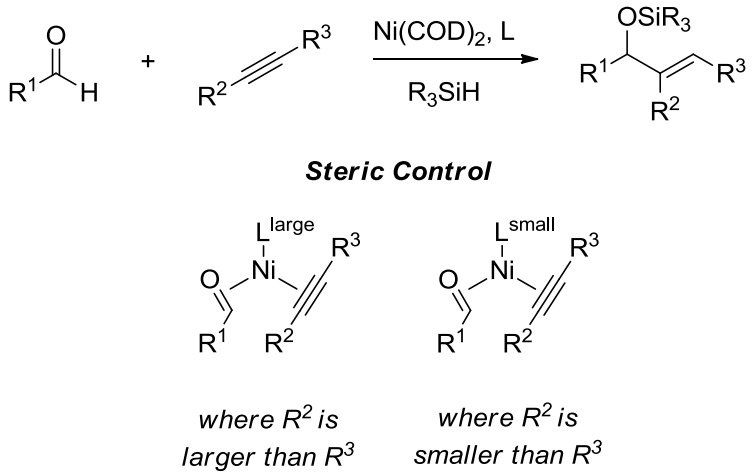

1.4.4 Diastereoselective Reaction

Exploring the impacts of neighboring functional groups on the selectivity of stereocenter formation, it was found that the coupling reaction between an α-silyloxyaldehyde and an alkynylsilane produced very high anti diastereoselectivity (Scheme 1.23).[51] The diastereoselectivity seems to be largely determined by sterics, based on the dependence on both the size of the α-silyloxyaldehyde silane, and the necessity of alkynylsilanes over other alkynes like internal and terminal alkynes. To demonstrate the power of these diastereoselective coupling reactions in synthesis, D-*erythro*-sphingosine was synthesized using similar conditions, utilizing an α-aminoaldehyde to direct the anti formation of the the 1,2-aminoalcohol (Scheme 1.24).[52]

Scheme 1.23. Anti Selectivity in the Coupling of α-Silyloxyaldehyde and Alkynylsilanes

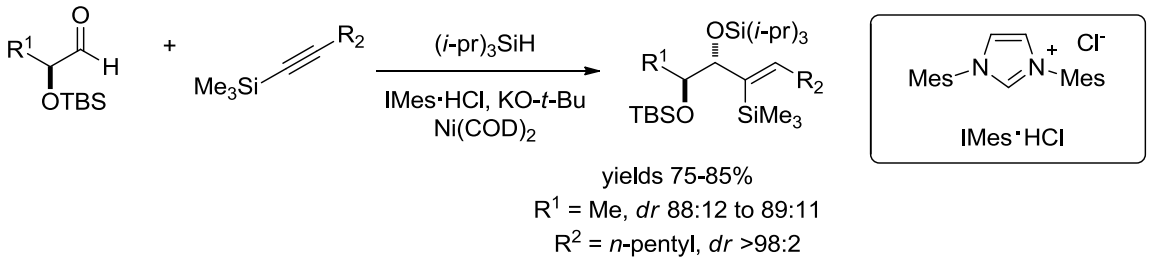

Scheme 1.24. Synthesis of D-*erythro*-Sphingosine

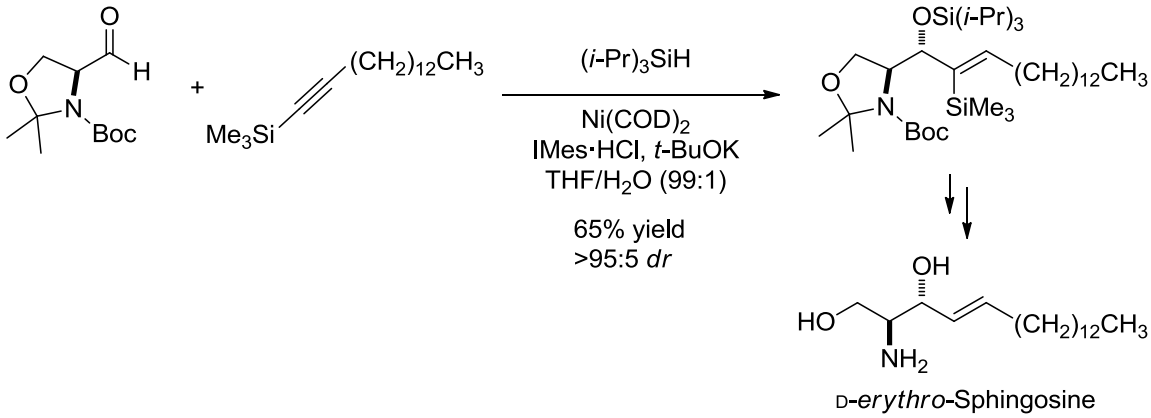

The total synthesis of aigialomycin D was achieved, with the key step being a nickel-catalyzed aldehyde-alkyne macrocyclization.[1] Initially, the strategy involved the

coupling of an alkynyl silane with an alpha-siloxy aldehyde, to take advantage of the diastereoselectivity we had observed in intermolecular couplings. Unfortunately, it was found that the alkynyl silane was sufficiently unreactive for the reductive coupling that a competing reaction occurred instead between the styrene and the aldehyde to produce a 5-membered ring (Scheme 1.25). It was known that the reaction rate of alkynyl silanes was slower than that of terminal alkynes based on experience within our lab, therefore the macrocyclization was instead performed with the terminal alkyne, which successfully produced the macrocycle in 61% yield.

Scheme 1.25. Key Macrocyclization Step of Aigialomycin D Synthesis

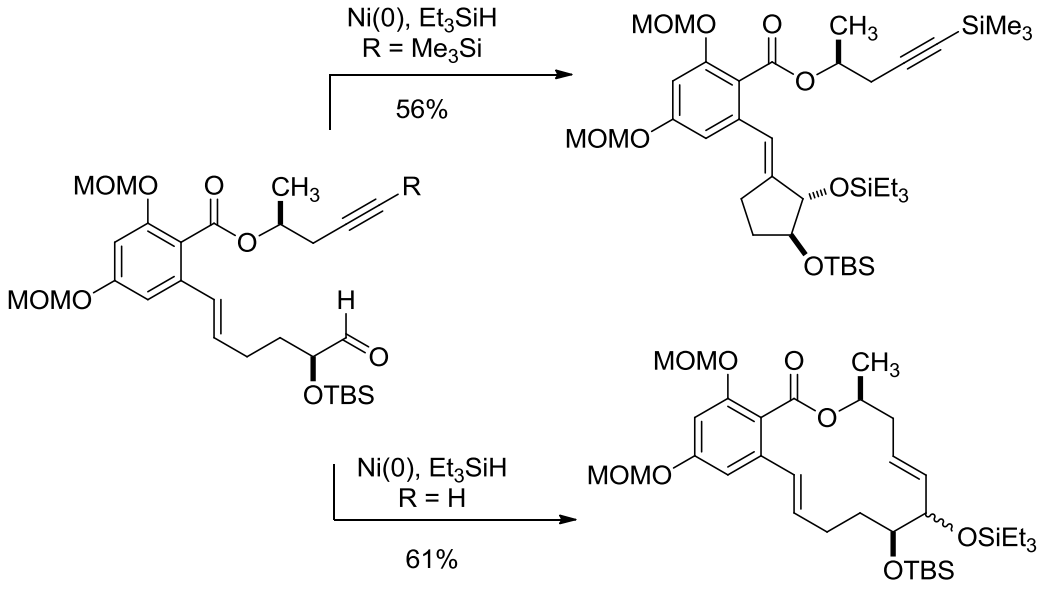

1.5 Summary of Introduction

Multiple methods for the aldehyde-alkyne coupling have been developed, though none with as broad of a scope as the nickel-catalyzed variant, using NHCs as ligands. The nickel-catalyzed reductive coupling has the potential to be used in a variety of applications, since its scope allows for a large variety of aldehydes and alkynes, in intermolecular couplings, intramolecular couplings, and macrocyclizations. As such, we believed it was important to control the reaction's regiochemistry and enantioselectivity, ideally through ligand design. These studies are the focus of this thesis.

Chapter 2

Enantioselective Nickel-Catalyzed Aldehyde-Alkyne Coupling

2.1 Enantioselective Nickel-Catalyzed Aldehyde-Alkyne Coupling Background

2.1.1 Methods to Enantioselectivity Produce Allylic Alcohols

There are a variety of different methods to enantioselectively produce allylic alcohols. Many of the methods described in Chapter 1 also have enantioselective variants. Lipshutz has developed a copper-catalyzed, enantioselective 1,2-reduction of enones with high enantioselectivity, though the substrates are in general limited to compounds with aromatic substitution (Scheme 2.1).[53] The primary challenge in developing the 1,2-reduction of enones is suppressing the competitive 1,4-reduction, limiting the types of ligands that can be used in this methodology.

Scheme 2.1. Copper-Catalyzed Enantioselective 1,2-Reductions of Enones

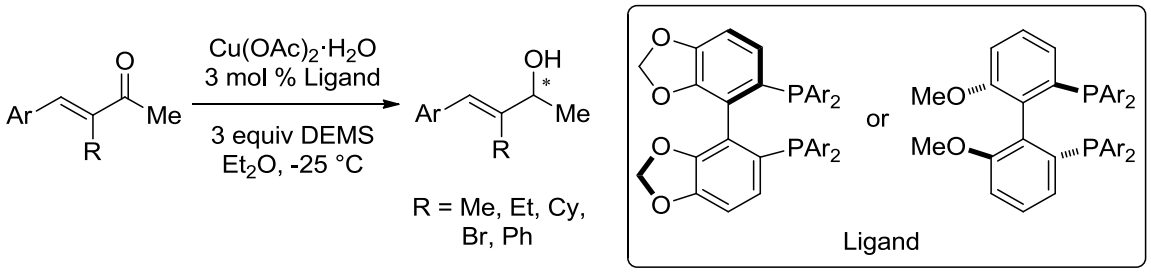

The Nozaki-Hiyama-Kishi coupling has been developed as an asymmetric reaction (Scheme 2.2).[54] Both internal and terminal alkenyl halides were capable of undergoing enantioselective reactions. While the examples given in this specific example are diastereoselective, the pre-existing stereocenters on the aldehydes have no bias for either isomer. It is important to note that the conditions developed take advantage of the Fürstner modification,[13] lowering the equivalents of chromium down to catalytic amounts

by using stoichiometric amounts of manganese. The unique ligand class used in this methodology is easily tunable as well, allowing for fast screening.

Scheme 2.2. Asymmetric Nozaki-Hiyama-Kishi Coupling

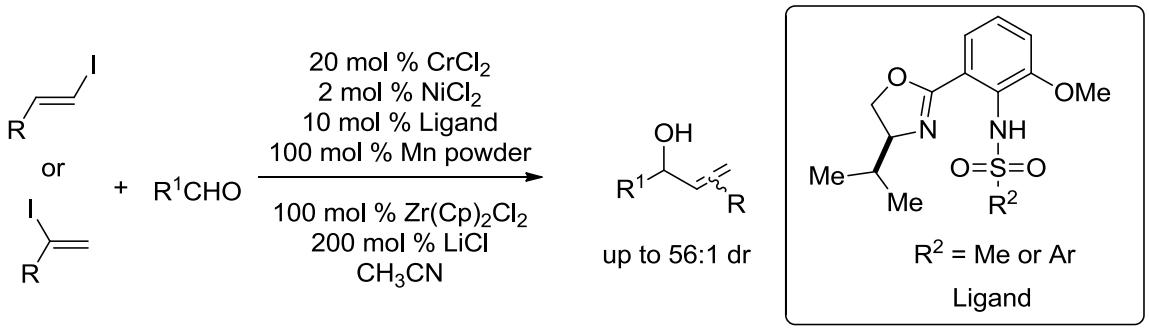

2.1.2 Enantioselective Aldehyde Couplings

As discussed in Chapter 1, Oppolzer has developed enantioselective variants of the reductive couplings of terminal alkynes and aldehydes through a hydrometallation-addition pathway (Scheme 2.3).[15] The core limitation of these methodologies is that they can only result in 1,2-substituted trans-alkene products, as the hydrometallation step requires a terminal alkyne. This strategy has also successfully been applied to macrocyclizations, where the hydroboration of the alkyne occurred selectively in the presence of an unhindered aldehyde leading to the macrocycle in 75% yield and 92% *ee*.[16]

Scheme 2.3. Asymmetric Aldehyde-Alkyne Reductive Coupling via Alkyne Hydroboration followed by Aldehyde Addition

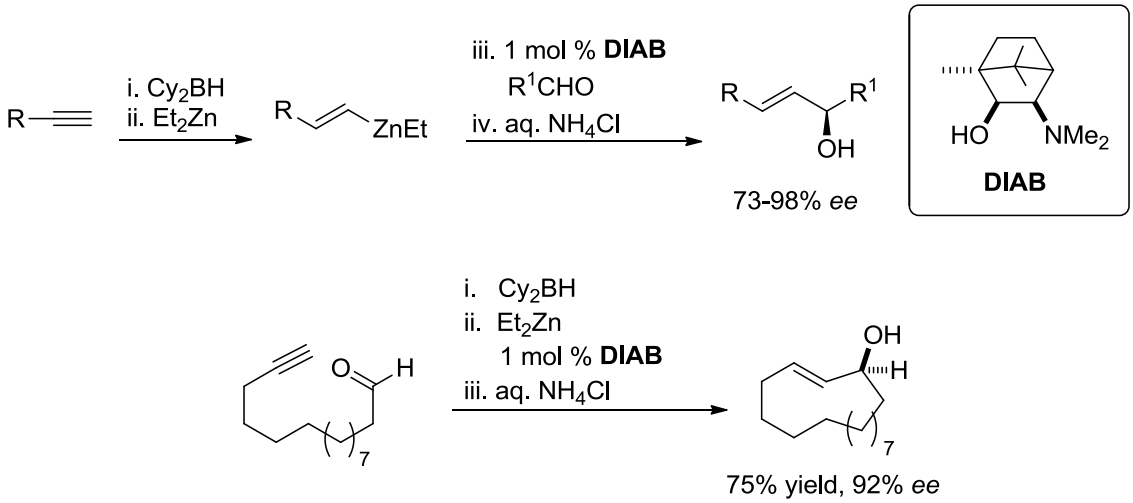

Krische has developed an enantioselective catalyst system for the hydrogenative coupling of aldehydes and alkynes, though the substrate scope is generally limited to conjugated or aromatic alkynes, and has so far been limited to a α-ketoaldehydes, α-ketoesters and heterocyclic aromatic aldehydes (Scheme 2.4).[26] It is possible that these vicinal aldehyde structures are simply more electrophilic, though when heterocyclic aromatic aldehydes were studied in the presence of chiral acids it appeared clear that the additional heteroatoms were involved in the protonation of the aldehyde.[25]

Scheme 2.4. Rhodium Catalyzed Asymmetric Hydrogenative Coupling of Aldehydes and Alkynes

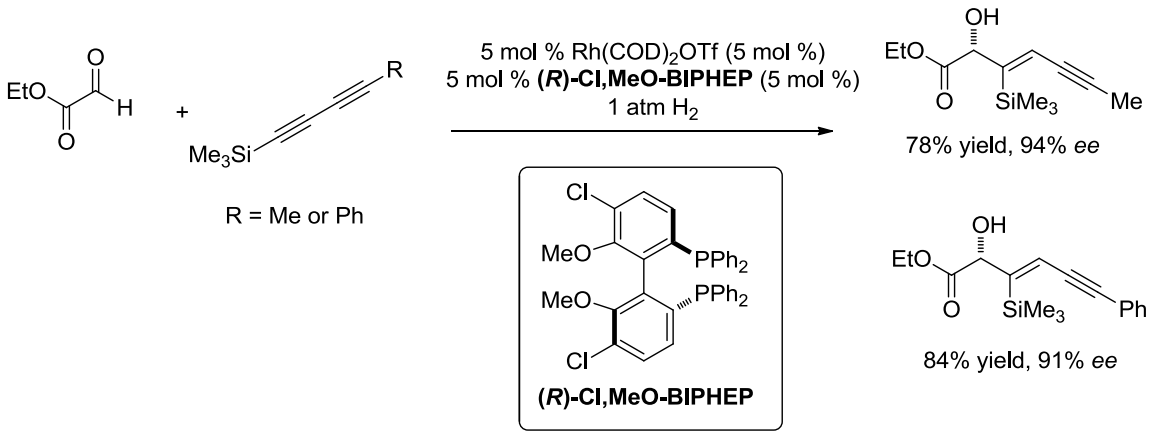

Using a (+)-NMDPP ligand, in a nickel-catalyzed aldehyde-alkyne reductive coupling, Jamison was able to observe up to 96% *ee* (Scheme 2.5). The methodology is most successful with aromatic internal alkynes.[55] The use of an alkynylsilane results in only 43% yield, while use of di-alkyl substituted alkyne results in both low yield and low enantioselectivity. The reaction conditions required were cumbersome, requiring an eight hour syringe drive addition to a reaction mixture at -25 ˚C, followed by stirring at that temperature for 36 hours.

Scheme 2.5. Asymmetric Nickel-Phosphine Catalyzed Aldehyde-Alkyne Reductive Coupling

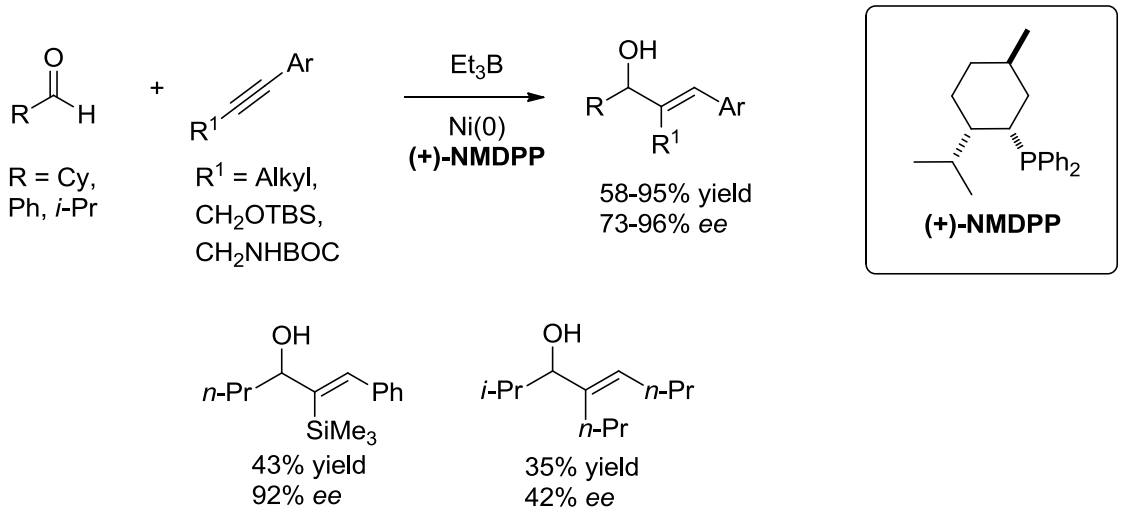

2.1.3 *N*-Heterocyclic Carbenes in Asymmetric Catalysis

Due to the lack of generality for any processes to produce allylic alcohols directly from aldehydes and alkynes, we decided to explore NHC complexes as enantioselective catalysts. We based our initial focus on enantioselective ligands that share common structure with the NHCs that have been shown to be effective as ligands in nickel-catalyzed aldehyde-alkyne couplings. One of the most recognized catalyst systems that have used IMes as a ligand are the ruthenium metathesis catalysts.[56] Grubbs explored a class of NHCs that can be derived in two steps from commercially available chiral 1,2 diamines and aryl-halides as ligands for ruthenium in an enantioselective ring closing metathesis reaction (Scheme 2.6).[57] NHCs derived from (1*R*,2*R*)-diphenylethylenediamine and *ortho*-substituted aromatics yielded very high enantioselectivity in the desymmetrization of achiral trienes (Scheme 2.7). It was observed that the NHC salt had high stability (stable to column chromatography), and that the chiral NHC-ruthenium complex was just as stable as the Grubbs second generation catalyst. A crystal structure of the isolated complex illustrated that the *ortho*-substituents were pointing away from the metal center.

Scheme 2.6. Ligand Synthesis from (1*R*,2*R*)-Diphenylethylenediamine

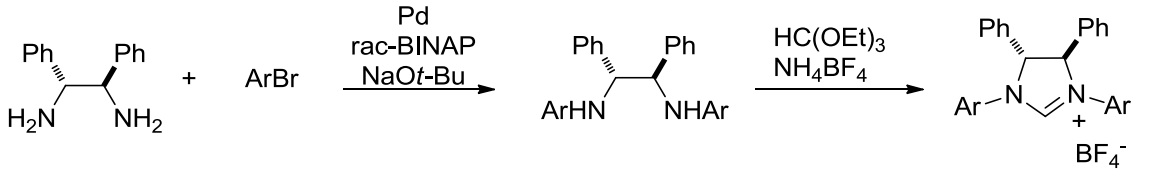

Ar = Mes, *o*-tol, *o*-*i*-PrPh

Scheme 2.7. Asymmetric Desymmetrization of Achiral Trienes

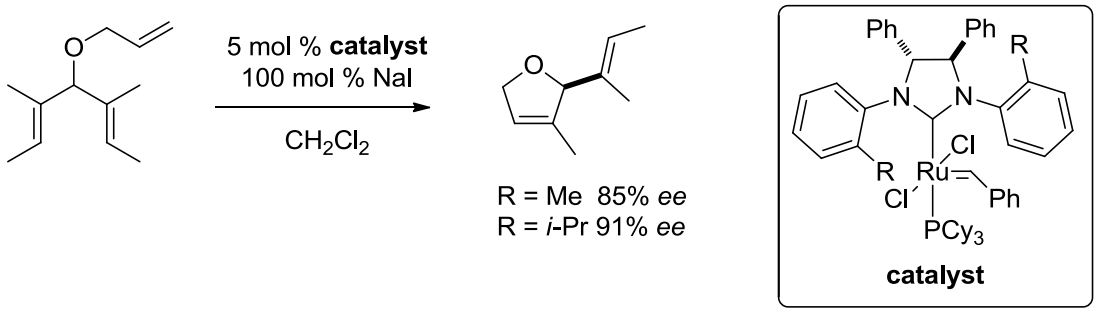

2.2 Developing an Enantioselective NHC Ligand for Nickel-Catalyzed Aldehyde-Alkyne Couplings

2.2.1 Enantioselective Goal

Our goal was to create a catalyst system that would provide high enantioselectivity and chemical yields over a broad set of aldehydes and alkynes in nickel-catalyzed aldehyde-alkyne reductive couplings. Every other method to asymmetrically produce allylic alcohols from aldehydes and alkynes has a scope limited to either terminal or aromatic alkynes. We wanted to expand this scope to include aliphatic alkynes, as well as provide alternative conditions for the asymmetric reductive couplings of terminal and aromatic alkynes.

2.2.2 Enantioselective Ligand Screening

Mani Chaulagain and I began our exploration of enantioselective nickel-catalyzed aldehyde-alkyne reductive couplings[58] using the ligands from Grubbs' asymmetric metathesis work described above. Ligand precursors were generally synthesized following same procedures, a Pd-catalyzed *N*-arylation of (1*R*,2*R*)-diphenylethylenediamine followed by cyclization using triethylorthoformate in the presence of ammonium tetrafluoroborate (Scheme 2.6). Initially, the *ortho*-substitution

was varied to include Me, Ph, *i*-Pr or Cy (Table 2.1). The ligand with *ortho*-Cy substitution gave significantly higher enantioselectivity than the other ligands, though the yield was limited. Using a Ph in the *meta*-substitution also had a weak impact on enantioselectivity. After a general base and solvent screen, the maximum yield for the coupling of benzaldehyde and phenylpropyne using **L4** was 60%, while enantioselectivities appeared to be constant (Table 2.2).

Table 2.1. Initial Screening of Ligands for the Enantioselective Aldehyde-Alkyne Reductive Coupling

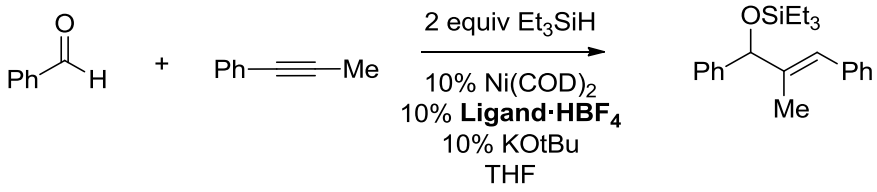

ligand	% *ee*	% yield
L1	27	50
L2	29	50
L3	45	40
L4	72	60
L5	30	50

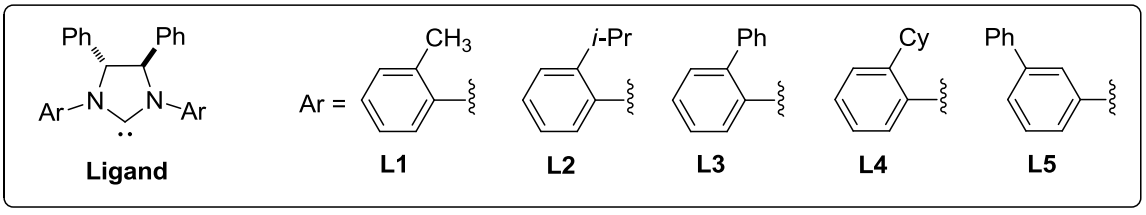

Table 2.2. Ligand **L4** Yield Optimization

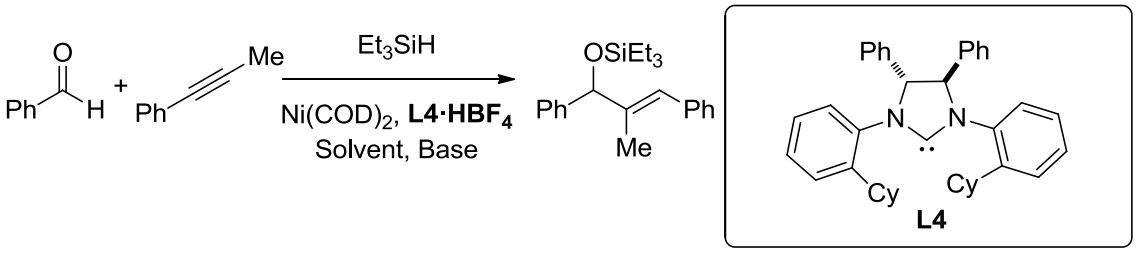

solvent	base	% yield	% *ee*
Et_2O	*t*-BuOK	43	76
Tol	*t*-BuOK	43	75
THF	*t*-BuOK	60	76
THF	BuLi	54	74
THF	Me_3SiOK	37	76

There are a variety of explanations for why yields are lower with ligands that lack *ortho,ortho*-disubstitution; catalyst formation may be reduced due to carbene dimerization, free carbene formation may be slow due to the base adding into the imidazolinylidene instead of doing a direct deprotonation, or side reactions including alkyne trimerization, alkyne hydrosilylation and aldehyde hydrosilylation may br preferred. Because we had seen much higher yields using IMes as a ligand we decided to screen a ligand with methyl in each *ortho* position (Scheme 2.8), synthesized by the standard pathway (Scheme 2.6). Yields dramatically improved to 79%, but enantioselectivity dropped to 30% *ee*. This increase in yield was proof that we needed a ligand with *ortho,ortho*-disubstitution on the *N*-aryl rings, but we wanted to maintain a cyclohexyl in the *ortho* position to get the high enantioselectivities.

Scheme 2.8. Impact of *ortho,ortho*-Disubstitution on Yields

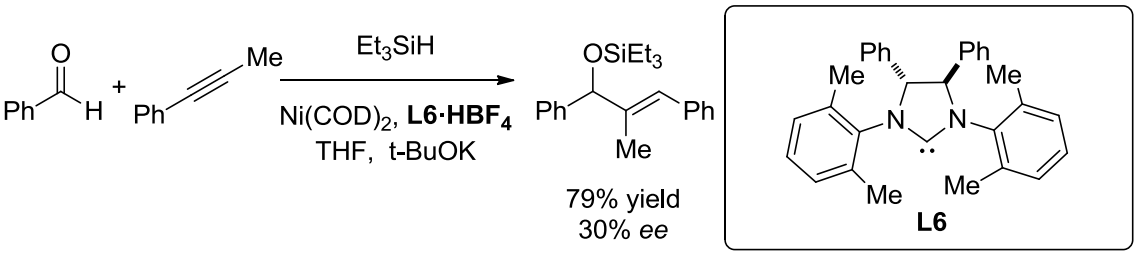

The synthesis of our ligand with an *ortho*-cyclohexyl and *ortho*-methyl on each *N*-aryl ring required first the synthesis of our precursor aryl halide, since there was no commercially available aryl halide that would lead to this motif. Through a Friedel-Crafts reaction of toluene and cyclohexyl bromide in the presence of aluminum(III) chloride, 3,5-dicyclohexyltoluene is produced (Scheme 2.9). While initially it is likely that 2,4-dicyclohexyltoluene is produced via 2 sequential electrophilic aromatic substitutions, the presence of excess aluminum(III) choride is capable of catalyzing a 1,2 alkyl migration to produce the more energetically stable 1,3,5 substitution pattern.[59] This product was then brominated, where of the three possible aromatic bromination sites, two of the sites are equivalent. A small amount of the bromination product with the bromine between the cyclohexyls was also produced, but it was found to be unreactive in the next step, *N*-arylation, based on recovered aryl halide.

Scheme 2.9. Aryl Halide Synthesis for $I_{Me,Cy}$

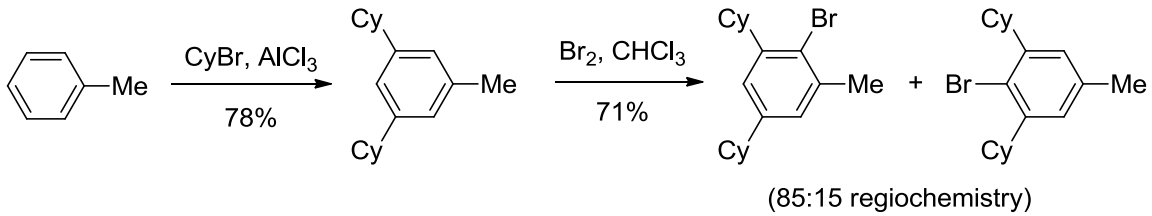

While it had been noting previously that the *N*-arylation of a similar aryl halide proceeded poorly,[60] we decided it pertinent to make this specific ligand. Standard conditions using racemic BINAP gave none of the desired product (entry 1, Table 2.3). Using a ligand developed specifically for bulky *N*-arylations also gave no increase in yield. Upon increasing the temperature of the reaction to 105 ˚C, 10% yield was observed. By increasing the temperature to refluxing conditions, increasing the concentration of the reaction and boosting the catalyst loading we were able to achieve 83% yield for the *N*-arylation product. The *N*-arylation product was then cyclized under standard conditions to produce the $I_{Me,Cy}$ (Scheme 2.6).

Table 2.3. Optimizing *N*-Arylation Conditions

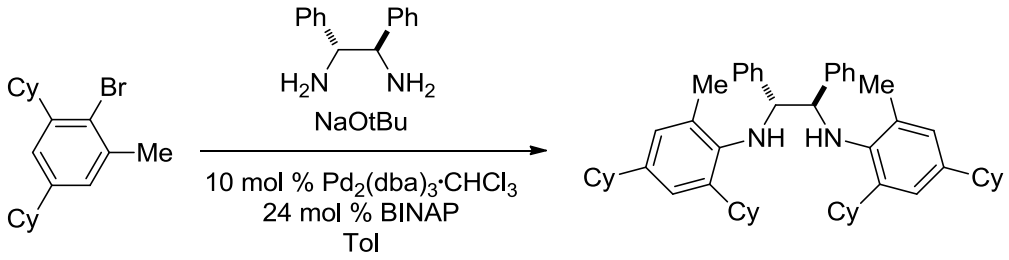

entry	temperature	concentration (diamine) mol/L	catalyst/ligand	yield
1	90 ˚C	0.1	5% Pd, 12% BINAP	0%
2	90 ˚C	0.1	5% Pd, 12% 2-Diphenylphosphino-2'-(N,N-dimethylamino)biphenyl	0%
3	105 ˚C	0.1	5% Pd, 12% BINAP	10%
4	110 ˚C	0.1	5% Pd, 12% BINAP	15%
5	110 ˚C	0.6	5% Pd, 12% BINAP	27%
6	110 ˚C	0.6	10% Pd, 24% BINAP	83%

With this ligand in hand, we were encouraged by the fact that it produced both high enantioselectivity and yields when applied to the reductive coupling of benzaldehyde and phenylpropyne. Even more exciting was the fact that for this substrate combination, 98% yield could be achieved with only 2% catalyst loading (Scheme 2.10).

Scheme 2.10. Enantioselectivity of $I_{Me,Cy}$

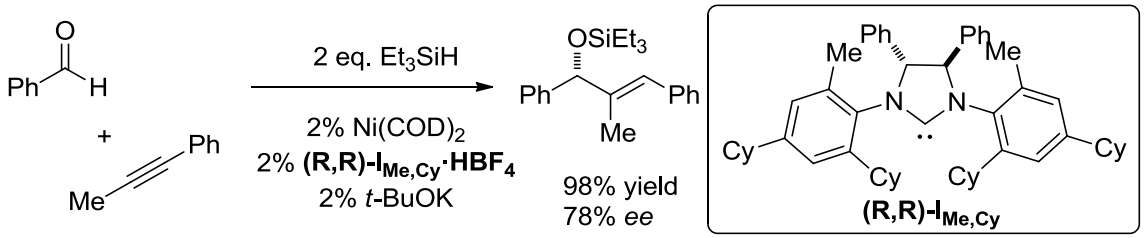

2.2.3 Enantioselective Ligand Scope

With the use of the standard 10% catalyst loading, synthetically useful yields and enantioselectivities were observed for the intermolecular coupling of a wide range of aldehydes (linear alkyl, branched alkyl, aromatic) and alkynes (aromatic, internal and terminal) (Table 3.4). Free alcohols were also tolerated with no loss in enantioselectivity.

Table 2.4. Substrate Scope of Chiral Ligand

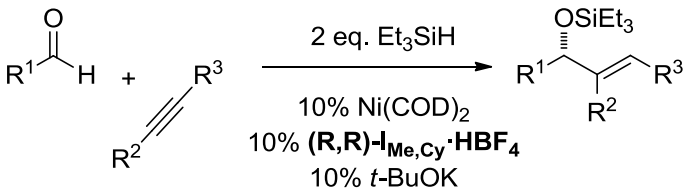

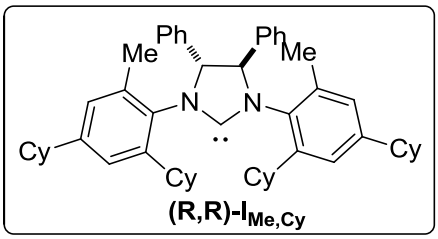

Entry	R^1	R^2	R^3	% yield	% *ee*	regioselectivity
1	Ph	Me	Ph	98[a]	78	10:1
2	Ph	Et	Et	82	70	
3	*i*-Pr	Me	Ph	86	70	>19:1
4	*i*-Pr	$(CH_2)_2Ph$	Me	86	75	3:1
5	Cy	Et	Et	84	85[b]	
6	$(CH_2)_2Ph$	Et	Et	75	78	
7	Cy	Me	Ph	78	81	>19:1
8	Cy	H	*n*-hex	64	65	>19:1
9	*n*-hex	Me	Ph	70	73	10:1
10	Cy	$(CH_2)_4OH$	Ph	99	79	9:1

[a]2% catalyst loading

[b](S,S) $I_{Me,Cy}$ used producing opposite enantiomer

One interesting observation was the stark contrast in regiochemistry for ligands **L4** and (R,R)-$I_{Me,Cy}$ for the coupling of 2-octyne with cyclohexylcarboxaldehyde (Scheme 2.11). Both ligands demonstrated high enantioselectivity, but depending on the ligand either regioisomer could be produced, though the yields for ligand **L4** are still moderate. These trends follow the ligand based regioselectivity trends observed in our previous macrocyclization work (Scheme 1.22).

Scheme 2.11. Regioselectivity Switch in Enantioselective Coupling

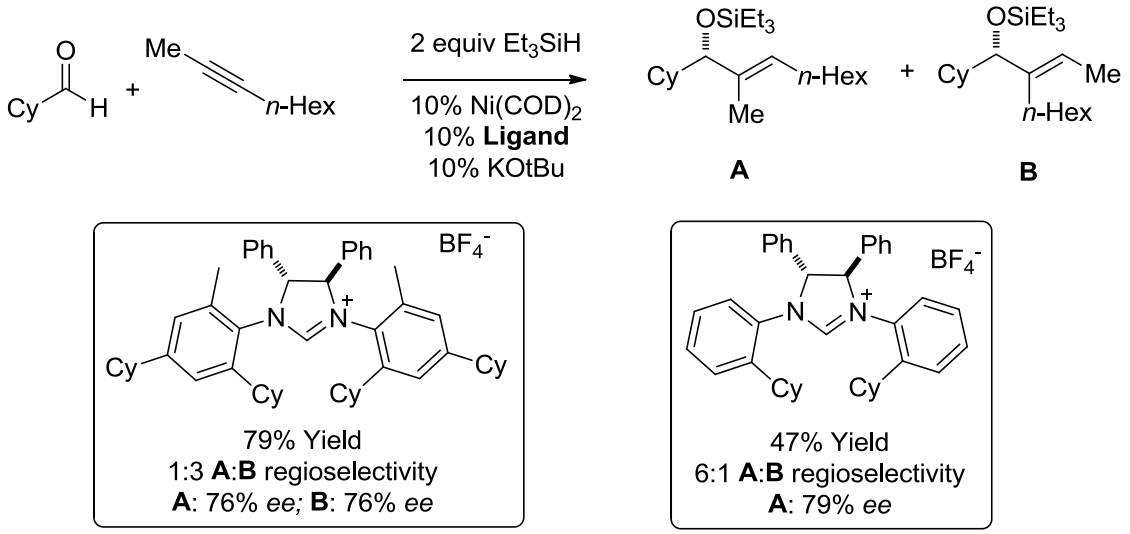

Ligand (R,R)-$I_{Me,Cy}$ was also applied in a macrocyclization to produce a 86:14 mixture of endo:exo product (Scheme 2.12). Similar to the previous macrocyclizations including nickel-catalyzed aldehyde-alkyne reductive couplings,[50] very dilute conditions were required in order to minimize intermolecular dimerization. The endo product was produced in 79% *ee*, indicating these ligands are effective for conferring enantioselectivity in macrocyclizations.

Scheme 2.12. Macrocyclization using (*R*,*R*)-$I_{Me,Cy}$

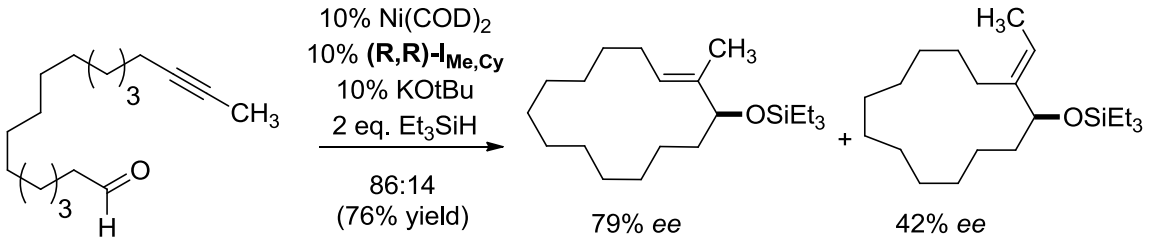

2.2.4 Determination of Absolute Stereochemistry

There are many methods that can be used to determine the absolute stereochemistry of a compound. If a compound has been synthesized previously or exists in nature and has been characterized, comparison of optical rotations can be used. Crystal structures can also be used as a method to determine absolute stereochemistry. After derivatization with an enantiopure reagent of known configuration, NMR studies

can be used through either chemical shifts or NOE studies for compounds with a predictable and rigid conformation. One of the most well known methods of determining the absolute stereochemistry of a secondary alcohol is Mosher's ester analysis (Scheme 2.13).[61] The Mosher's ester highly favors a conformation where the trifluoromethyl group eclipses the ester's carbonyl, which eclipses the proton of the secondary alcohol's chiral center. It is important to note that ester formation must go to completion in order to give an accurate measurement of enantiomeric excess, as it is possible that one alcohol enantiomer will react faster with the chiral Mosher's acid.

Scheme 2.13. Mosher's Ester Conformation

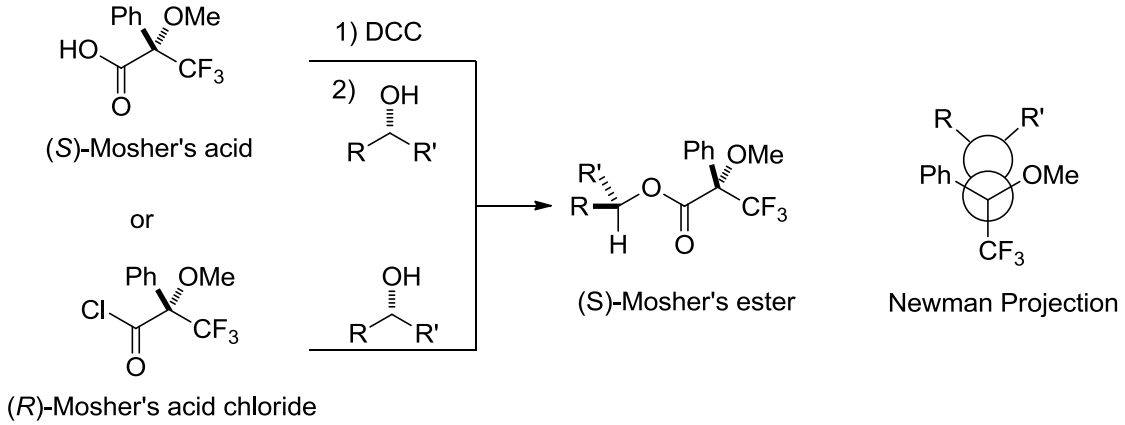

The importance of this conformation is that the phenyl and methyl ether substituents of the Mosher's ester can interact with the substrate, leading chemical shift differences between the Mosher's ester of the two enantiomers of the allylic alcohol (Scheme 2.14). While the phenyl group shields the group it eclipses, resulting in an upfield shift, the methyl ether deshields the group it eclipses, resulting in a downfield shift. It is also important to note that the alcohol substituents can interact with the Mosher's ester, when either an aromatic or alkenyl group is present near the methyl ether, a methyl ether upfield shift would be expected.

Scheme 2.14. Chemical Shift Effects of Mosher's Esters

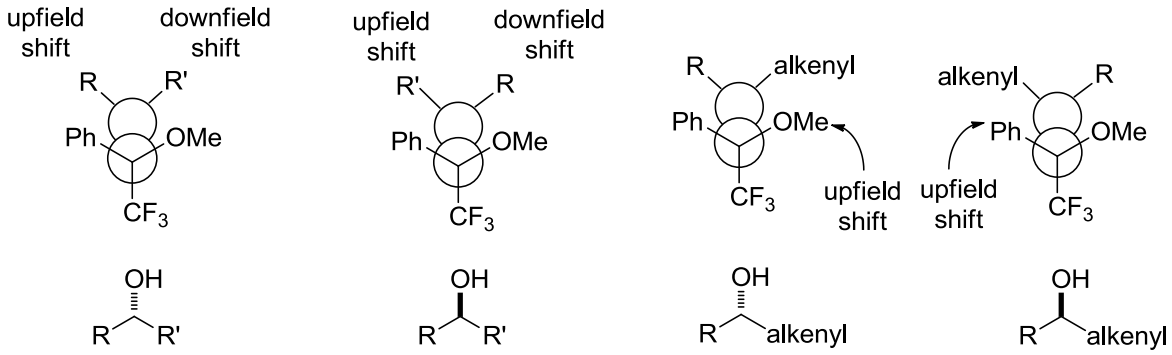

To ensure the absolute stereochemistry of our products, we resynthesized ligand (R,R)-$I_{Me,Cy}$ using (1*R*,2*R*)-diphenylethylenediamine, confirming its absolute stereochemistry by optical rotation. Using this ligand, three examples were synthesized, desilylated using TBAF, then the (*S*)-Mosher's Esters were synthesized from the (*R*)-Mosher's acid chloride. The stereochemistry of the (*R*)-Mosher's acid chloride was confirmed by synthesis of an (*S*)-Mosher's ester using the (*R*)-Mosher's acid chloride, followed by NMR comparison with the (*S*)-Mosher's ester synthesized from the same alcohol sample and (*S*)-Mosher's acid, after confirming the (*S*)-Mosher's acid absolute stereochemistry by optical rotation. The first example was analyzed by only Mosher's ester analysis alone, where the alkene proton was clearly shifted downfield in the major product relative to the minor product, matching the left model (Scheme 2.15). While the methyl ether signal was also clearly separated by NMR, the alcohol was substituted with two π-systems which may not be clearly differentiated. The other two compounds that were synthesized had literature optical rotations, which allowed us to confirm absolute configuration by optical rotation[55] in addition to Mosher's ester analysis (Scheme 2.16). The product absolute stereochemistry was also confirmed by the comparison of compounds (*R,E*)-Triethyl(2-methyl-1,3-diphenylallyloxy)silane (Table 2.4, Entry 1)[58] and (*S,E*)-(1-Cyclohexyl-2-methyl-3-phenylallyloxy)triethylsilane (Table 2.4, Entry 7)[62] chiral HPLC traces of those reported previously.[55]

Scheme 2.15. Absolute Stereochemistry by Mosher's Ester Analysis

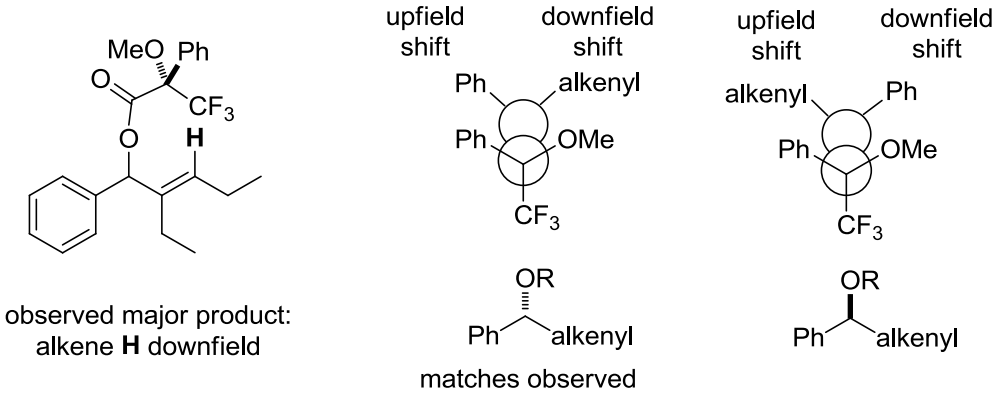

Scheme 2.16. Compounds with Known Optical Rotations, Absolute Stereochemistry by Mosher's Ester Analysis

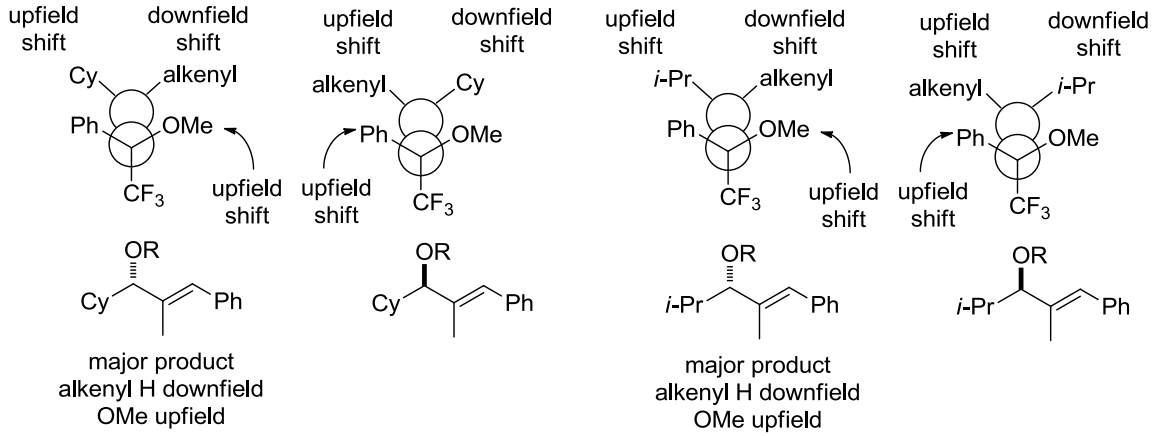

2.2.5 Ligand Salt Atropisomers

While characterizing $I_{Me,Cy}$•HBF_4 we observed what appeared to be three compounds by NMR, in a ratio of 50:33:17, each containing all the components of our desired imidazolium but with slightly different chemical shifts (Scheme 2.17). Two of these compounds were *C2*-symmetric, while the third (**A2**) lacked this symmetry causing the backbone protons to couple to each other and have different chemical shifts (Figure 2.1). To distinguish between the two *C2*-symmetric atropisomers, the backbone proton of the major atropisomer was irradiated in an NOE experiment, resulting in a through-space excitation of the methyl of the *N*-aryl ring (Figure 2.2). This methyl signal indicated that in the major atropisomer the methyl was oriented towards the backbone, as expected in atropisomer **A1**.

Scheme 2.17. Atropisomerization of $I_{Me,Cy}$•HBF_4

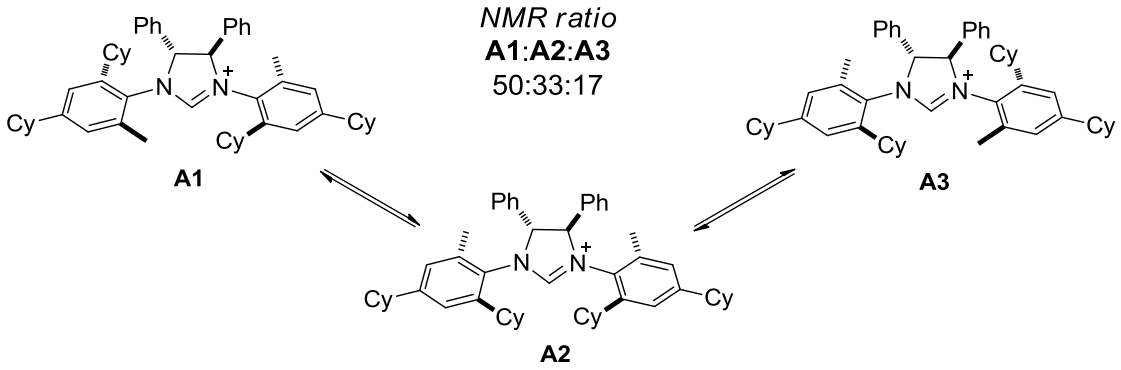

Figure 2.1. Assigning Atropisomer **A2**

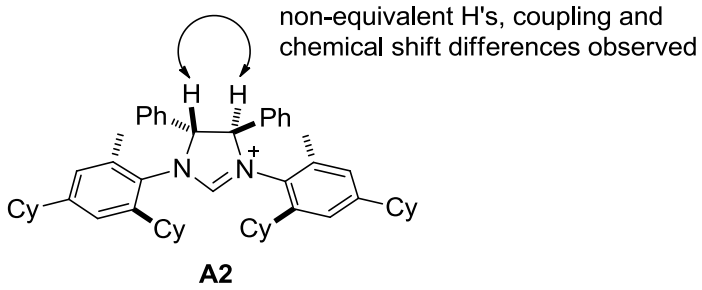

Figure 2.2. Assigning Major Atropisomer

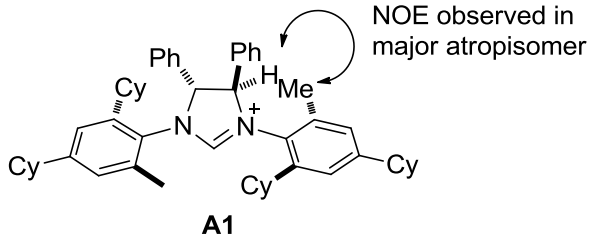

We also wanted to know how quickly these atropisomers could interconvert. Initially we changed the temperature of the NMR acquisition, hoping to observe a chance in the ratio of regioisomers, but no significant change was observed. NOE experiments were then performed on the imidazolium C-H (Scheme 2.18). When **A2** was irradiated **A1** and **A3** also appeared to be irradiated with a 1.0 second mixing time. Increasing the mixing time to 2.0 seconds increased the signal intensity **A1** and **A3**. When either **A1** or **A3** were irradiated conversion was primarily to **A2**, which supports our model that **A2** is an intermediate between **A1** and **A3**.

Scheme 2.18. Observation of Atropisomer Interconversion by NMR

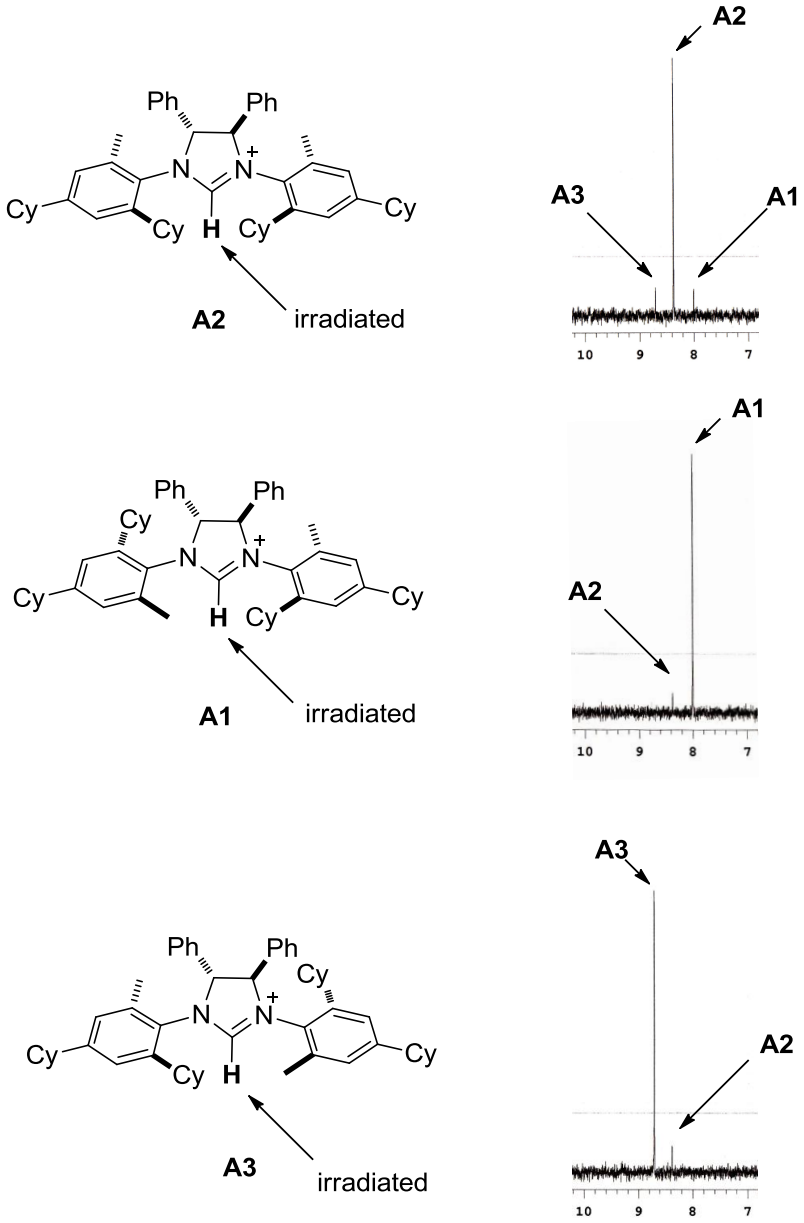

2.2.6 Origin of Enantioselectivity

Our model for the conformation of this class of NHCs in asymmetric catalysis is roughly based on the crystal structures of Grubbs' metathesis catalyst (Scheme 2.17).[57] We predict that the substrates bind to the faces of the nickel-catalyst, perpendicular to the plane of the imidazolinylidene, similar to trigonal nickel-NHC complexes characterized by Nolan.[56] The phenyls in the backbone cause the *N*-aryl rings to rotate, placing the *ortho*-substituent on the right-front of the catalyst face down into the metal center while

the left-front *ortho*-substituent is pointing up and away from the metal center, creating a preferred pocket for aldehyde binding. After oxidative cyclization, which we consider to be irreversible, the stereochemistry is established. The resulting metallacycle can then undergo σ-bond metathesis and reductive elimination (Scheme 1.18), leading to our observed product.

Scheme 2.19. Model for Asymmetric Induction

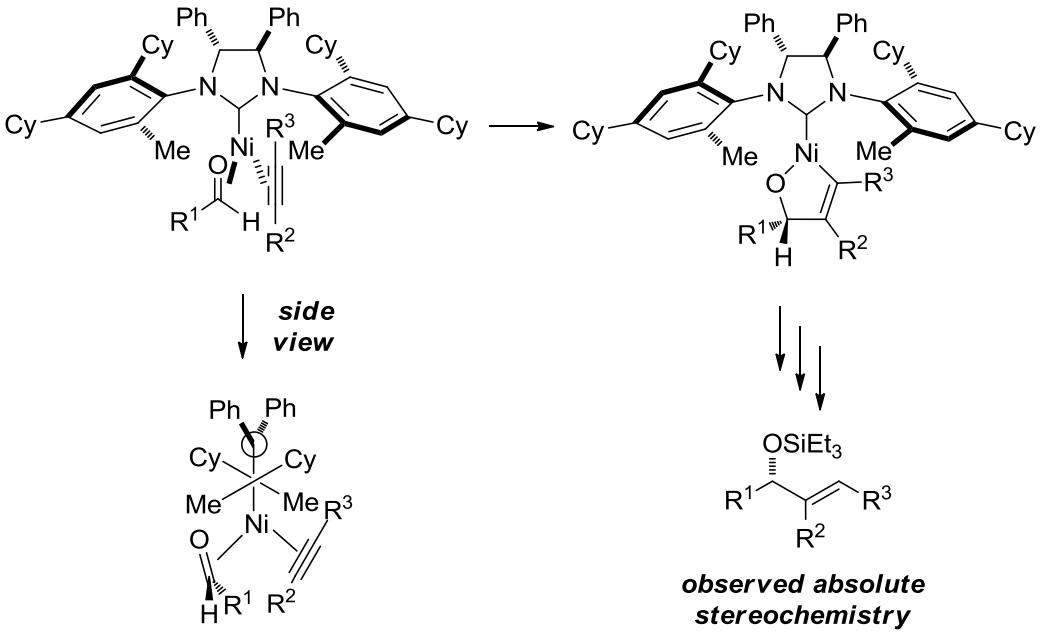

Though the crystal structures of the Grubbs metathesis catalyst placed the *ortho*-substituents of both *N*-aryl rings up towards the hydrogens of the backbone, it is possible that the active catalyst in this reaction is a different atropisomer. An alternative is that both *ortho*-cyclohexyls orient themselves on the side of the catalyst the aldehyde binds, and both *ortho*-methyls are oriented towards the alkyne, lowering the steric interactions with the alkyne (Scheme 2.18). This would result in directing the larger *ortho*-substituent into the metal center on the face of the metal that the aldehyde binds. It is also possible that multiple atropisomers exist as competent catalysts for this reaction, each with its own enantioselectivity, and the observed enantioselectivities are an averaging of an extremely selective catalyst and less reactive non-selective catalysts.

Scheme 2.20. Alternative Catalyst Atropisomer

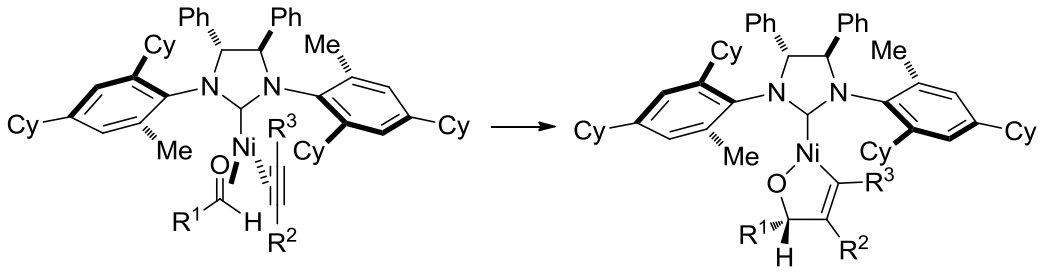

2.3 Additional Ligand Screening

2.3.1 Interesting Backbones and *N*-Substituents

In addition to screening the ligand prepared from (1*R*,2*R*)-diphenylethylenediamine, Grubbs[57] also screened ligands prepared from (1*R*,2*R*)-1,2-diaminocyclohexane. Even though the ligands derived from the cyclic backbone produced lower enantioselectivity for metathesis, we thought it necessary to screen our best aromatic substitution pattern since the enantiopure diamine was commercially available and we were dealing with a different catalytic system. **L7** was produced in 36% overall yield from the diamine and the arylhalide using the optimized conditions to produce $I_{Me,Cy}$ (Scheme 2.19) Unfortunately, when **L7** was used as a catalyst for the nickel-catalyzed aldehyde-alkyne reductive coupling only 11% *ee* was observed, indicating that this backbone is less capable of promoting enantioselectivity (Scheme 2.20).

Scheme 2.21. Synthesis of **L7** from (1*R*,2*R*)-1,2-Diaminocyclohexane

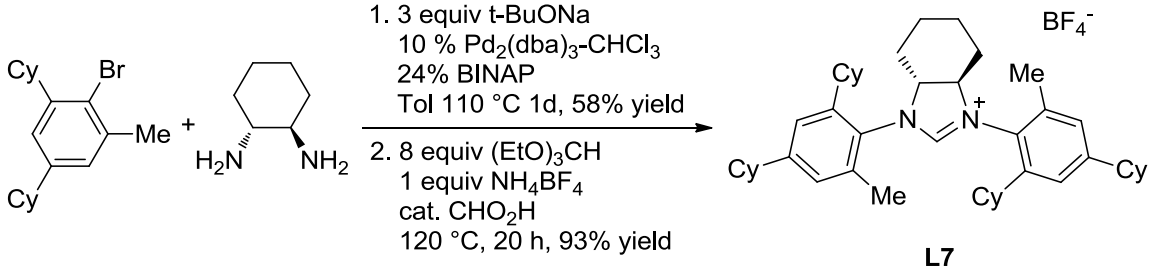

L7

Scheme 2.22. Reductive Coupling using **L7** as a Ligand

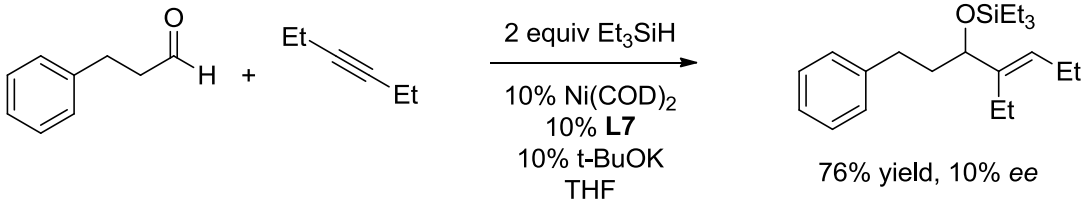

One well known catalyst in metathesis is Hoyveda's catalyst **L8**, which was shown to be highly enantioselective in catalytic enantioselective ring-opening metathesis and cross-metathesis.[63] It has a unique feature where the *N*-aryl substituent, a phenol, can bind the metal reversibly. After synthesizing this ligand via the 8-step route, this ligand was applied towards the aldehyde-alkyne reductive couplings but was not catalytically active (Scheme 2.21). We suspected this was due to a lack of tolerance of phenols in our reductive coupling reaction, so 2,4,5-trimethylphenol was added to a reaction using IMes as a ligand and only trace yield was observed. The methyl ether adduct **L9** was synthesized by cyclization of an intermediate in the synthesis of **L8**. We had hoped that as the methyl-ether we would still be able to utilize a loose coordination, without having the acidity issues of a free phenol. This ligand was effective as a catalyst and produced 70% yield in the reductive coupling of benzaldehyde and phenylpropyne, but the enantioselectivity was only poor, at only 20% *ee*.

Scheme 2.23. Ligands with Potential Coordination Effects

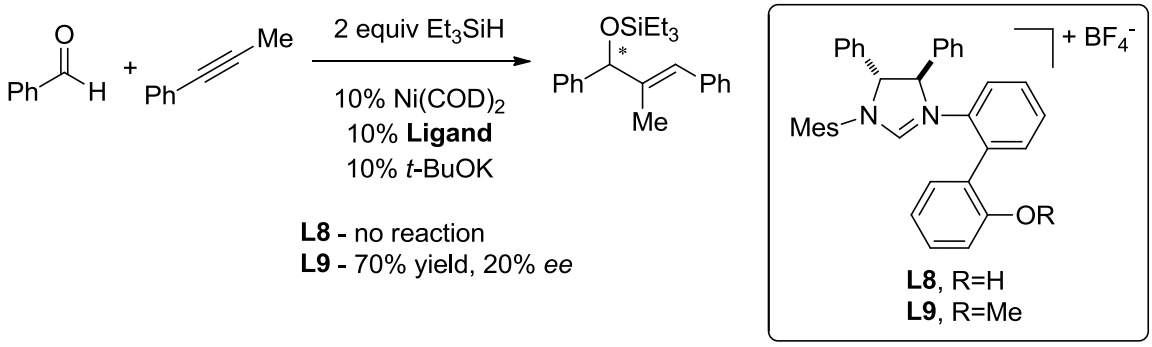

2.3.2 Fused Ring Systems

In order to probe what *ortho*-substituent of the aromatic ring (Scheme 2.17) was oriented into the metal center's reaction sphere we decided to make a rigid fused ring

system which would force a methyl into in the metal center (Scheme 2.22). Initially we envisioned we could make a fused ring system using diethyl tartrate as a readily available chiral source. Ligand **L10** was produced in 10% overall yield over 10 linear steps from diethyl tartrate. Ligand **L11** was produced following the same pathway.

Scheme 2.24. Oxygen Linked Fused Pentacyclic Ligand Synthesis

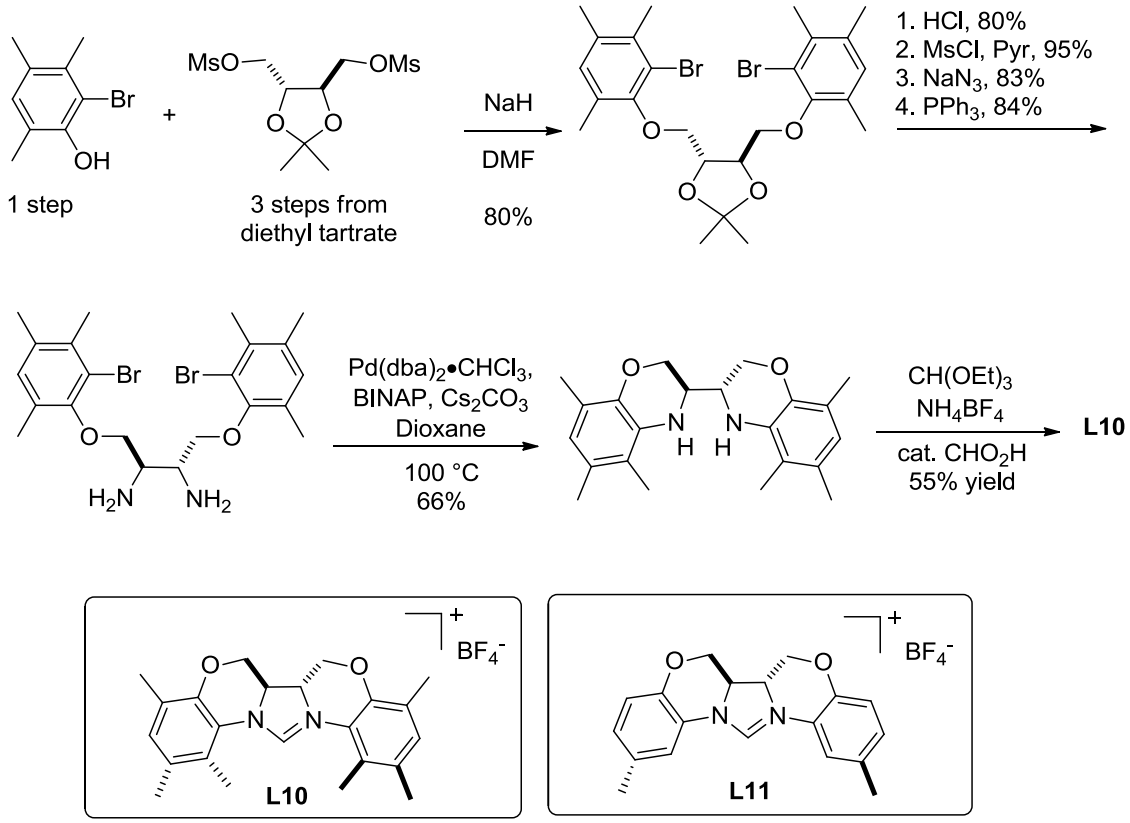

Unfortunately, this ligand was not catalytically active in the nickel-catalyzed aldehyde-alkyne reductive coupling reaction. Due to the decomposition issues in the *N*-arylation reaction, where a mild base was crucial to afford the product, there was a concern that the oxygen linkage was not base stable in this fairly strained ring system. When mild bases such as cesium carbonate were used to deprotonate the ligand, this ligand was still not productive in nickel couplings. When the ligand was treated with *t*-BuOK and observed by NMR, followed by quenching the carbene with acid, the original compound was not recovered, but rather some product which appeared to contain a phenol. Following the same procedure on IMes resulted in the reformation of IMes.

Our next step was to make a more stable system with an all carbon backbone. Without the oxygen linkage, decomposition should not occur. While initially we tried to use similar routes to our original approach, these we not successful and we instead decided that a much shorter racemic route would be preferred (Scheme 2.23). The racemic ligand could be used as a measure of the reactivity of the ligand, and the diamine intermediates could potentially be separated later using crystallization techniques with tartaric acid.[64] The diimine was formed using a simple condensation reaction from glyoxal and the corresponding aniline. Grignard addition into the diimine produced a 6:1 mixture of racemic:meso, the racemic compound was isolated in 78% yield as a single diastereomer after column chromatography. Treatment of the racemic diamine with sulfuric acid yielded the desired polycyclic product at 50 ˚C. Interestingly lower temperatures failed to promote the reaction, and at 60 ˚C, decomposition predominated. The imidazolium salt **L12** was then produced under standard cyclization conditions. An analog **L13** was also produced, following the same procedure.

Scheme 2.25. Carbon Linked Fused Pentacyclic Ligand Synthesis

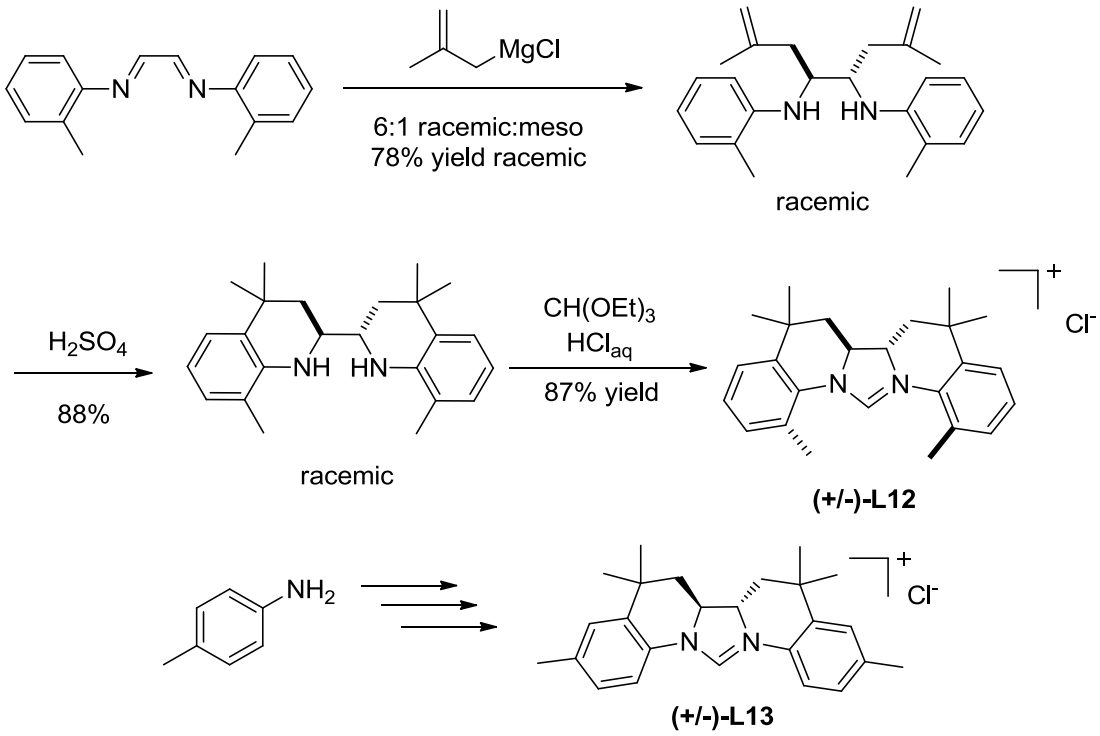

Unfortunately, these ligands were not productive in reductive coupling reactions under the conditions we screened. It is possible that the angles of the *N*-aryl rings are too far from perpendicular to the imidazolium face, and as such are interfering with either nickel binding to the NHC or the alkyne binding (Scheme 2.24). For other chiral systems the orientation of the *N*-aryl rings are actually very close to perpendicular to the imidazolium face, and are able to turn away from the alkyne as needed. Because these angles are maintained by covalent bonds, there is no flexibility to make room for alkyne binding, and the *N*-aryls are therefore locked in an unfavorable position.

Scheme 2.26. Pentacyclic Fused Ring System Conformation

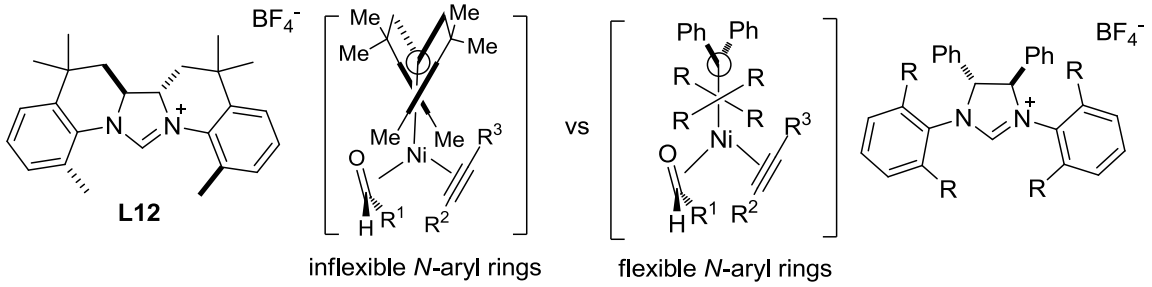

2.4 Enantioselectivity Conclusions

A series of chiral NHC ligands were synthesized, and screened in the nickel-catalyzed reductive couplings of aldehydes and alkynes. High enantioselectivities and yields were observed for $I_{Me,Cy}$ with a remarkably high substrate scope, far broader than the any of the existing asymmetric aldehyde-alkyne coupling reactions. The enantioselectivity was achieved using a chiral backbone that directs the *N*-aryl groups of the NHC ligand, forcing them into aldehyde coordination site in a way where they interfere with the binding of one prochiral face. Further directions for the enantioselective reductive coupling involve boosting enantioselectivity further through designs based on modeling, and designing ligands which are both enantioselective and regioselective, which will be discussed in Chapter 4.

Chapter 3

Regioselective Nickel-Catalyzed Aldehyde-Alkyne Coupling

3.1 Regioselectivity Nickel-Catalyzed Aldehyde-Alkyne Coupling Background

3.1.1 Regioselectivity in Alkyne Coupling Reactions

Regiocontrol in the reductive couplings of unsymmetrical alkynes has been a longstanding issue as it has been largely controlled by substrate bias. Commonly, the alkyne regioselectivity is controlled by silyl-substitution (Scheme 3.1), aromatic systems or conjugation (Scheme 3.2).[65] Reactions of terminal alkynes that involve initial hydroboration or hydrozirconation both tend to favor hydride addition at the internal position of terminal alkyne, and metal addition at the terminal position,[15-18] while chromium(II) mediated aldehyde-alkyne couplings have preferred C-C bond formation at the internal site of the terminal alkyne (Scheme 3.3).[32,33]

Scheme 3.1. Substrate Based Regiocontrol in Coupling Reactions of Alkynylsilanes

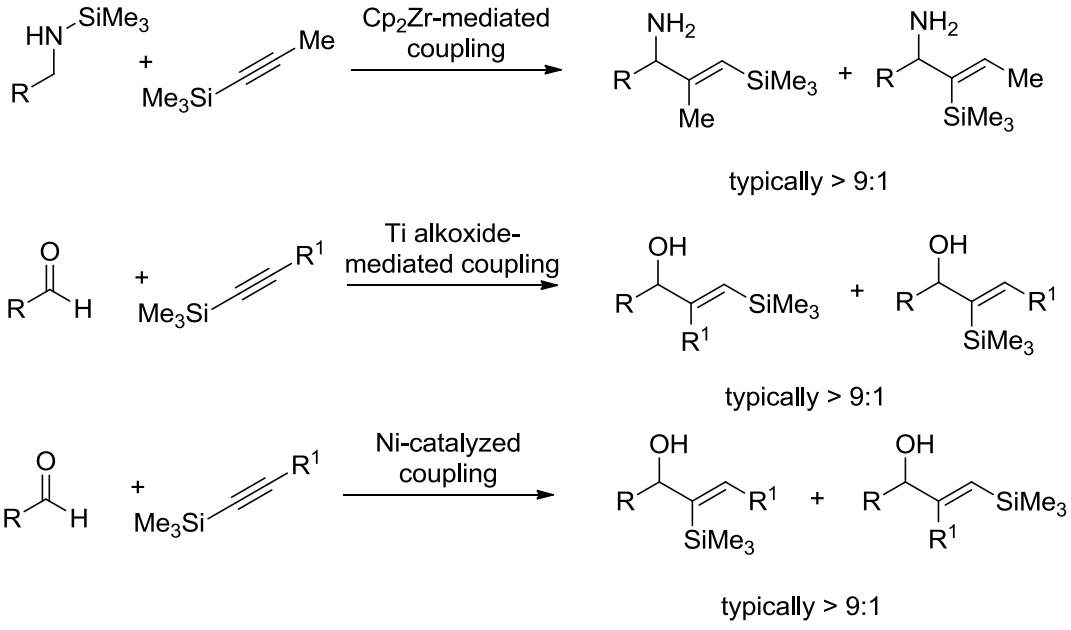

Scheme 3.2. Substrate Based Regiocontrol in Coupling Reactions of Unsymmetrical Internal Alkynes

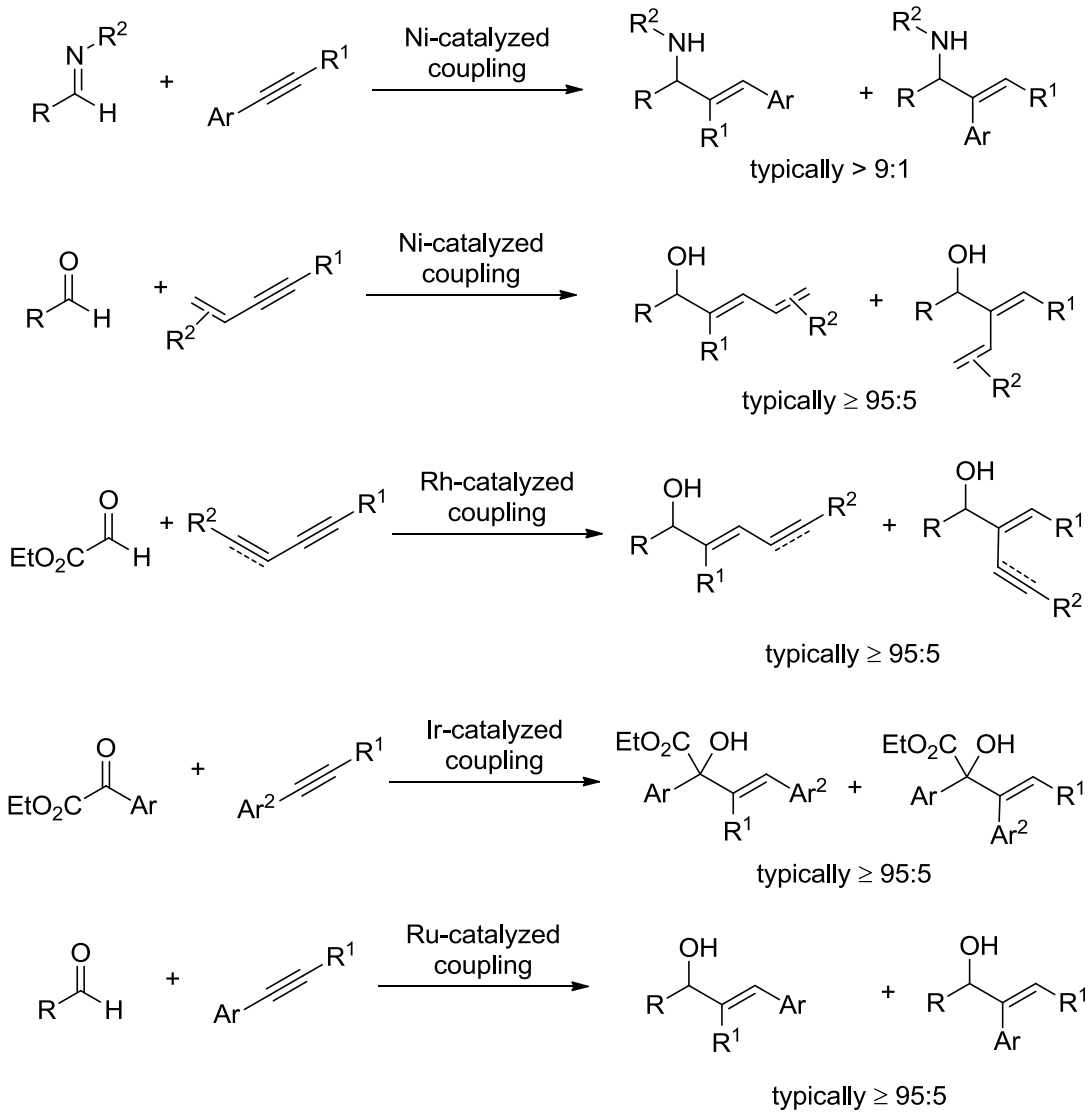

Scheme 3.3. Substrate Based Regiocontrol in Coupling Reactions of Terminal Alkynes

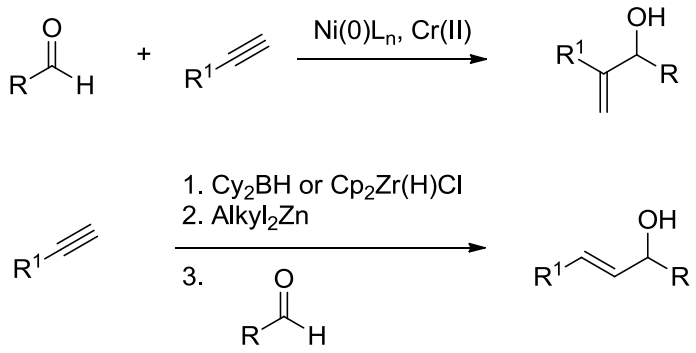

Other strategies have taken advantage of distal directing groups. Jamison found that 1,6-enynes can participate in aldehyde-alkyne reductive couplings in high regioselectivity. [66] In this case, regioselectivity may be reversed in the presence of a bulky phosphine ligand (Scheme 3.4). It was postulated that in the absence of a bulky phosphine the alkene occupies the coordination site that allows for C-C bond formation at carbon B, so the aldehyde binding occurs near carbon A, leading to regioisomer A. In the presence of the bulky phosphine, there is no free coordination site until the alkene dissociates from the metal, and the aldehyde binds where the alkene was, adjacent to carbon B, which leads to regioisomer B.

Scheme 3.4. Regiocontrol in the Coupling of Aldehydes and 1,6-Enynes

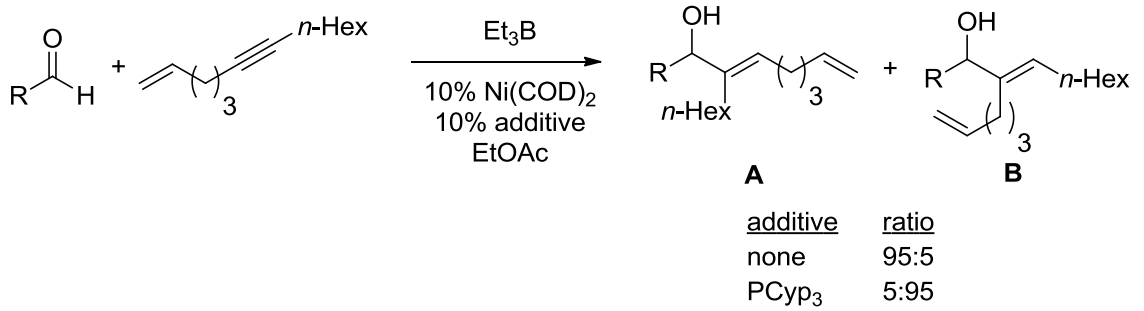

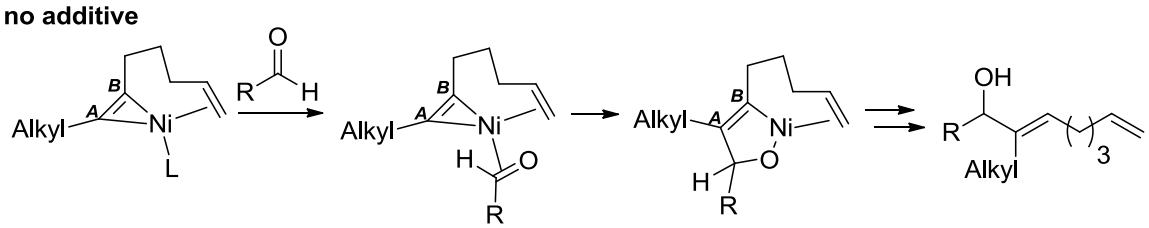

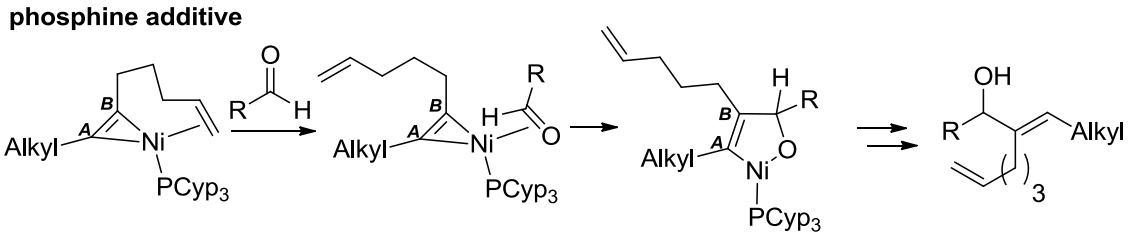

Recently, advances from Micalizio have been made in the reductive coupling of ynols to other π-systems using a titanium catalyst (Scheme 3.5).[20] Similar to the transition states of the ligand-free nickel-catalyzed couplings of 1,6-enynes and aldehydes, the free alcohol of the ynol binds to the titanium in addition to the alkyne. The only available site for the binding of the coupling partner is adjacent to carbon A,

which leads to selective C-C bond formation at carbon A. The scope of this reaction includes coupling with terminal alkynes, internal alkynes, imines and aldehydes. While this system does reliably control the regiochemistry of these reactions, it lacks the ability to reverse the selectivity through condition changes.

Scheme 3.5. Mechanism of Regioselectivity in Titanium-Mediated Coupling of Ynols

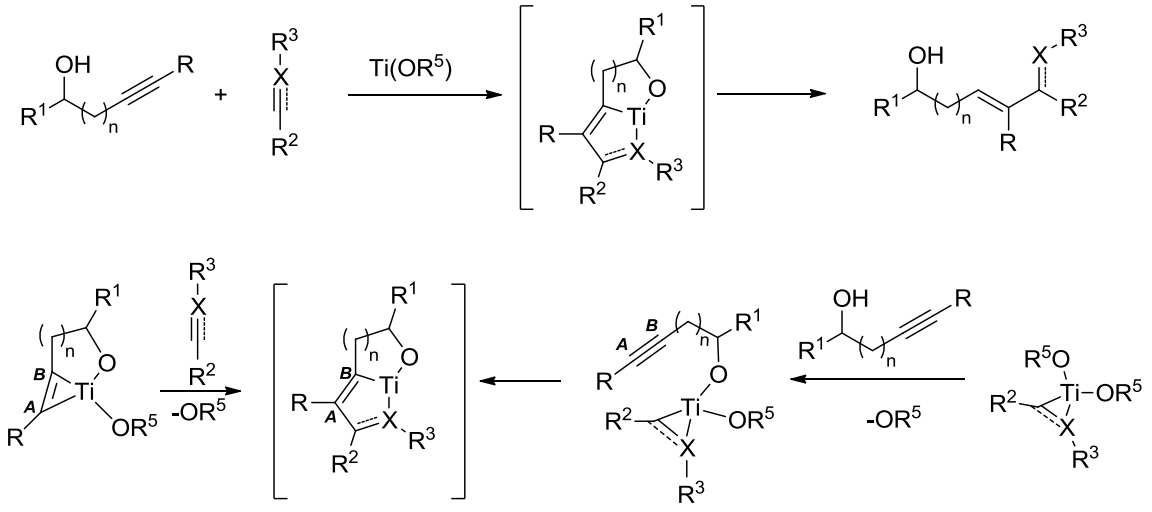

3.1.2 Regioselectivity in Nickel-NHC-Catalyzed Aldehyde-Alkyne Coupling Reactions

In our initial publication of the nickel-IMes catalyzed aldehyde-alkyne coupling reaction, there were a variety of alkynes whose functionality could direct regiochemistry through electronic biases (Scheme 3.6).[34] Terminal alkynes and aromatic alkynes both resulted in >98:2 selectivity. Later, alkynylsilanes were also shown to exhibit similarly high regioselectivity.[51] Unfortunately, 2-hexyne, an internal alkyne with dialkyl substitution, showed only 1.3:1 selectivity when coupled to benzaldehyde using IMes as a ligand (Scheme 3.7).

Scheme 3.6. Alkynes with Electronic Biases

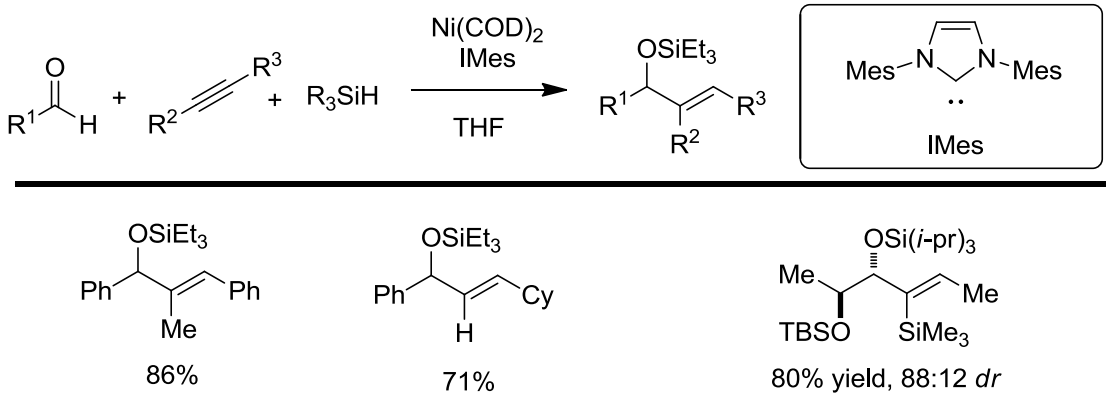

Scheme 3.7. Regioselectivity in the Coupling of 2-Hexyne

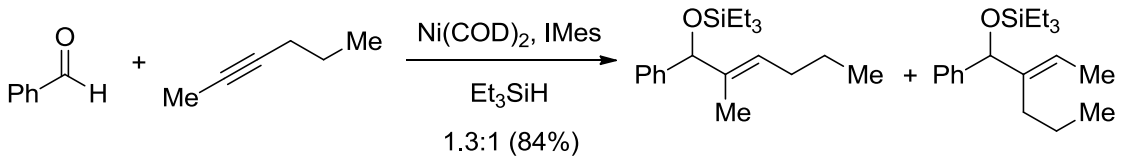

3.1.3 Strategies to Control Regioselectivity

Regioselectivity can be controlled from two fundamentally different approaches: catalyst based and substrate based. In the study of macrocyclizations by our lab, both strategies were utilized. When an internal alkyne containing a methyl substituent was cyclized using the nickel-catalyzed aldehyde-alkyne coupling using IMes as a ligand, no regioselectivity was observed (Scheme 3.8). Changing the ligand allowed the production of either regioisomer with modest selectivity. Alternatively, by changing the alkyne's methyl substituent to a phenyl the exocyclic product was formed exclusively.

Scheme 3.8. Ligand and Substrate Control in Macrocycles

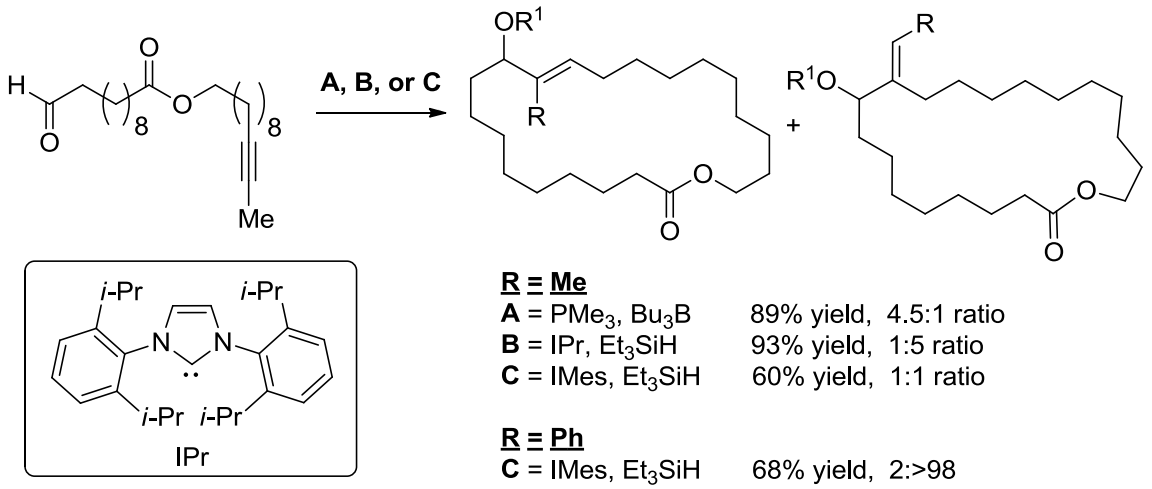

Later, we utilized the electronic biases of propargyl alkynes to control regioselectivity.[67] Using an unprotected propargyl alkyne in a coupling with heptaldehyde yielded 80:20 selectivity, an improvement over the 67:33 selectivity that was observed in the absence the alcohol (Scheme 3.9). After optimization it was found that using a *t*-butyldimethylsilyl protecting group for the alcohol boosted the selectivity to 87:13 indicating that this removable group could be used as a handle for regiocontrol. Based on this work and our work with macrocyclizations, we have developed a general predictive model for regiochemistry (Scheme 3.10).

Scheme 3.9. Controlling Regiochemistry using Propargyl Alcohols

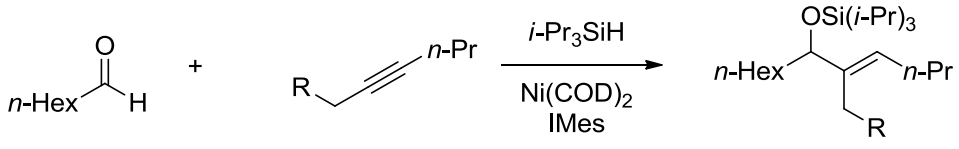

Scheme 3.10. Model for Regioselectivity

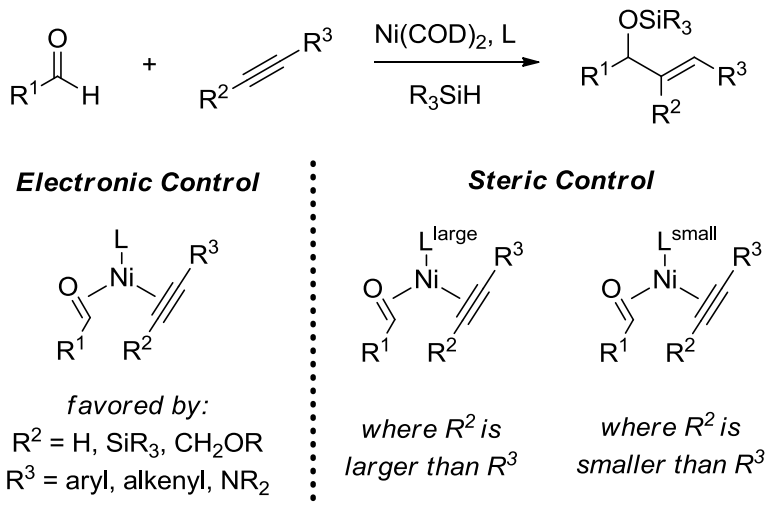

3.2 Developing a Regioselective NHC Ligand for Nickel-Catalyzed Aldehyde-Alkyne Couplings

3.2.1 Regioselectivity Goals

Hasnain Malik and I had two primary goals in developing regioselective aldehyde-alkyne coupling strategies.[68] First, we wanted to drive reactions that traditionally show poor regioselectivity to produce either regioisomer with high selectivity (Scheme 3.11). Secondly, we wanted to reverse the selectivity on electronically biased substrates, to selectively form the opposite regioisomer. While, the high selectivity in electronically biased alkynes can be useful, the ability to form either regioisomer is highly desired, to both increase the scope of the reaction and to allow for late stage diversification in medicinal chemistry applications.

Scheme 3.11. Regioselectivity Goals

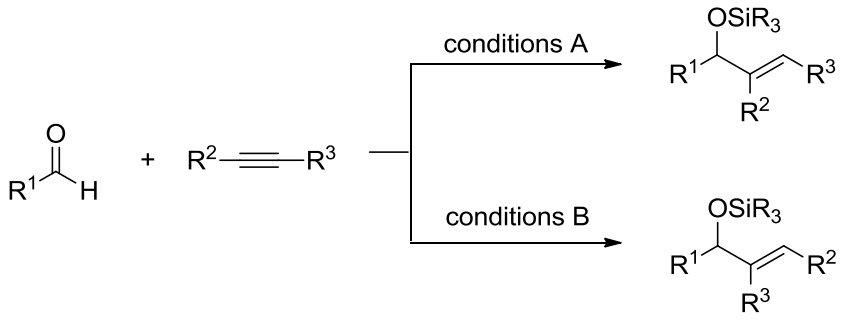

3.2.2 Initial Regioselectivity Hit

In our efforts to make a chiral ligand with *i*-Pr substitution in all ortho positions, ligand **L14** was synthesized. The yield of the *N*-arylation in this synthesis was only 5%, and at the time was not reproducible, so additional material could not be produced. Using the small amount of material that was product, the coupling reaction between benzaldehyde and phenylpropyne was screened, and produced the first reversal of selectivity we had observed with phenylpropyne in a 1.85:1 ratio (Scheme 3.12). This was a significant change in selectivity over what we had considered to be our "biggest" ligand, IPr which gave a 1.3:1 ratio favoring the electronically favored product.

Scheme 3.12. First Reversal in Regiochemistry of Phenylpropyne in Reductive Coupling Reaction

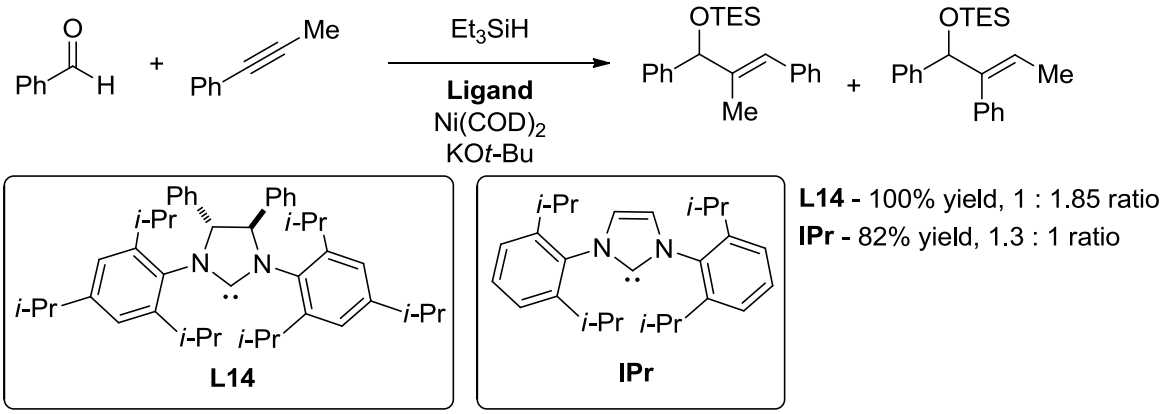

3.2.3 Ligand Synthesis

Due to our interest in controlling regioselectivity and the potential of our initial finding, we decided that it was imperative to make ligand **L14** on a larger scale. Because the *N*-arylation reaction involved in this synthesis was both low yielding and difficult to reproduce (though it was improved at a later time, see Chapter 4), we decided that a different synthesis was necessary to produce the large quantities that would be required for a thorough screen of reactivity, and for adaption beyond our lab (Scheme 3.13). We looked to an alternative diamine synthesis by Sigman, where a simple imine was homocoupled in a pinacol type reaction.[60] The synthesis was followed to produce both the meso and racemic compounds, which were separated from each other by

crystallization in methanol. First, the meso compound was subjected to standard cyclization conditions to produce the imidazolium salt, but only decomposition was observed. We then subjected the racemic product to standard cyclization conditions and found it cyclized well to make our carbene salt (+/-)-DP-IPr, a close analog to **L14** though it lacks the *i*-Pr's in the para positions of the *N*-aryl rings.

Scheme 3.13. Synthesis of (+/-)-DP-IPr via Pinacol-Type Coupling

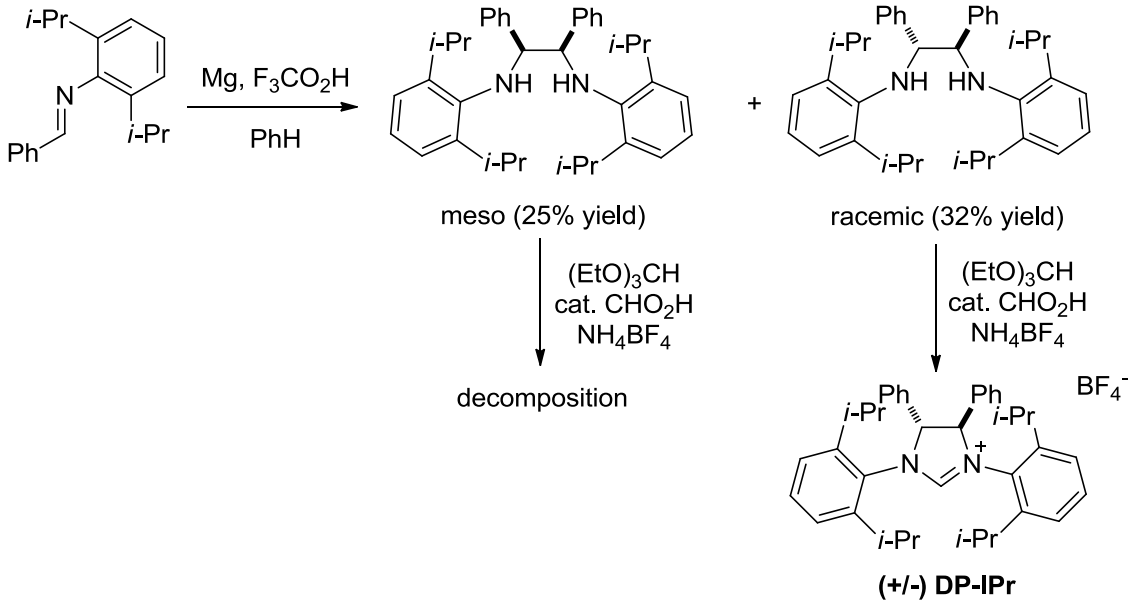

3.2.4 Ligand Screening

In collaboration with Hasnain Malik, a variety of known and new ligands were screened for regioselectivity. Overall, NHC ligands that had larger *ortho*-substituents on their *N*-aryl rings tended to show large ligand selectivity, while the ITol ligands with no *ortho*-substituents gave very high small ligand selectivity (Table 3.1). Both ITol and *i*-Pr-BAC provided small ligand selectivity for the coupling of 2-hexyne with heptaldehyde, though under the standard screening conditions the yields were very low. After optimization of base and silane, yields were improved to synthetically useful levels. It was observed that lower amounts of aldehyde hydrosilylation were produced using the $(t\text{-Bu})_2SiH_2$ for both of these ligands, which likely was responsible for the dramatic yield increases. With larger ligands it was observed that SIPr worked similar to (+/-)-DP-IPr for use on internal alkynes. It was found that the use of smaller silanes with (+/-)-DP-IPr, and BuLi as a base produced higher yields for the couplings of terminal alkynes (Table

3.2). It is likely that the σ-bond metathesis step is slower in the presence of both the bulky ligand and the bulky silane.

Table 3.1. Regioselective Ligand Screening

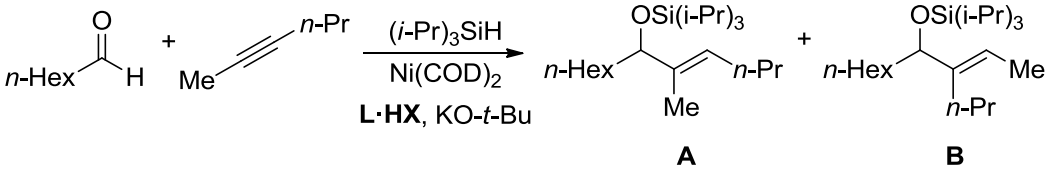

entry	ligand	ratio (**A**:**B**)	yield
1	ITol	87:13	18% (62% optimized)
2	*i*-Pr-BAC	86:14	29% (78% optimized)
3	L4	75:25	22%
4	IMes	67:33	83%
5	SIMes	61:39	73%
6	IAd	44:56	64%
7	$I_{Me,Cy}$	29:71	86%
8	IPr	20:80	84%
9	SIPr	7:93	85%
10	DP-IPr	6:94	69% (94% optimized)

L·HX =

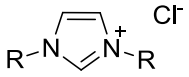

ITol R = *p*-tolyl
IMes R = mesityl
IAd R = adamantyl
IPr R = 2,6-di-isopropylphenyl

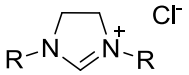

SIMes R = mesityl
SIPr R = 2,6-di-isopropylphenyl

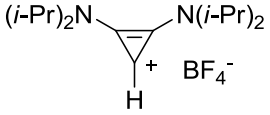

***i*-Pr-BAC**

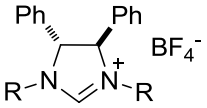

L4 R = 2-cyclohexylphenyl

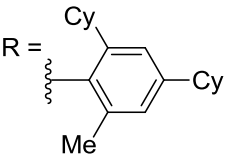

(+/-)-DP-IPr R =2,6-di-isopropylphenyl

Table 3.2. Yield Optimization of (+/-) DP-IPr

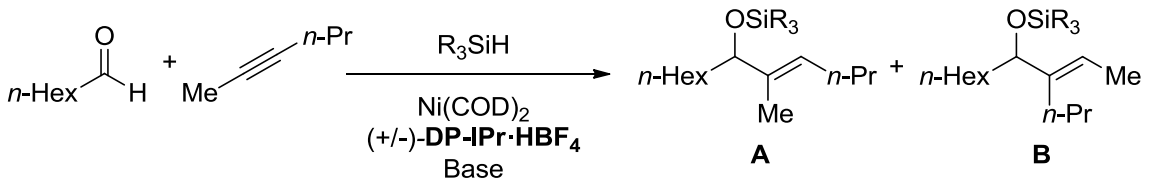

silane	base	ratio (**A**:**B**)	yield
Et_3SiH	*t*-BuOK	9:91	77%
Et_3SiH	BuLi	6:94	94%
i-Pr_3SiH	*t*-BuOK	6:94	69%

3.2.5 Regioselectivity Scope

We screened our smallest ligand *i*-Pr-BAC, both of our large ligands, SIPr and (+/-)-DP-IPr, as well as IMes and IPr to get a baseline understanding of that system's regioselectivity. These studies were conducted with 2-hexyne and a variety of aldehydes, and a small aldehyde effect on regiochemistry was observed (Entries 1-3, Table 3.3). When the steric difference between the two sides of the alkyne was increased by having branching on the more hindered side, the small ligand regioselectivity was enhanced to 97:3, while the large ligand selectivity was 10:90 (Entry 4). For compounds containing strong electronic biases, IMes functioned as a small ligand with high regioselectivity, so *i*-Pr-BAC was not screened (Entries 5-6). Use of SIPr allowed for the reversal of regioselectivity for both phenylpropyne and the conjugated enyne, indicating that our model was capable of reversing selectivity in some electronically biased systems.

Table 3.3. Regioselective Coupling of Internal Alkynes

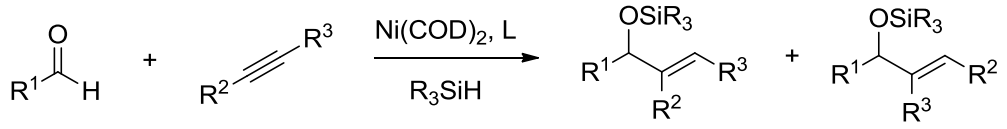

entry	R^1	R^2	R^3	ligand				
				i-Pr-BAC[a]	IMes[b]	IPr[b]	SIPr[b]	(+/-)DP-IPr[c]
1	*n*-Hex	Me	*n*-Pr	88:12 (78%)	67:33 (83%)	20:80 (84%)	7:93 (85%)	6:94 (94%)
2	*c*-Hex	Me	*n*-Pr	82:18 (75%)	62:38 (89%)	21:79 (83%)	5:95 (91%)	9:91 (96%)
3	Ph	Me	*n*-Pr	84:16 (72%)	67:33 (98%)	19:81 (95%)	2:>98 (86%)	2:>98 (95%)
4	Ph	Me	*i*-Pr	97:3 (85%)	76:24 (87%)	16:84 (93%)	10:90 (89%)	9:91 (66%)
5	Ph	Me	Ph	-	>98:2 (84%)	50:50 (81%)	19:81 (99%)	31:69 (96%)
6	*n*-Hex	Me	1-*c*-Hexene	-	97:3 (99%)	-	9:91 (77%)	9:91 (72%)

Reaction conditions employed:
[a] $Ni(COD)_2$, *i*-Pr-BAC, *n*-BuLi, $(t\text{-Bu})_2SiH_2$, THF
[b] $Ni(COD)_2$, NHC, *t*-BuOK, $(i\text{-Pr})_3SiH$, THF
[c] $Ni(COD)_2$, DP-IPr, *n*-BuLi, Et_3SiH, THF

Terminal alkynes are also quite electronically biased, with high selectivity for the trans-1,2 alkene when reductively coupled using IMes as a ligand (Table 3.4). Using IPr and SIPr as ligands, selectivity was poor across all examples indicating that (+/-)-DP-IPr is necessary to get strong stereochemical reversal. Using an aryl aldehyde, coupling with either terminal linear aliphatic alkynes or terminal propargylsilyl ethers afford high selectivities (entries 1-2). Using an aliphatic aldehyde coupled with either of these alkynes resulted in poor selectivity (entries 3-4), indicating that the aldehyde plays a key role in the selectivity of these reactions. This is expected as placing the larger group towards the aldehyde should cause a steric interaction that will be dependent on both

aldehyde size and geometry. Using a terminal alkyne with a branched aliphatic substitution led to exceptionally high selectivity for either product (entry 5).

Table 3.4. Regioselective Coupling of Terminal Alkynes

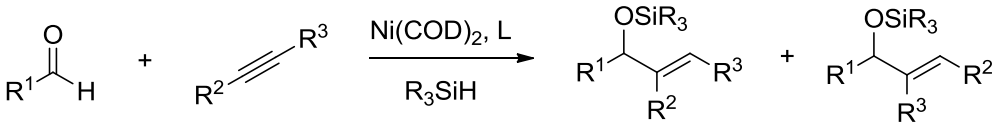

entry	R^1	R^2	R^3	ligand			
				IMes[a]	IPr[a]	SIPr[a]	(+/-)DP-IPr[b]
1	*n*-Hex	H	CH_2OTBS	>98:2 (86%)	65:35 (82%)	63:37 (75%)	28:72 (50%)
2	*n*-Hex	H	*n*-Hex	>98:2 (76%)	70:30 (87%)	69:31 (84%)	28:72 (84%)
3	Ph	H	CH_2OTBS	93:7 (88%)	50:50 (77%)	35:65 (43%)	15:85 (85%)
4	Ph	H	*n*-Hex	97:3 (82%)	55:45 (79%)	50:50 (63%)	12:88 (71%)
5	*n*-Hex	H	*i*-Pr	>98:2 (74%)	75:25 (72%)	59:41 (40%)	5:95 (76%)

Reaction conditions employed:
[a] $Ni(COD)_2$, NHC, *t*-BuOK, $(i\text{-Pr})_3SiH$, THF
[b] $Ni(COD)_2$, DP-IPr, *n*-BuLi, Et_3SiH, THF

Other aldehyde-alkyne combinations were also screened for their regioselectivity, though were not selective. When coupling phenylacetylene, the bulky ligand was completely unselective producing a 50:50 mixture of products (Entry 1, Table 3.5). Coupling of an alkynyl silane yielded the electronically biased product in all cases (Entry 2). The coupling of a branched aliphatic aldehyde with 1-octyne yielded slightly lower regioselectivity than that observed for linear aliphatic aldehydes (Entry 3). Coupling of phenyl propyne to heptaldehyde produced the product in a 25:75 ratio (Entry 4).

Table 3.5. Additional Regioselective Ligand Scope Screening

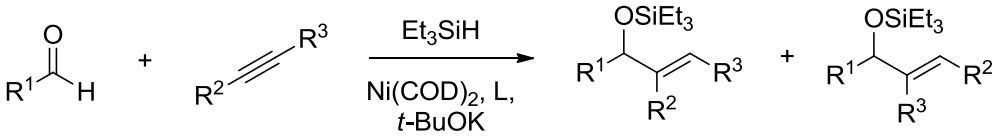

Entry	R^1	R^2	R^3	Ligand	
				IPr	(+/-)DP-IPr
1	*n*-Hex	H	Ph	95:5 (ND)	50:50 (ND)
2	*n*-Hex	$SiMe_3$	Me	>98:2 (71%)	>98:2 (80%)
3	Cy	H	*n*-Hex	92:8 (12%)[a]	36:64 (59%)
4	*n*-Hex	Me	Ph	55:45 (79%)	25:75 (95%)

[a]Unoptimized yield.

3.2.6 Modeling

In order to understand what interactions were leading to high regioselectivity, we began a collaboration with Ken Houk with the hopes of using that this understanding to allow us to design more selective ligands. Houk has been responsible for the computational modeling of a variety of systems, including the phosphine/Et_3B mediated nickel-catalyzed aldehyde-alkyne coupling, and therefore was well positioned to explore how our ligands were impacting regioselectivity.[69] We were excited to see that the computationally predicted regiochemistries for a variety of ligands were similar to those that we had observed experimentally (Table 3.6).

Table 3.6. Computational and Experimental Regioselectivities

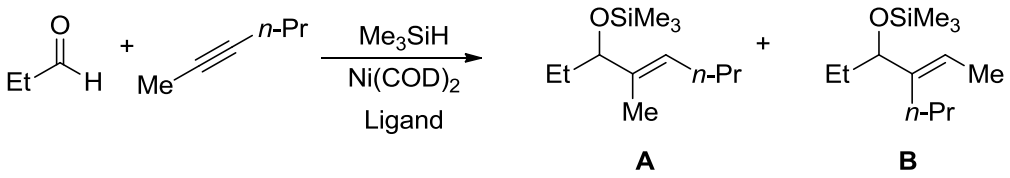

ligand	predicted ratio A:B	experimental ratio A:B[a]
IToL	79:21	87:13
i-Pr-BAC	64:36	86:14
IMes	57:43	67:33
SIMes	59:41	61:39
IAd	11:89	44:56
IPr	6:94	20:80
SIPr	4:96	7:93

[a]Using heptaldehyde and $(i\text{Pr})_3\text{SiH}$

Based on modeling, the *ortho*-substituents of the *N*-aryl rings interact directly with the alkyne, at both the first methylene and the second methylene (Figure 3.1, Figure 3.2). Interestingly, when IPr is used as a ligand, the distance between the *i*-Pr group and the second methylene is shorter (2.21 Å) than that of the *i*-Pr distance to the first methylene (2.51 Å), which could explain the high regioselectivity.

Figure 3.1. Small Ligand Interaction (B3LYP/LANL2DZ-6-31G* free energies)

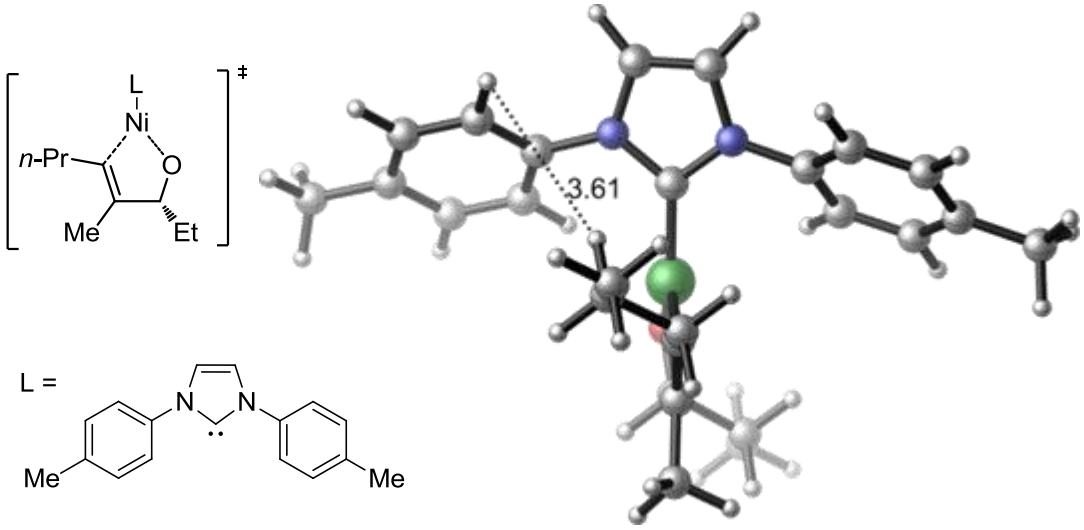

Figure 3.2. Large Ligand Interaction (B3LYP/LANL2DZ-6-31G* free energies)

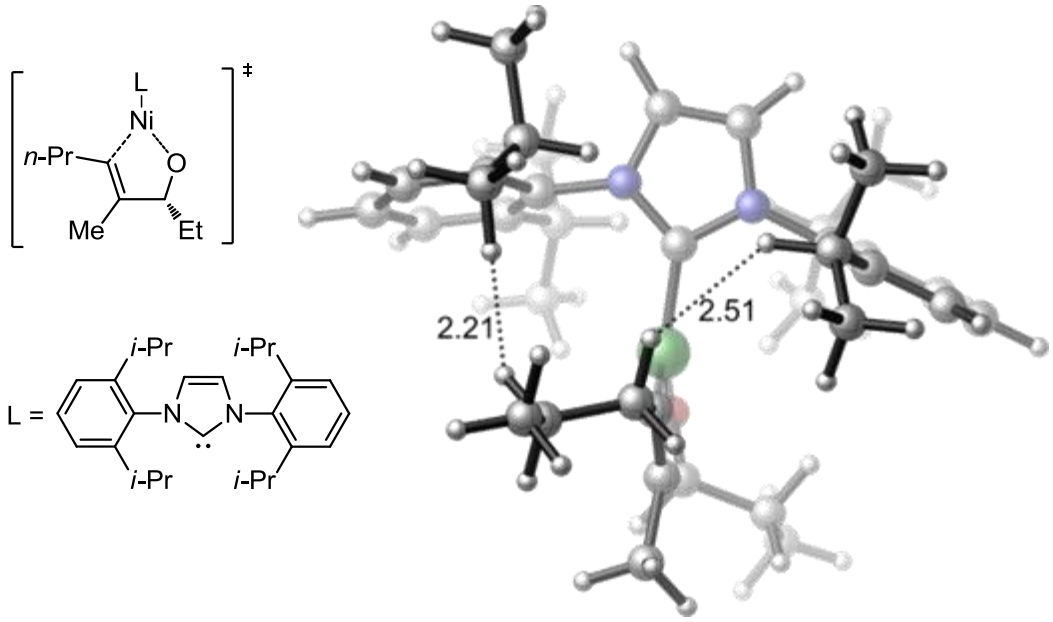

Based on the modeling of ITol, it is apparent that the aryl rings have a tilted conformational away from their typical horizontal orientation (Figure 3.3). This tilt creates an open pocket for the alkyne substituent that is oriented towards the ligand, reducing the steric interactions that lead to large ligand selectivity. The ring orientation indicates that in addition to the *ortho*-substitution of the *N*-aryl rings, the flexibility of the *N*-aryl rings plays a large role in the ability of a ligand to produce small ligand

regioselectivity. The *N*-aryl ring flexibility of ITol is in contrast to IPr, where the *N*-aryl rings are nearly horizontal (Figure 3.4). Here it is clear the *i*-Pr groups are positioned in the same space as the *n*-Pr of the alkyne, favoring the *n*-Pr to be oriented towards the aldehyde.

Figure 3.3. Small Ligand Conformation (B3LYP/LANL2DZ-6-31G* free energies)

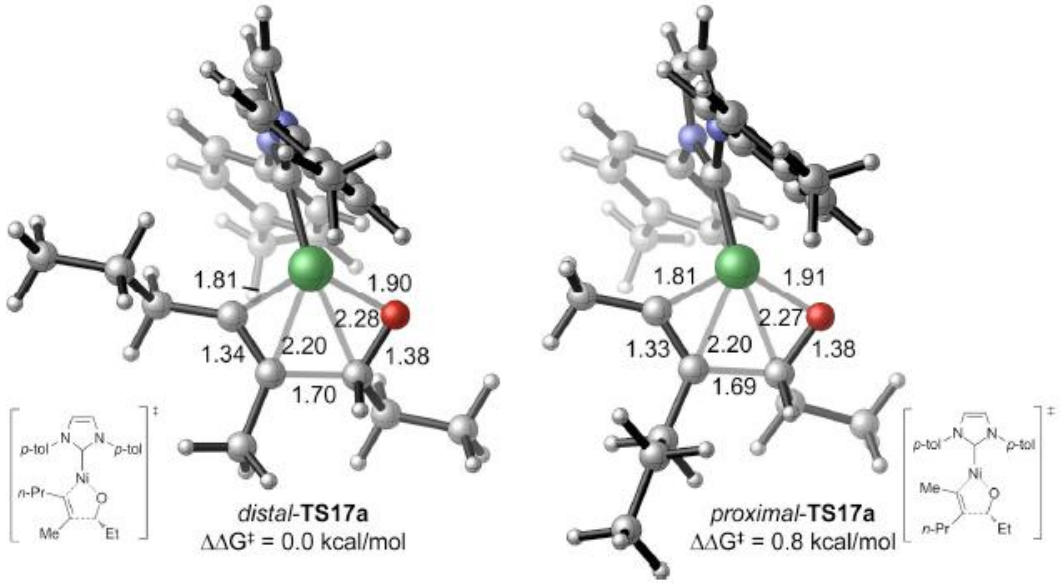

Figure 3.4. Large Ligand Conformation (B3LYP/LANL2DZ-6-31G* free energies)

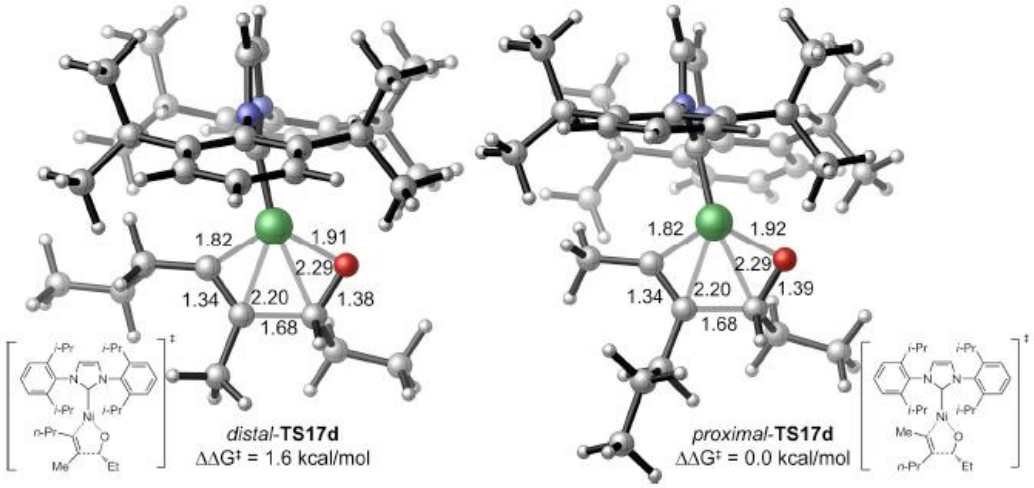

3.3 Conclusions

We have developed aldehyde-alkyne reductive coupling reactions that allow for ligand directed alkyne regioselectivity. Where other methodologies have utilized substrate bias and directing groups placed within the substrate,[65] we have developed conditions that can either allow those biases to control the regioselectivity, or reverse the selectivity to produce the opposite product using steric control. This methodology has shown strong reversal in a variety of internal alkynes, as well as terminal alkynes. While the regiocontrol in many cases was very high for either product, there is still room for improvement, as the coupling of terminal unbranched alkynes with aliphatic aldehydes is still limited to only 2.6:1 selectivity for the exo-methylene product. Ultimately, it is likely that the ligand capable of selectively reversing terminal alkyne regioselectivity in the more challenging cases will be unable to participate in couplings of internal alkynes, as that area of the binding pocket will be occupied. While the scope is not yet optimal, it is important to acknowledge that this advancement in regiocontrol is not only an advancement for the reductive couplings of aldehydes and alkynes, but rather a general advancement in the demonstration of ligand-based regiocontrol of π-systems.

Chapter 4

Enantioselective and Regioselective Nickel-Catalyzed Aldehyde-Alkyne Coupling

4.1 Background

4.1.1 Goal

As described in Chapter 2 and Chapter 3, we have developed methods to control either regiochemistry or stereochemistry, but ultimately we would like to control both of these variables simultaneously. While the NHK reaction could potentially provide each of these products, it requires selective alkenyl halide formation (Scheme 4.1). A stereoselective and regioselective aldehyde-alkyne coupling would allow for a mild coupling reaction directly from the alkyne (Scheme 4.2). In addition to this, it would allow for late stage diversification in synthesis from a single starting material.

Scheme 4.1. NHK Reaction in Product Diversification

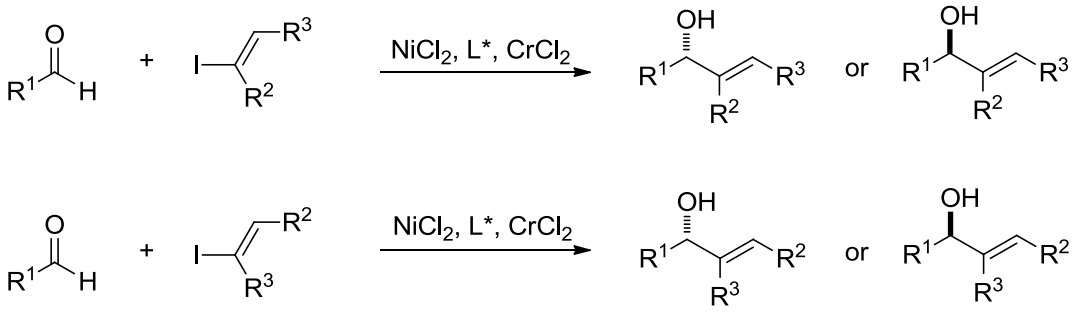

Scheme 4.2. Goal for the Regioselective and Enantioselective Reductive Couplings

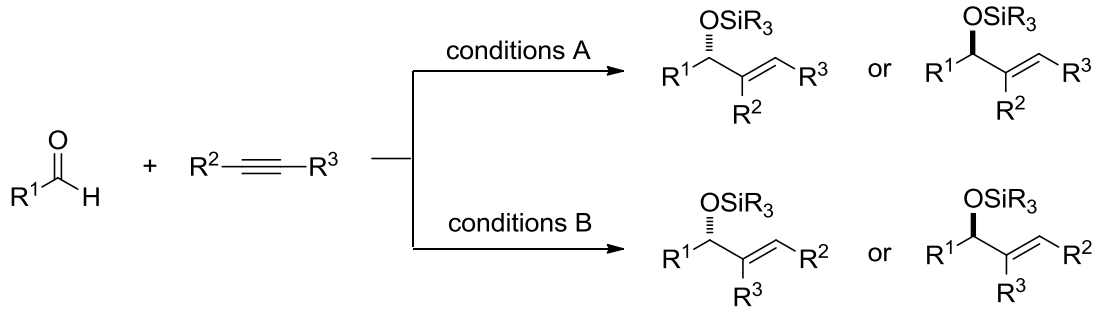

4.1.2 Precedent for Regioselective and Enantioselective Couplings

While working on enantioselectivity, the contrast between **L4** and $I_{Me,Cy}$ in the enantioselective couplings gave a good indication that this concept was achievable, as we had demonstrated a moderate level of regiocontrol, with good enantioselectivity (Scheme 4.3).[58] Because these levels of regiocontrol are far below that those observed in our regiocontrol study, we decided it pertinent to improve upon these ligands.

Scheme 4.3. Regioselectivity Switch in Enantioselective Coupling

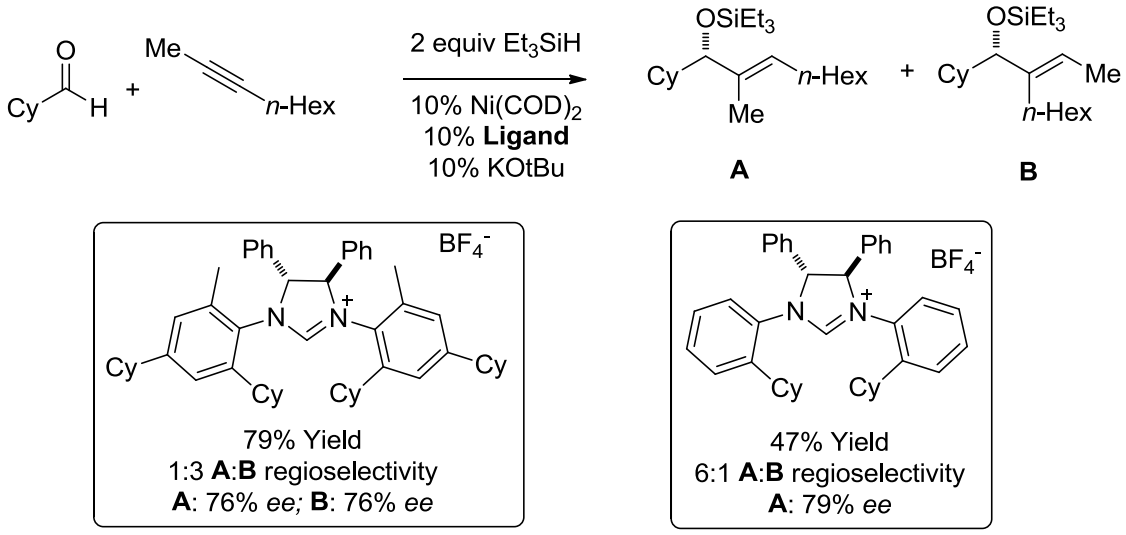

4.1.3 Modeling Insights

Through our collaboration with Houk, we have received some insights into the source of enantioselectivity in our reductive coupling reactions. Modeling a ligand with small sterics, containing both *ortho*-substitution and *meta*-substition, it was determined that both rings oriented their substituents away from the alkyne (Figure 4.1). An

interaction between the *meta*-substituent and the aldehyde was observed, indicating that stereochemistry could be directed by a meta substituent. Also, modeling implies that the meta position does not interact with the alkyne. Since, the meta substituent interacts with the aldehyde but not the alkyne, we believe that the can use the meta substituents to control enantioselectivity while maintaining small ligand regioselectivity.

Figure 4.1. Modeling of *meta*-Substitution on Enantioselectivity

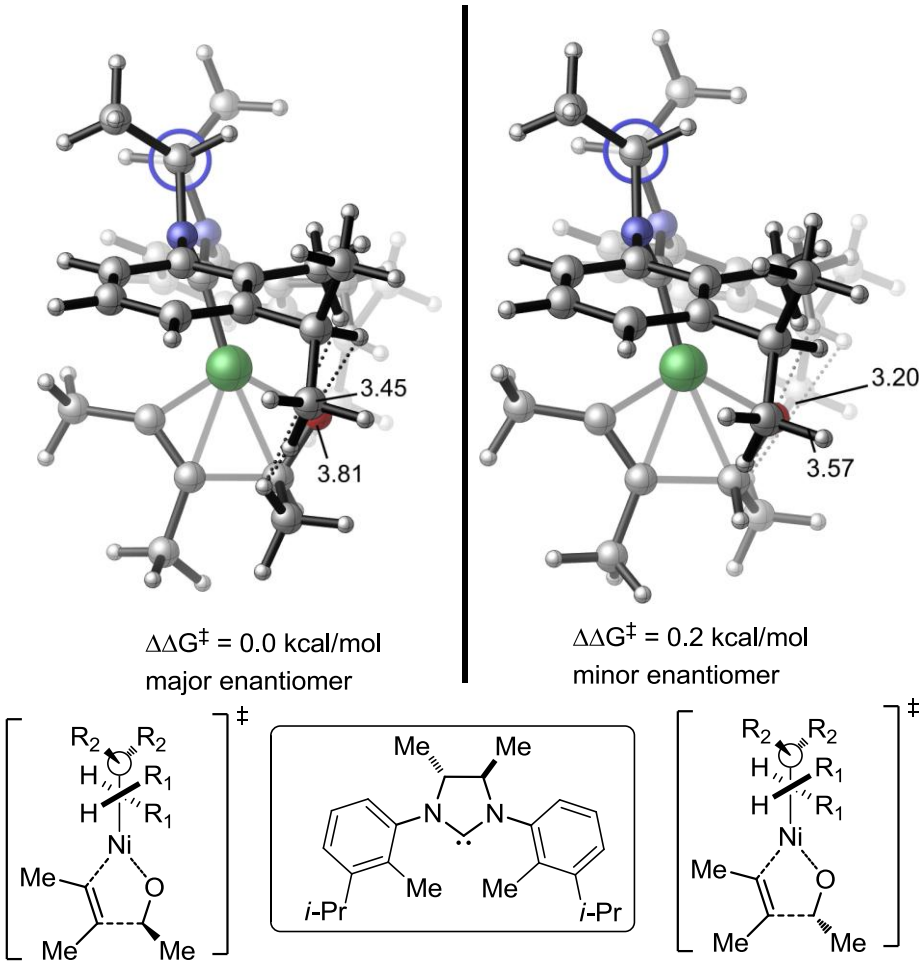

With the goal of understanding how large ligands will react with high enantioselectivity, a close analog to our DP-IPr ligand was modeled, with the backbone simplified from Ph to Me to reduce computational complexity (Figure 4.2). This example demonstrated that the *ortho* position of the NHC *N*-aryl rings can direct both stereochemistry and regiochemistry.

Figure 4.2. Large Ligand Modeled Regiocontrol and Enantiocontrol

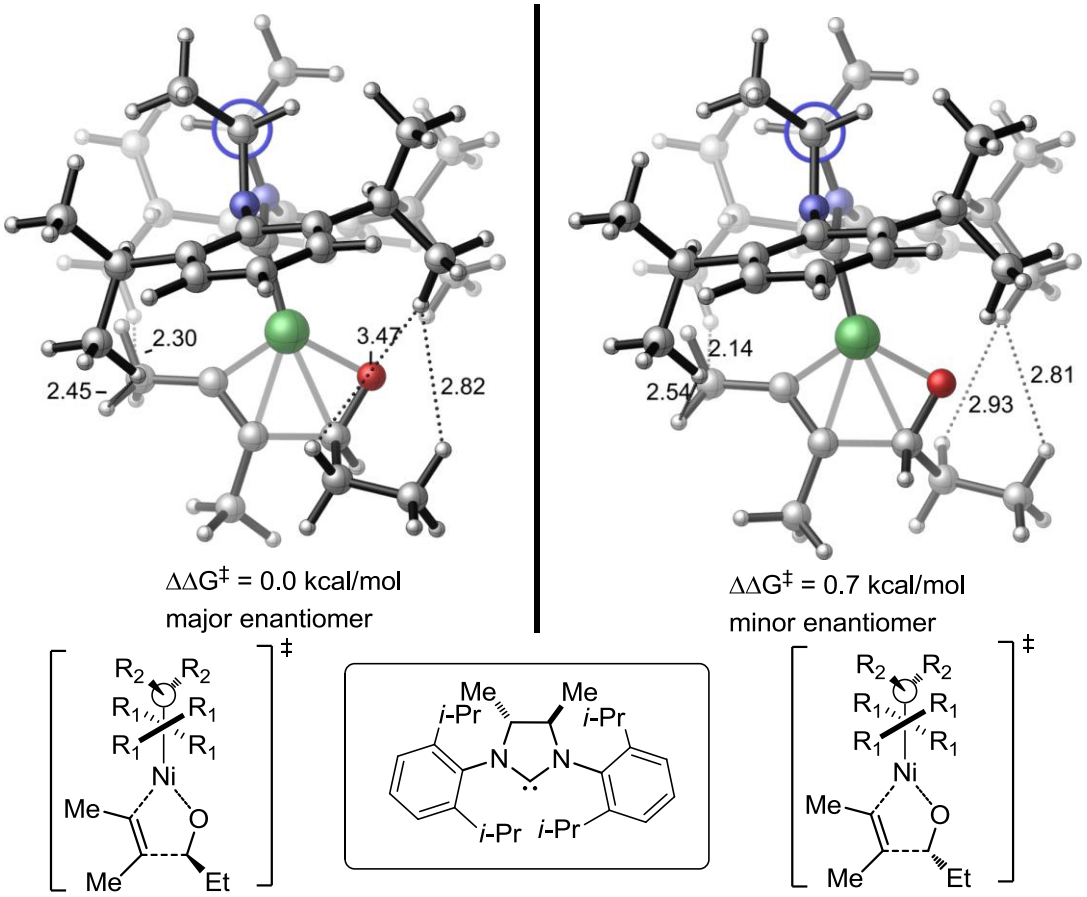

4.2 Ligand Screening

4.2.1 Ligand Synthesis

Hasnain Malik and I screened a variety of ligands we believed may produce high enantioselectivity and regioselectivity. My efforts focused on exploring additional substitution patterns on the 1,2-diphenyl backbone tha we had used previously,[58] and Hasnain Malik's efforts focused on new backbone substituents (Figure 4.3). The 1,2 diphenyl backbone ligands would allow for the exploration of the impact of *ortho*-substitution and *meta*-substitution patterns, while the C1-symmetric backbones allow for the synthesis of the ligands where both aryl rings can freely bend away from the alkyne, potentially allowing for larger substitution patterns to potentially produce smaller ligand selectivity.

Figure 4.3. General Ligand Structures for Regiocontrol and Enantiocontrol

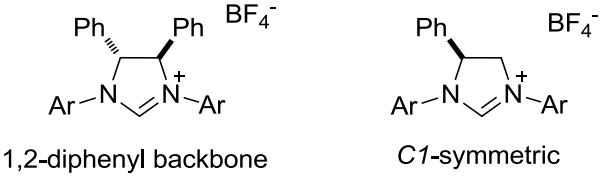

In general, ligands with little or moderate amounts of sterics in the *ortho* positions of the N-aryl rings synthesized with the 1,2-diphenyl backbone were produced via the same procedure used by Grubbs (Scheme 4.4). Using a bulkier aryl halide leads to reduced reactivity in the *N*-arylation step, and the aryl halide required to make a chiral variant of DP-IPr requires *i*-Pr in both *ortho*-positions. To accommodate this steric congestion, alternative conditions were used (Scheme 4.5). The reaction was run at the same catalyst loading required to make ligand **L14**, the temperature was increased and four equivalents of the aryl bromide were used as the solvent. This produced the desired diamine **A** in 17% yield, and the monosubstituted diamine **B** in 47% yield. Diamine **A** was then cyclized to produce **L14**, while the monosubstituted diamine **B** underwent an additional *N*-arylation reaction followed by cyclization to produce **L17** and **L18**.

Scheme 4.4. Synthesis of Small *C2*-Symmetric Ligands

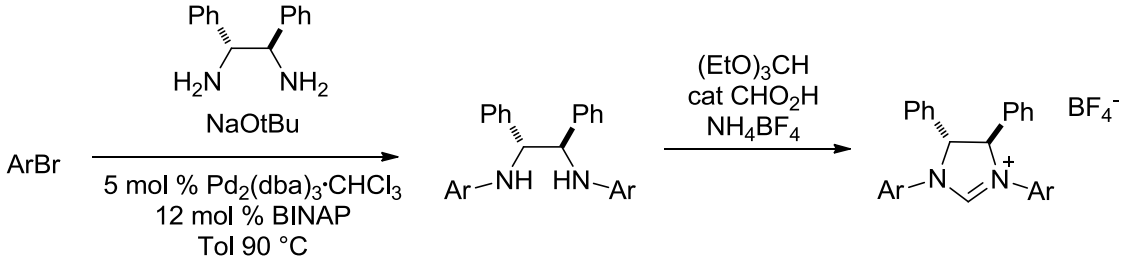

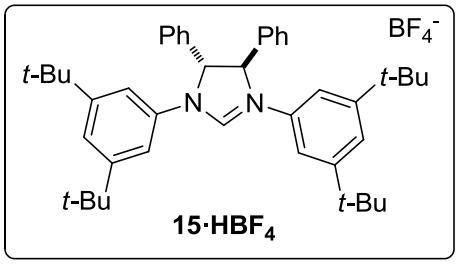

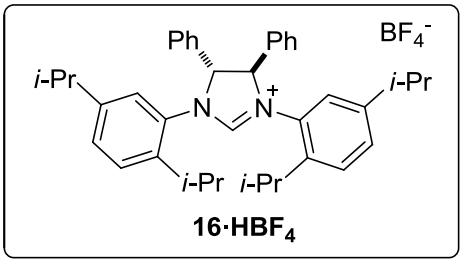

Scheme 4.5. Hindered Ligand Synthesis and *C1*-Symmetric Ligands

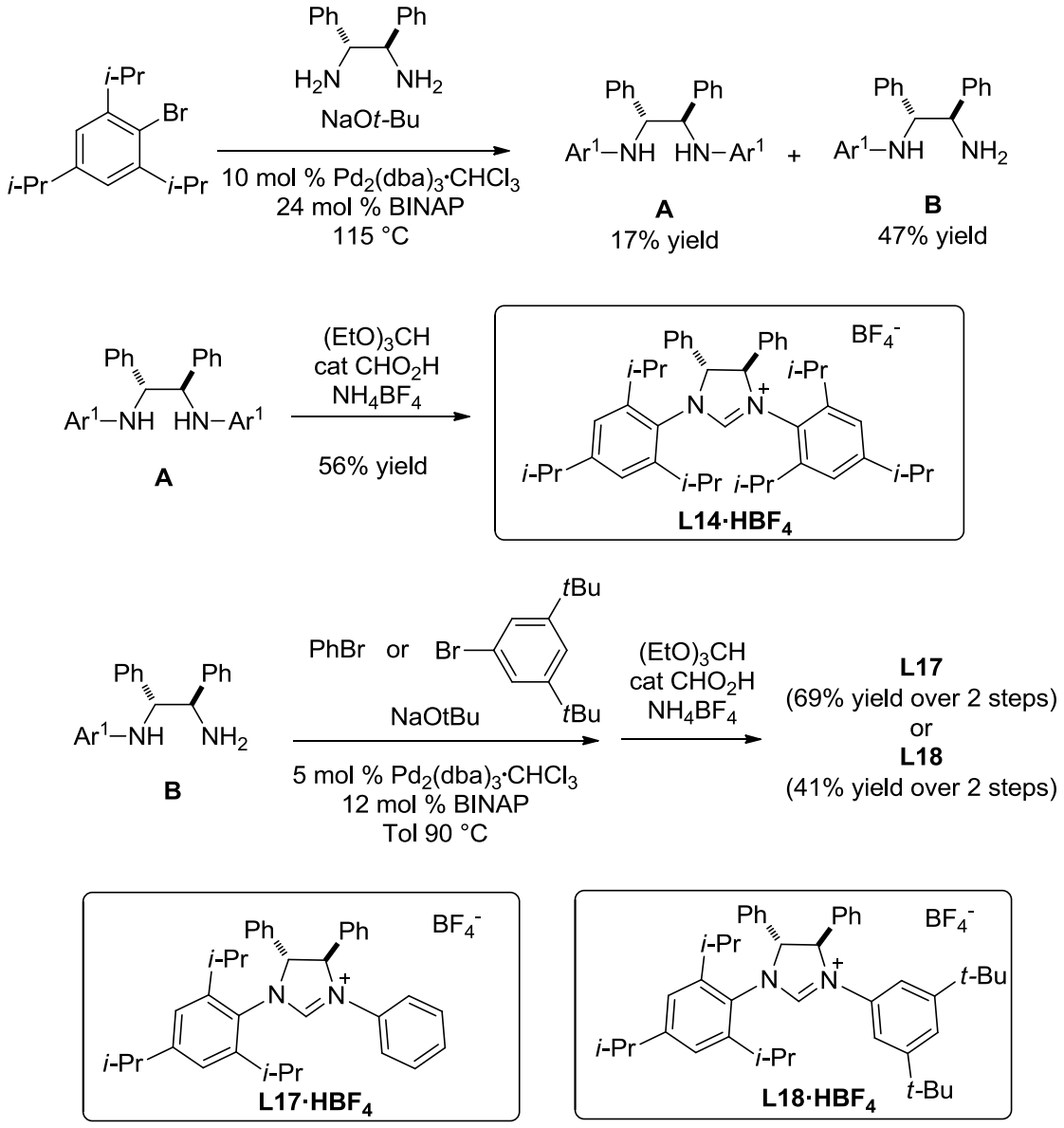

4.2.2 Ligand Reactivity

First we chose substrates for the screening that would produce a mixture of regioisomers and that possessed a UV active group for chiral HPLC detection. We decided that the product of the coupling of benzaldehyde and 2-hexyne was ideal since it portrayed a wide selectivity range in our regioselectivity studies.[68] A screen was done based on the reaction conditions that were optimal for the different silanes and bases we used in the aldehyde-alkyne coupling reactions. Based on this, we assumed these

conditions were sufficiently similar to each other that we could get a reasonable understanding of regioselectivities and enantioselectivities using conditions that were likely to be optimal for yields (Table 4.1)

Table 4.1. Variation of Regioselectivity and Enantioselectivity Based on Conditions

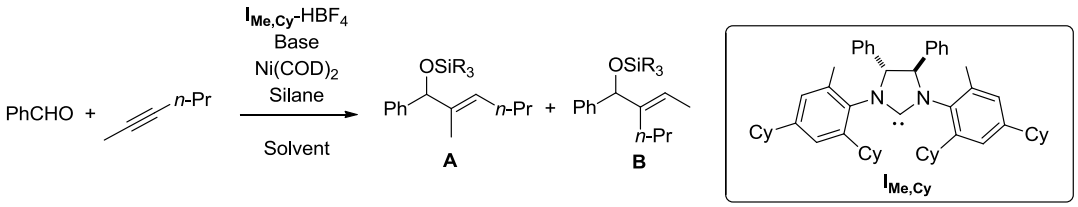

solvent	base	silane	yield	**A**:**B**	*ee* (**A**)	*ee* (**B**)
THF	*t*BuOK	Et_3SiH	77%	25:75	55%	55%
Tol	*t*BuOK	Et_3SiH	76%	28:72	56%	55%
THF	BuLi	Et_3SiH	84%	27:73	54%	61%
THF	*t*BuOK	iPr_3SiH	77%	27:73	46%	39%
THF	*t*BuOK	$(tBu)_2SiH_2$	62%	37:63	46%	54%

We then screened our ligands (Table 4.2) in the reductive coupling of benzaldehyde and 2-hexyne, in each case using the silane and base that we predicted would produce the highest yield. Ligand **14** provided high selectivity for regioisomer **B**, but provided low enantioselectivity for this regioisomer, while producing good enantioselectivity for regioisomer **A** (Entry 1). Ligand **L15** indicated that the *meta* position was indeed able to interact with the aldehyde while having no impact on the regioselectivity, matching our highest small ligand selectivity for this reaction. While it provided higher enantioselectivity than $\mathbf{I_{Me,Cy}}$, the yields were very low (Entry 2). Ligand **L16** with *ortho,meta*-disubstitution provided moderate regioselectivity, favoring **A**, while yielding moderate enantioselectivity (Entry 3). The *C1*-symmetric ligands (Entries 4-8) generally produced moderate to low enantioselectivity, and low yields with the exception of **L20**, which has the advantage of *ortho,ortho*-disubstitution on one ring. Ligand **L19** differed from ligand **L15** in that it contained a di-*t*-butyl backone instead of a diphenyl backbone; it produced moderate selectivity and yield (Entry 9).

Table 4.2. Ligand Screening for Regioselectivity and Enantioselectivity

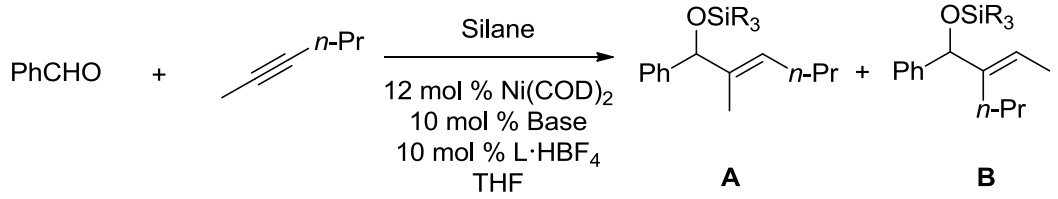

entry	ligand	silane	yield	**A**:**B**	*ee* (**A**)	*ee* (**B**)
1	**L14**	Et_3SiH	79%	5:95	75%	36%
2	**L15**	$(t\text{Bu})_2SiH_2$	10%	88:12	79%	73%
3	**L16**	$i\text{Pr}_3SiH$	Trace	80:20	42%	46%[a]
4	**L17**	Et_3SiH	12%	34:66	34%	32%
5	**L18**	Et_3SiH	16%	55:45	31%	16%
6	**L19**	$(t\text{Bu})_2SiH_2$	NR	-	-	-
7	**L20**	$(t\text{Bu})_2SiH_2$	55%	77:23	40%	18%
8	**L21**	$(t\text{Bu})_2SiH_2$	Trace	90:10	29%	54%
9	**L22**	$(t\text{Bu})_2SiH_2$	27%	86:14	64%	52%

[a]Opposite enantiomer was formed as major enantiomer.

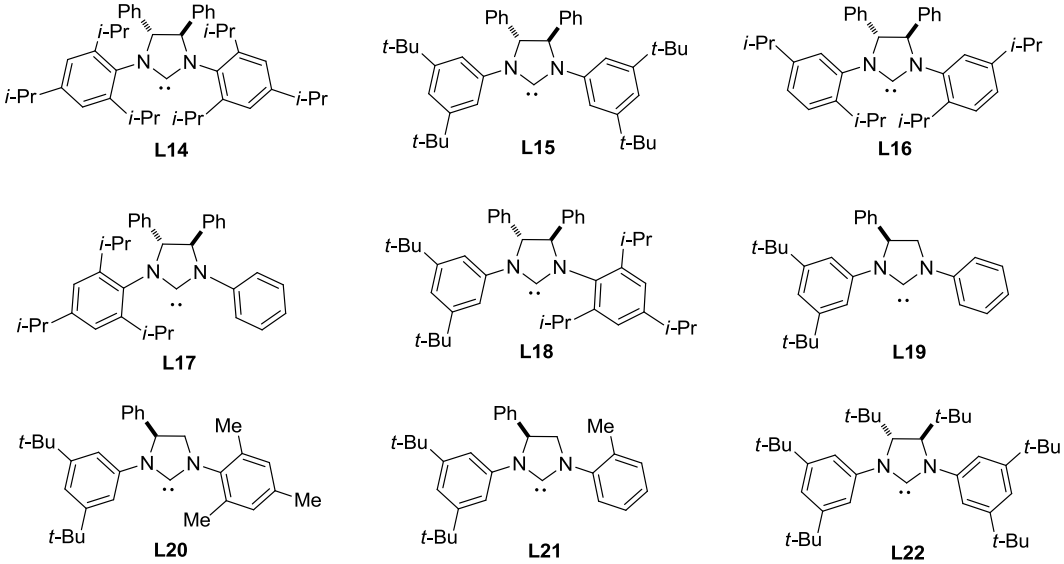

Due to the high yields and regioselectivity of ligand **L14** we decided it would be important to screen it against other substrate combinations (Scheme 4.6). Coupling a terminal alkyne with cyclohexylcarboxaldehyde provided a 50:50 mixture of regioisomers, with moderate enantioselectivity for the linear product and very low

enantioselectivity for the exomethylene product. Interestingly, the regioselectivity of this reaction differed from that when (+/-) DP-IPr was used, where the only structural difference is the para-isopropyls. This indicates that the para-group may interact with the substrates. There seemed to be a trend in enantioselectivity with respect to the size of the alkyne substituent facing the ligand in the transition state. We used 3-hexyne as the alkyne in the coupling reaction so an ethyl would face the ligand in the transition state, and found that it provides 72% *ee* when coupled to benzaldehyde (Scheme 4.7). Overall this supports the trend that larger alkyne substituents provide higher enantioselectivities for this ligand, which is troubling as it implies that enantiocontrol using *i*-Pr *ortho*-substituents will not be effective on any compounds where the small alkyne substituent is smaller than ethyl.

Scheme 4.6. Ligand **L14** Reactivity with Terminal Alkynes

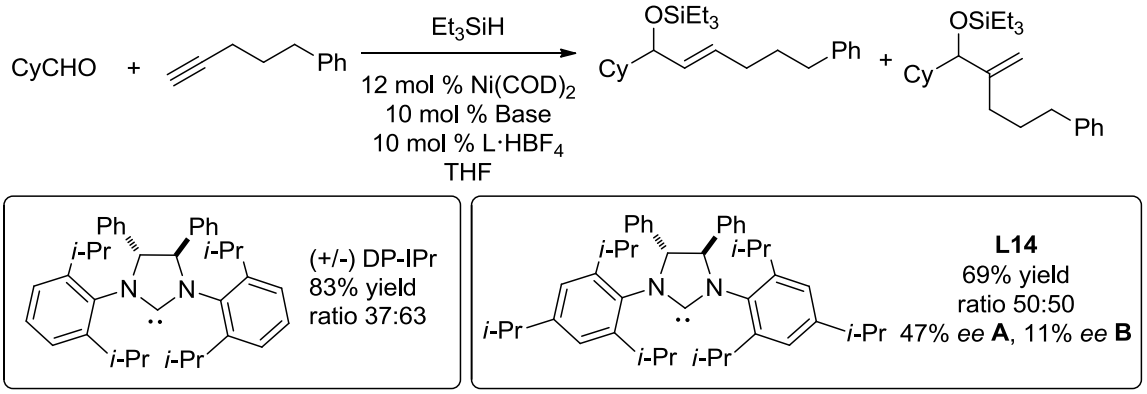

Scheme 4.7. Ligand **L14** Reactivity with 3-Hexyne

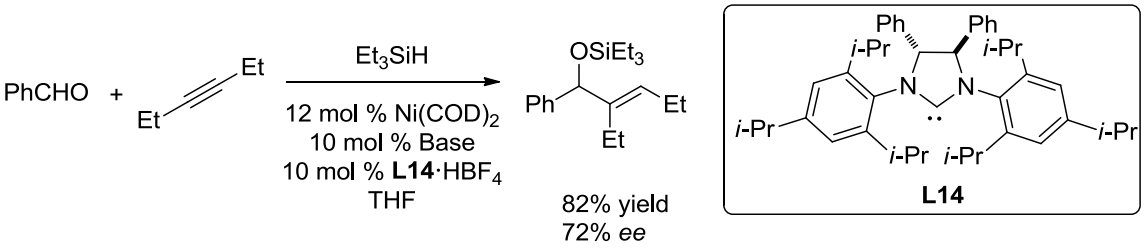

To showcase the regioselectivity and enantioselectivity of ligand **L14**, an alkyne was synthesized which contained ethyl as the sterically smaller group (Table 4.3). When this compound was coupled with (+/-)-DP-IPr the regioselectivity was 5:95 favoring the large ligand product **B**. Using chiral ligand **L14** the regioselectivity dropped slightly to

8:92, with 82% *ee* for the major product. Using our best small ligand **L16**, only trace yields were produced, but with >97:3 regiochemistry and 90% *ee*.

Table 4.3. Ligand **L14** and **L16** Reactivity with But-1-yn-1-ylcyclohexane

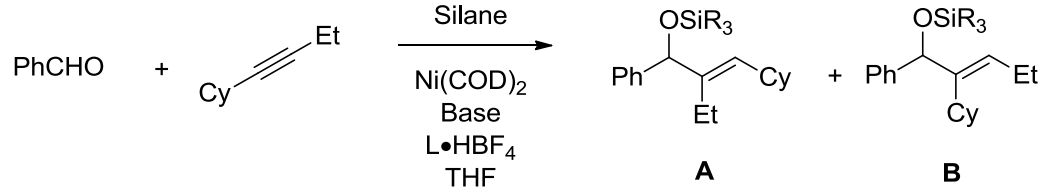

Entry	Ligand	Silane	Yield	**A**:**B**	*ee* (**A**)	*ee* (**B**)
1	(+/-)-DP-IPr	Et_3SiH	59%	5:95	-	-
2	**L14**	Et_3SiH	28%	8:92	ND	82%
3	IMes[a]	iPr_3SiH	75%	78:22	-	-
4	**L16**	iPr_3SiH	Trace	>97:3	90%	ND

[a]HCl Salt

4.3 Conclusions and Future Directions

We have developed a series of ligands that probes the opportunity to reverse regioselectivity using small and large ligands, while exhibiting enantiocontrol. The *meta*-position of the aromatic ring was shown to direct enantioselectivity without impacting regioselectivity, allowing for small enantioselective ligands. Interestingly we did find that the *para*-position was important as well, as it had a small impact on regioselectivity, while its impact on enantioselectivity is yet to be explored. Many of the observations made were in agreement with the computational modeling done by our collaborator Ken Houk, indicating that computation-directed ligand design is a valid strategy for this system.

Our best large ligand exhibited regioselectivity similar to our previous regioselectivity results, and for a limited set of alkynes also produced high enantioselectivity for a subset of alkynes. There are a variety of products, including the exomethylenes produced from a terminal alkyne, which still require new ligand design. It is likely that additional ligand screening, using groups such as *ortho*-cyclohexyls, or using compounds that have both *ortho* and *meta* substitution may lead to a more general large ligand (Figure 4.4). The biggest challenge to this process is the synthesis of these ligands, as the high amounts of steric congestion around the *N*-aryl bond hinders the *N*-

arylation reaction from occurring. Changing the backbone of the DP-IPr ligand from 1,2-diphenyl to 1,2-di(2,6-dimethylphenyl), may cause additional interaction with the *N*-aryl rings leading to higher regioselectivities and possibly enantioselectivities (Figure 4.5). The main advantage of this ligand is the fact that the precursor diamine has been made previously with reported chiral HPLC conditions, the disadvantage is that it is likely problematic to separate the enantiomers via crystallization.[60]

Figure 4.4. Future Chiral Large Ligand Designs

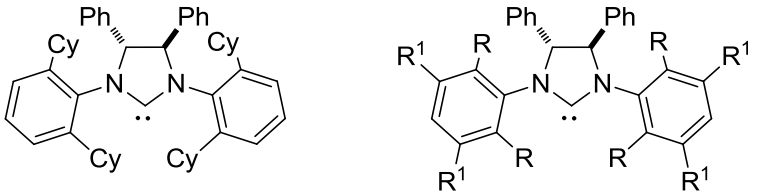

Figure 4.5. Future Bulky Ligand Design

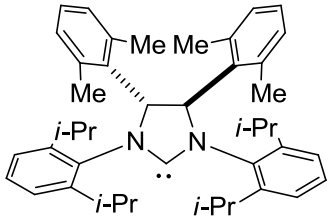

Our ability to control the enantioselectivity with a ligand (**L15**) that provides the small ligand product proved to be quite powerful. Unfortunately the yields are still very low, which means we need to explore optimization of ligand structure and reaction condition. These low yields could be the result of either side reactions or poor catalyst formation. While the side reactions can be minimized by careful silane choice and slow addition of reactants, alterations to the ligand structure may also be required to afford high yields. Alternatively, the ligand design may not be well suited for the catalyst generation by the methods we currently employ. Our lab has limited experience with alternative methods for catalyst formation for use in these couplings (Scheme 4.8). Catalyst formation by production of the free carbene in the presence of nickel(II) instead of nickel(0) may lead to higher nickel-NHC complex formation, which can then be reduced *in situ*.[70] Treatment of nickel with the free carbene or the carboxylate salt may also provide higher catalyst formation.[71] With the high regiochemistry and stereochemistry demonstrated, it is clear that this general system is worth optimizing.

Scheme 4.8. Alternative Methods of Catalyst Formation

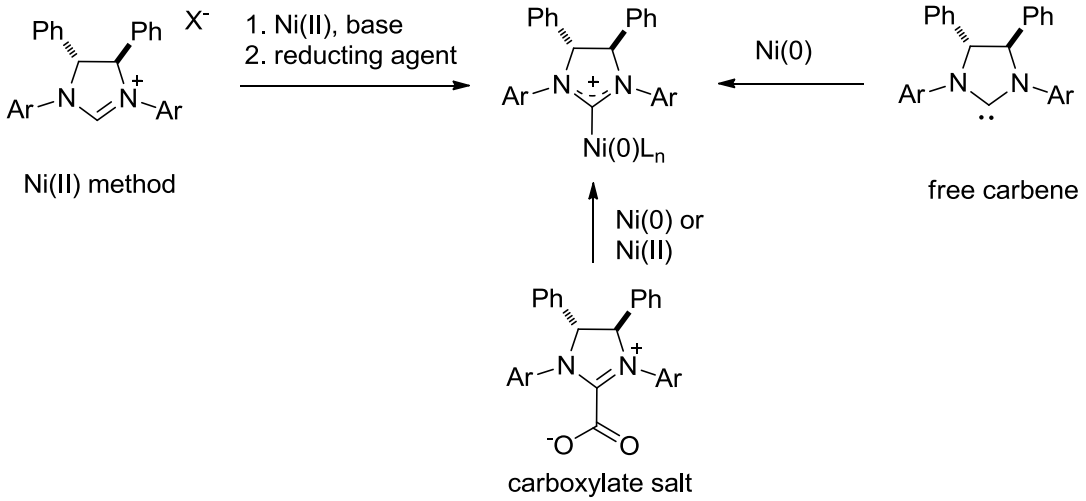

Chapter 5

Experimental

5.1 General Statement

All reagents were used as received unless otherwise noted. Solvents were purified under nitrogen using a solvent purification system (Innovative Technology, inc., Model # SPS-400-3 and PS-400-3. Aldehydes were distilled prior to use. $Ni(COD)_2$ (Strem Chemicals, Inc., used as received), 1,3-Bis(2,4,6-trimethyl-phenyl)imidazolium chloride (IMes·HCl), 1,3-Bis(2,6-di-*iso*-propylphenyl)imidazolium chloride (IPr·HCl), and potassium *tert*-butoxide were stored and weighed in an inert atmosphere glovebox. All reactions were conducted in flame-dried glassware under nitrogen atmosphere. 1H and 13C spectra were obtained in $CDCl_3$ at rt (25 ^oC), unless otherwise noted, on a Varian Mercury 400 or Varian Unity 500 MHz instrument. Chemical shifts of ^1H NMR spectra were recorded in parts per million (ppm) on the δ scale from an internal standard of residual chloroform (7.27 ppm). Chemical shifts of ^{13}C NMR spectra were recorded in ppm from the central peak of $CDCl_3$ (77.0 ppm) on the δ scale. High resolution mass spectra (HRMS) were obtained on a VG-70-250-s spectrometer manufactured by Micromass Corp. (Manchester UK) at the University of Michigan Mass Spectrometry Laboratory. Regioisomeric ratios were determined on crude reaction mixtures using NMR or GC. GC analyses were carried out on an HP 6890 Series GC System with an HP-5MS column (30m x 0.252mm x 0.25 μm). Chiral HPLC analyses were carried out using an Agilent Technologies 1100 series instrument and chiralcel OD-H column from Chiral Technologies Inc.

5.2 Chapter 2 Experimental

5.2.1 Ligands $I_{Me,Cy}$, L1 to L9

Ligands **L1**, **L2**, **L3**, **L5** and were prepared as described by reference 57. The preparation of Ligand **L8** is described in reference 63.

General procedure of the coupling of the chiral diamines and aryl bromide followed by cyclization

(*1R,2R*)-(+)-1,2-diphenylmethylenediamine (1.00 equiv), $Pd_2(dba)_3$•$CHCl_3$ (0.05 equiv), BINAP (0.12 equiv) and sodium tert-butoxide (3.00 equiv) were weighed in a flask with a stir bar in an oxygen free glove box and sealed with a rubber septum. A solution of the aryl bromide (2.4 equiv) in toluene (3 mL/mmol) was added to the mixture and heated at 90 °C under nitrogen (unless otherwise noted). The crude reaction mixture was filtered through celite washed with methylene chloride, concentrated and purified by column chromatography (SiO_2, 1:10 ethyl acetate/hexanes) to afford bis *N*-arylated products as soft pale yellow solids after the removal of solvents under high vacuum.

The bis-(aryl amine) was dissolved in triethyl orthoformate (10.0 equiv based on the starting diammines) followed by the addition of ammonium tetrafluoroborate (1.0 equiv) and catalytic (1 drop) formic acid. The mixture was heated under nitrogen atmosphere at 120 °C for 12 h. The crude reaction mixture was purified by column chromatography (SiO_2, 1:10 methanol/CH_2Cl_2) to afford 3,4-dihydroimidazolium tetrafluoroborate as hard foam pale yellow solids after removal of the solvents under high vacuum.

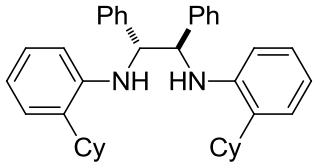

1*R*,2*R*-N^1,N^2-Bis(2-cyclohexylphenyl)-1,2-diphenylethane-1,2-diamine

Using the general procedure, (*1R,2R*)-(+)-1,2-diphenylmethylenediamine (212 mg, 1.00 mmol), 1-bromo-2-cyclohexylbenzene (526 mg, 2.20 mmol), $Pd_2(dba)_3$•$CHCl_3$ (52 mg, 0.05 mmol), racemic-BINAP (74 mg, 0.12 mmol) and sodium *tert*-butoxide (288 mg, 3.00 mmol) were employed to afford *1R,2R-*N^1,N^2-bis(2-cyclohexylphenyl)-1,2-diphenylethane-1,2-diamine (482 mg, 0.91 mmol, 91%) after column chromatography (SiO_2, 1:20 ethyl acetate/hexanes) as a light orange solid.

^{1}H NMR (400 MHz, $CDCl_3$) δ 7.52 (d, *J* = 8.0 Hz, 4H) 7.40 (t, *J* = 7.6 Hz, 4H) 7.28-7.34 (m, 2H) 7.11 (dd, *J* = 8.0, 1.6 Hz, 2H) 6.90 (td, *J* = 8.0, 1.6 Hz, 2H) 6.70 (td, *J* = 7.6, 1.2 Hz, 2H) 6.23 (d, *J* = 8.0 Hz, 2H) 4.80 (s, 2H) 4.66 (s, 2H) 2.44-2.51 (m, 2H) 2.15 (d, *J* = 11.2 H, 2H) 1.67 (d, *J* = 11.2 Hz, 2H) 1.82-2.05 (m, 8H) 1.30-1.56 (m, 12H).

^{13}C (125 MHz, $CDCl_3$) δ 143.6, 140.1, 132.2, 129.0, 127.8, 126.8, 126.4, 125.3, 117.8, 112.3, 63.9, 38.7, 32.9, 32.6, 27.5, 27.4, 26.5.

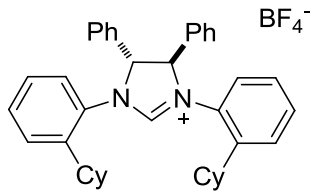

4*R*,5*R*-1,3-bis(2-cyclohexylphenyl)-4,5-dihydro-1H-imidazol-3-ium tetrafluoroborate (L4•HBF_4)

Following the general procedure, ammonium tetrafluoroborate (105 mg, 1.0 mmol), triethyl orthoformate (1.60 mL, 10.0 mmol) and 1 drop formic acid along with the crude *N*-arylated product were employed to afford pure *4R,5R*-1,3-bis(2-cyclohexylphenyl)-4,5-diphenyl-4,5-dihydro-1*H*-imidazol-3-ium tetrafluoroborate (520 mg, 0.83 mmol, 83% over 2 steps) after column chromatography (SiO_2, 1:20 methanol/methylene chloride) as a light yellow solid foam.

^{1}H NMR (400 MHz, $CDCl_3$) δ 8.32 (s, 1H) 7.54 (d, *J* = 7.6 Hz, 2H) 7.11-7.46 (m, 16H) 5.67 (s, 2H) 2.61-2.72 (m, 2H) 1.65-1.98 (m, 8H) 1.28-1.55 (m, 8H) 1.20-1.28 (m, 4H).

^{13}C (125 MHz, $CDCl_3$) δ 157.4, 143.5, 133.8, 130.8, 130.6, 130.4, 129.7, 128.5, 128.1, 127.7, 127.6, 77.2, 39.5, 34.8, 34.0, 27.1, 27.0, 25.7.

HRMS (EI) m/*z* calculated for $[M]^+$ 539.3426, found 539.3430.

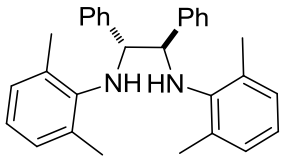

1*R*,2*R*-N^1,N^2-bis(2,6-dimethylphenyl)-1,2-diphenylethane-1,2-diamine

Using the general procedure, (*1R,2R*)-(+)-1,2-diphenylmethylenediamine (106 mg, 0.50 mmol), 2-bromo-1,3-dimethylbenzene (222 mg, 1.20 mmol), $Pd_2(dba)_3$•$CHCl_3$ (26 mg, 0.025 mmol), BINAP (37 mg, 0.06 mmol) and sodium *tert*-butoxide (144 mg, 3.00 mmol) were employed to afford 1*R*,2*R*-N^1,N^2-bis(2,6-dimethylphenyl)-1,2-diphenylethane-1,2-diamine (180 mg, 0.43 mmol, 86%) after column chromatography (SiO_2, 1:20 ethyl acetate/hexanes) as a light yellow solid.

^{1}H NMR (400 MHz, $CDCl_3$) δ 7.06-7.12 (m, 6H), 6.91-6.95 (m, 4H), 6.82 (d, *J* = 7.2 Hz, 4H), 6.65 (t, *J* = 7.2 Hz, 2H), 4.83 (s, 2H), 4.02 (bs, 2H), 2.09 (s, 12H).

^{13}C (125 MHz, $CDCl_3$) δ 144.2, 140.3, 129.1, 128.3, 128.0, 127.7, 127.2, 120.9, 66.1, 19.5.

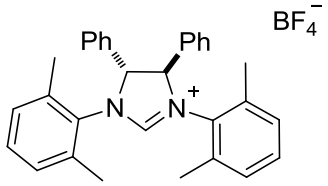

4*R*,5*R*-1,3-Bis(2,6-dimethylphenyl)-4,5-diphenyl-4,5-dihydro-1*H*-imidazol-3-ium tetrafluoroborate (L6•HBF_4)

Following the general procedure, ammonium tetrafluoroborate (53 mg, 0.50 mmol), triethyl orthoformate (0.83 mL, 10.00 mmol) and 1 drop formic acid along with the crude *N*-arylated product were employed to afford pure *4R,5R*-1,3-bis(2,6-dimethylphenyl)-4,5-diphenyl-4,5-dihydro-1*H*-imidazol-3-ium tetrafluoroborate (199 mg, 0.39 mmol, 77% over 2 steps) after column chromatography (SiO_2, 1:10 methanol/methylene chloride) as light yellow solid foam after.

^{1}H NMR (500 MHz, $CDCl_3$) δ 8.63 (s, 1H), 7.25-7.35 (m, 10H), 7.05-7.15 (m, 4H), 6.86 (t, *J* = 4.0 Hz, 2H), 6.01 (s, 2H), 2.66 (s, 6H), 1.92 (s, 6H).

^{13}C (125 MHz, $CDCl_3$) δ 157.9, 136.5, 134.7, 131.1, 131.0, 130.8, 130.3, 129.4, 128.8, 72.7, 19.0, 18.2.

HRMS (EI) m/z calculated for $[M]^+$ 431.2487, found 431.2385.

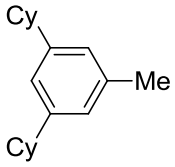

3,5-Dicyclohexyl toluene

A solution of aluminum chloride (3.266 g, 24.5 mmol) in toluene (1.078 g, 11.7 mmol) was cooled to 0 °C. Cyclohexyl bromide (4.006 g, 24.5 mmol) was added dropwise. The reaction was stirred for 45 min, warming to rt. The reaction was then quenched with 15 mL ice, and diluted with 25 mL ether. The layers were separated, and the ether layer was washed twice with 10 mL water and 10 mL brine. The organic layer was then dried with

$MgSO_4$, filtered and concentrated to afford 3,5-dicyclohexyl toluene after column chromatography (SiO_2, hexanes) as a colorless oil (2.344 g, 9.14 mmol, 78 %).

^{1}H NMR (CDCl3, 400 MHz) δ 6.85 (s, 3H), 2.43 (m, 2H), 2.31 (s, 3H), 1.80 (m, 8H), 1.69 (m, 2H), 1.35 (m, 8H), 1.21 (m, 2H).

13C NMR (CDCl3, 100 MHz) δ 148.0, 137.5, 125.1, 122.6, 44.6, 34.5, 27.0, 26.2, 21.5;

IR (thin film, KBr, cm-1) 3017, 2924, 2850, 1601, 1447, 847, 707.

HRMS (ES+) calculated for $C_{19}H_{28}$ [M]+ 256.2191, found 256.2196.

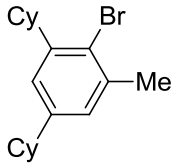

2-Bromo-3,5-dicyclohexyl toluene

3,5-dicyclohexyltoluene (0.6441 g, 2.512 mmol) was dissolved in 0.75 mL of chloroform and cooled to 0 °C. Bromine (0.4014 g, 2.512 mmol) was added slowly over 15 min. The solution was allowed to warm to rt, then stirred for 16 h. The reaction was diluted with 5 mL dichloromethane, which was washed with water. The water layer was extracted with dichloromethane twice and organics were combined and washed with 5 mL 10% NaOH, then brine, then dried with MgSO4, filtered and concentrated to afford a mixture of isomers (85:15), 2-bromo-3,5-dicyclohexyl toluene and 4-bromo-3,5-dicyclohexyltoluene, as a colorless oil (0.6002 g, 1.78 mmol, 71 %) after column chromatography (SiO2/hexanes). The minor isomer does not undergo *N*-arylation in the following step based on recovery of starting material.

1H NMR (CDCl3, 400 MHz) δ 6.88-6.90 (m, 2Hmajor), 6.87 (s, 2Hminor), 3.00-3.09 (m, 1Hmajor + 2Hminor), 2.39-2.43 (m, 4Hmajor), 2.22 (s, 3Hminor), 1.50-1.90 (m, 10H), 1.20-1.45 (m, 10H).

13C NMR (CDCl3, 100 MHz) δ 146.7, 146.3, 137.9, 136.6 (minor isomer), 126.8, 125.6 (minor isomer), 124.2, 123.2, 44.2, 44.0 (minor isomer), 43.7, 34.4, 33.4, 26.9, 26.8, 26.3, 26.1, 24.4.

IR (thin film, KBr, cm-1) 2924, 2850, 1461, 1447, 1017, 857;

HRMS (ES+) calculated for $C_{19}H_{27}Br$ [M]+ 334.1296, found: 334.1287.

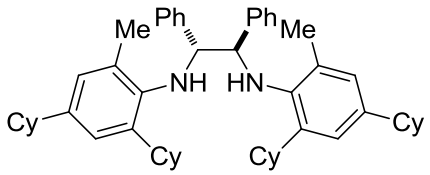

1*R*,2*R*-*N*^{1},*N*^{2}-bis(2,4-dicyclohexyl-6-methylphenyl)-1,2-diphenylethane-1,2-diamine

Following the general procedure, (*1R,2R*)-(+)-1,2-diphenylmethylenediamine (212 mg, 1.00 mmol), 2-bromo-3,5-dicyclohexyltoluene (801 mg, 2.40 mmol), $Pd_2(dba)_3$•$CHCl_3$ (104 mg, 0.10 mmol), BINAP (148 mg, 0.24 mmol) and sodium *tert*-butoxide (288 mg, 3.00 mmol) and tol (0.6 mL) were heated at 110 °C to afford *1R,2R*-*N*^{1},*N*^{2}-bis(2,4-dicyclohexyl-6-methylphenyl)-1,2-diphenylethane-1,2-diamine (598 mg, 0.83 mmol, 83%) after column chromatography (SiO_2, 1:20 ethyl acetate/hexanes) as a light orange solid.

^{1}H NMR (400 MHz, $CDCl_3$) δ 6.90-7.10 (m, 10H), 6.79 (s, 2H), 6.68 (s, 2H), 4.50 (s, 2H), 4.04 (bs, 2H), 2.81-2.92 (m, 2H), 2.28-2.36 (m, 2H), 2.03 (s, 6H), 1.58-1.83 (m, 20H), 1.10-1.39 (m, 20H).

^{13}C (125 MHz, $CDCl_3$) δ 142.4, 141.4, 140.8, 140.7, 131.4, 128.5, 127.7, 126.8, 126.5, 123.2, 68.0, 44.0, 38.0, 35.0, 34.5, 33.9, 27.2, 27.0, 26.7, 26.3, 26.2, 19.5.

HRMS (EI) m/*z* calculated for $[M+H]^+$ 721.5461, found 721.5468.

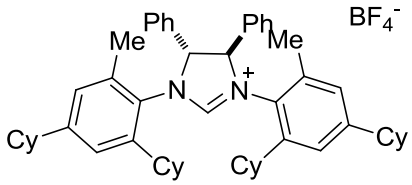

4*R*,5*R*-1,3-bis(2,4-dicyclohexyl-6-methylphenyl)-4,5-diphenyl-4,5-dihydro-1*H*-imidazol-3-iumtetrafluoroborate ($I_{Me,Cy}$•HBF_4)

Following the general procedure, ammonium tetrafluoroborate (105 mg, 1.00 mmol), triethyl orthoformate (1.66 mL, 10 mmol) and 1 drop formic acid along with the crude *N*-arylated product were employed to afford pure *4R,5R*-1,3-bis(2,4-dicyclohexyl-6-methylphenyl)-4,5-diphenyl-4,5-dihydro-1*H*-imidazol-3-iumtetrafluoroborate (581 mg, 0.71 mmol, 71% over 2 steps) after column chromatography (SiO_2, 1:20 methanol: methylene chloride) as light yellow foam.

^{1}H NMR (400 MHz, $CDCl_3$) δ 8.70 (s, 0.17H), 8.37 (s, 0.33H), 8.00 (s, 0.50H) (correspond to the three rotamers of a single proton), 6.70-7.26 (m, 14H), 6.11 (s, 1.00H), 5.97 (d, *J* = 10.4 Hz, 0.33H), 5.85 (d, *J* = 10.4 Hz, 0.33H), 5.78 (s, 0.33H) (correspond to three rotamers of two protons of the nitrogen heterocycle), 2.79-2.95 (m, 1H), 2.65-2.78 (m, 3H), 1.05-2.45 (m, 46H).

^{13}C (125 MHz, $CDCl_3$) (due to existence of three rotamers, ^{13}C NMR spectrum appeared complex) δ 157.3, 156.7, 151.1, 150.7, 150.5, 145.9, 145.2, 144.1, 143.8, 134.2, 130.7, 129.8, 129.6, 129.4, 129.3, 129.2, 128.9, 128.8, 127.9, 126.9, 124.1, 75.0, 72.7, 72.2, 44.3, 44.2, 44.2, 40.4, 40.3, 39.6, 35.9, 34.1, 34.0, 33.9, 32.6, 31.9, 27.0, 26.8, 26.7, 26.6, 26.5, 25.9, 25.7, 19.6, 18.8, 18.6, 18.3.

HRMS (EI) m/*z* calculated for $[M]^+$ 731.5304, found 731.5306.

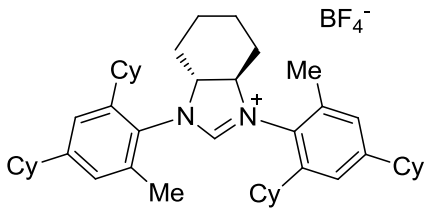

(*3aR,7aR*)-1,3-bis(2,4-dicyclohexyl-6-methylphenyl)-3a,4,5,6,7,7a-hexahydro-1H-benzo[d]imidazol-3-ium tetrafluoroborate (L7)

(*1R,2R*)-(+)-1,2-Diaminocyclohexane (46 mg, 0.40 mmol), 2-bromo-3,5-dicyclohexyltoluene (402 mg, 1.20 mmol), $Pd_2(dba)_3$•$CHCl_3$ (41 mg, 0.04 mmol), BINAP (60.3 mg, 0.10 mmol) and sodium *tert*-butoxide (288 mg, 3.00 mmol), and 1.0 mL of toluene were heated at 110 °C for 24 h to afford the diamine (144 mg, 0.23 mmol, 58 %) as a solid after a celite plug (washed with CH_2Cl_2) and column chromatography (SiO_2, 1:50 ethyl acetate/hexanes, rf = 0.45 in 1:20 ethyl acetate/hexanes). The diamine (94 mg, 0.15 mmol) was then heated to 120 ˚C for 20 h with formic acid (1 drop), triethyl orthoformate (179 mg, 1.2 mmol) and ammonium tetrafluoroborate (15.7 mg, 0.15 mmol). The resulting crude mixture was then concentrated, followed by column chromatography (SiO_2, 1:20 methanol/CH_2Cl_2, rf = 0.2). The imidazolium salt (102 mg, 94% yield) was then dried under vacuum at 50 ˚C for 12 h.

^{1}H (400 MHz, $CDCl_3$) (due to the existence of multiple rotamers, spectra appeared complex) δ 8.23 (s, 0.38H), 8.17 (s, 0.38H), 8.00-7.96 (m, 0.23H) 7.02-6.94 (m, 5H), 4.15-3.72 (m, 2H), 2.74-2.66 (m, 2H), 2.48-1.18 (m, 55H).

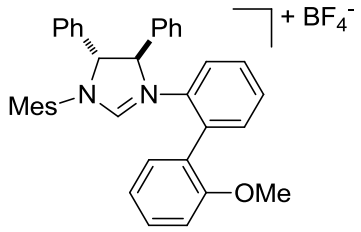

(*4R,5R*)-1-mesityl-3-(2'-methoxy-[1,1'-biphenyl]-2-yl)-4,5-diphenyl-4,5-dihydro-1H-imidazol-3-ium tetrafluoroborate (L9)

(*1R,2R*)-N^1-mesityl-N^2-(2'-methoxy-[1,1'-biphenyl]-2-yl)-1,2-diphenylethane-1,2-diamine (reference 63) (100 mg, 0.20 mmol) was heated to 100 ˚C for 16 h with formic acid (1 drop), triethyl orthoformate (231 mg, 1.56 mmol) and ammonium tetrafluoroborate (20.3 mg, 0.20 mmol). The resulting crude mixture was then concentrated, followed by column chromatography (SiO_2, 1:20 methanol/CH_2Cl_2, rf = 0.3 in 10% methanol/ CH_2Cl_2). The imidazolium salt (115 mg, 96% yield) was then dried under vacuum at 50 ˚C for 12 h.

1H (500 MHz, mixture of 2 atropisomers, $CDCl_3$) δ 8.72 (s, 0.66 H), 8.61 (s, 0.33 H), 7.98 (dd, *J* = 8.5 Hz, 1.5 Hz, 0.66 H), 7.72-7.64 (m, 1 H), 7.48-7.14 (m, 14.5 H), 6.96 (bs, 0.66 H), 6.91 (bs, 0.33 H), 6.8-6.2 (m, 1.5 H), 6.51 (d, *J* = 7.5 Hz, 1.33 H), 5.58 (d, *J* = 7.5 Hz, 0.33 H), 5.40 (d, *J* = 7.5 Hz, 0.33 H), 5.36 (s, 1 H), 3.818 (s, 1 H), 3.76 (s, 2 H), 2.61 (s, 2 H), 2.49 (s, 1 H), 2.21 (s, 2 H), 2.20 (s, 1 H), 1.70 (s, 2 H), 1.68 (s, 1 H).

5.2.2 Chapter 2 Reductive Coupling Products

General procedure of the enantioselective aldehyde-alkyne coupling

$Ni(COD)_2$ (0.1 equiv), ligand (0.1 equiv), and potassium *tert*-butoxide (0.1 equiv) were weighed in a flask inside the glove box and sealed with a rubber septum. The mixture was stirred in THF (8 mL/mmol,) under inert atmosphere for 10 min at rt. Triethylsilane (2.0 equiv) was added and stirred for 5 min at 0 °C. Neat aldehyde (1.0 equiv) and the solution of alkyne (1.2 equiv) in THF (2 mL/mmol) were added sequentially to the mixture at RT. The reactions usually completes in 30 min. The reaction was quenched by

stirring in air for 15 min followed by concentration and purification by column chromatography.

General procedure of TBAF deprotection

To the solution of the TES-ether (1 equiv) in THF (10 mL/mmol) was added tetrabutylammonium fluoride (TBAF) (2 equiv, 1M solution in THF) and the mixture was stirred at RT for 2h. The reaction mixture was then diluted with ether (10 mL/mmol) and washed with $NaHCO_3$ (10 mL/mmol). The organic layer was then dried over $MgSO_4$, filtered and concentrated. The crude product was purified by column chromatography.

General procedure to make Mosher's ester

A solution of (*R*)-(-)-α-methoxy- α-trifluoromethylphenyl acetyl chloride (*R*-MTPA-Cl) (2 equiv) (weighed in glove box in a vial) in 1mL/mmol CH_2Cl_2, was added to a solution of alcohol (1 equiv) in CH_2Cl_2 (1 mL/mmol) at 0 °C under nitrogen followed by the addition of pyridine (1 mL/mmol). The mixture was stirred until all the starting alcohol is consumed as judged by TLC analysis. The reaction mixture was filtered through a small silica plug and washed with CH_2Cl_2.

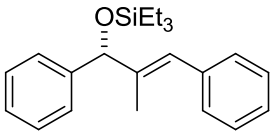

(*R*,*E*)-Triethyl(2-methyl-1,3-diphenylallyloxy)silane (Table 2.4, Entry 1). Following the general procedure, $Ni(COD)_2$ (6 mg, 0.02 mmol), ligand (*R*,*R*)-**$I_{Me,Cy}$•HBF_4** (16 mg, 0.02 mmol), *t*BuOK (2.5 mg, 0.02 mmol), triethylsilane (64 µL, 2.00 mmol), 1-phenyl-1-propyne (140 mg, 1.25 mmol) and benzaldehyde (100 µL, 1.00 mmol) were employed to give (R,*E*)-triethyl(2-methyl-1,3-diphenylallyloxy)silane (331 mg, 0.98 mmol, 98% yield, 10:1 regioselectivity), after column chromatography (SiO_2, hexanes) as a colorless oil. Spectral data of the compound were identical with the previously reported compound.[28] Following the general procedure, silyl deprotection followed by HPLC analysis (using chiral column chiralcel OJ 1.0 mL/min 99:1 hexanes/2-propanol) illustrated 78% ee (some variation in ee was observed ranging from 65-78%).

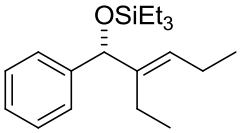

(*R*,*E*)-(2-Ethyl-1-phenylpent-2-enyloxy)triethylsilane (Table 2.4, Entry 2). Following the general procedure, $Ni(COD)_2$ (6 mg, 0.02 mmol), ligand (*R*,*R*)-**$I_{Me,Cy}$•HBF_4** (16 mg, 0.02 mmol), *t*BuOK (3 mg, 0.02 mmol), triethylsilane (64 µL, 0.4 mmol), 3-hexyne (20 mg, 0.24 mmol) and benzaldehyde (20 µL, 0.2 mmol) were employed to give (*R*,*E*)-(2-ethyl-1-phenylpent-2-enyloxy)triethylsilane (50 mg, 0.16 mmol, 82% yield), after column chromatography (SiO_2, hexanes) as a colorless oil.

^{1}H NMR (400 MHz, $CDCl_3$) δ 7.28-7.36 (m, 2H), 7.22-7.28 (m, 2H), 7.14-7.20 (m, 1H), 5.48 (t, *J* = 7.2 Hz, 1H), 5.07 (s, 1H), 2.03 (dquint, *J* = 7.6, 2.4 Hz, 2H), 1.86 (dq, *J* = 7.6, 3.2 Hz, 2H), 0.97 (t, *J* = 7.6 Hz, 3H), 0.88 (t, *J* = 8.0 Hz, 9H), 0.70 (t, *J* = 7.6 Hz, 3H), 0.56 (q, *J* = 8.0 Hz, 6H).

^{13}C (125 MHz, $CDCl_3$) δ 144.0, 142.7, 128.1, 127.6, 126.5, 126.2, 78.9, 20.7, 19.7, 14.34, 14.30, 6.8, 4.8.

HRMS (EI) *m*/*z* calculated for M^+ 304.2222, found 304.2218.

Following the general procedure, Mosher ester was synthesized (with *R*-MTPA-Cl) followed by ^{1}H and ^{19}F NMR analysis which illustrated 70% ee (some variation in ee was observed ranging from 60-70%)

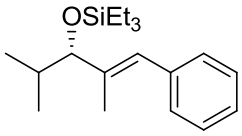

(*S*,*E*)-(2,4-Dimethyl-1-phenylpent-1-en-3-yloxy)triethylsilane (Table 2.4, Entry 3). Following the general procedure, $Ni(COD)_2$ (6 mg, 0.02 mmol), ligand (*R*,*R*)-**$I_{Me,Cy}$•HBF_4** (16 mg, 0.02 mmol), *t*BuOK (2.5 mg, 0.02 mmol), triethylsilane (64 µL, 0.4 mmol), 1-phenyl-1-propyne (28 mg, 0.24 mmol) and isobutyraldehyde (18 µL, 0.2 mmol) were employed to give (*S*,*E*)-(2,4-dimethyl-1-phenylpent-1-en-3-yloxy)triethylsilane (52 mg, 0.17 mmol, 86% yield), after column chromatography (SiO_2, hexanes) as a colorless oil.

^{1}H NMR (400 MHz, $CDCl_3$) δ 7.27-7.32 (m, 2H), 7.21-7.25 (m, 2H), 7.15-7.20 (m, 1H), 6.33 (s, 1H), 3.66 (d, *J* = 8.0 Hz, 1H), 1.77 (d, *J* = 1.2 Hz, 3H), 1.72-1.82 (m, 1H), 0.95 (d, *J* = 6.8 Hz, 3H), 0.93 (t, *J* = 8.0 Hz, 9H), 0.79 (d, *J* = 6.8 Hz, 3H), 0.58 (q, *J* = 0.8 Hz, 6H).

^{13}C (125 MHz, $CDCl_3$) δ 140.3, 137.9, 128.8, 128.0, 126.2, 126.1, 84.9, 32.2, 19.4, 18.9, 13.1, 6.9, 4.9.

IR (Thin film, KBr, cm^{-1}) 3021, 2954, 2875, 1454, 1064, 1009, 746, 698

HRMS (EI) *m/z* calculated for $[M+H]^+$ 305.2301, found 305.2312.

Following the general procedure, Mosher ester was synthesized (with *R*- MTPA-Cl) followed by ^{19}F NMR analysis which illustrated 70% ee.

(*S,E*)-(4-Ethylidene-2-methyl-7-phenylheptan-3-yloxy)triethylsilane (Table 2.4, Entry 4, major) and *S,E*-(2,4-Dimethyl-8-phenyl-oct-4-en-3-yloxy)triethylsilane (Table 2.4, Entry 4, minor).

Following the general procedure, $Ni(COD)_2$ (6 mg, 0.02 mmol), ligand (*R,R*), **$I_{Me,Cy}$•HBF_4** (16 mg, 0.02 mmol), *t*BuOK (2.5 mg, 0.02 mmol), triethylsilane (64 µL, 0.4 mmol), hex-4-ynylbenzene (38 mg, 0.24 mmol) and isobutyraldehyde (18 µL, 0.2 mmol) were employed to give a mixture of regioisomers (*S,E*)-triethyl(4-ethylidene-2-methyl-7-phenylheptan-3-yloxy)silane and *S,E*-(2,4-dimethyl-8-phenyl-oct-4-en-3-yloxy)triethylsilane (60 mg, 0.17 mmol, 86% yield, 3:1 regioselectivity), after column chromatography (SiO_2, hexanes) as a colorless oil.

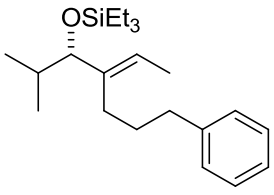

(*S,E*)-(4-Ethylidene-2-methyl-7-phenylheptan-3-yloxy)triethylsilane (Table 2.4, Entry 4, major)

^{1}H NMR (400 MHz, $CDCl_3$) δ 7.21-7.28 (m, 2H), 7.12- 7.18 (m, 3H), 5.31 (q, *J* = 6.8 Hz, 1H), 3.55 (d, *J* = 7.6 Hz, 1H), 2.60 (t, *J* = 8.0 Hz, 2H), 2.00 (t, *J* = 8.0 Hz, 2H), 1.58-1.74

(m, 3H), 1.53 (d, *J* = 6.8 Hz, 3H), 0.90 (t, *J* = 8.0 Hz, 9H), 0.84 (d, *J* = 6.4 Hz, 3H), 0.73 (d, *J* = 6.4 Hz, 3H), 0.53 (q, *J* = 8.0 Hz, 6H).

^{13}C (125 MHz, $CDCl_3$) δ 142.5, 141.3, 128.3, 128.2, 125.6, 121.5, 83.7, 36.7, 32.1, 31.0, 26.7, 19.9, 18.4, 12.9, 6.9, 4.9.

IR (Thin film, KBr, cm^{-1}) 3022, 2953, 2875, 1054, 1006, 740.

HRMS (EI) *m*/*z* calculated for [M^++Na] 369.2590, found 369.2584.

Following the general procedure, silyl deprotection followed by HPLC analysis (using chiral column chiralcel OJ 1 mL/min 99:1 hexanes/2-propanol) illustrated 75% ee. Absolute stereochemistry was assigned by analogy.

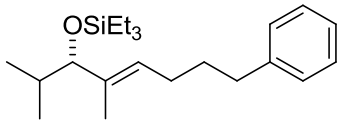

***S,E*-(2,4-Dimethyl-8-phenyl-oct-4-en-3-yloxy)triethylsilane (Table 2.4, Entry 4, minor)**

^{1}H NMR (400 MHz, $CDCl_3$) δ 7.21-7.28 (m, 2H), 7.12-7.18 (m, 3H), 5.26 (t, *J* = 7.2 Hz, 1H), 3.47 (d, *J* = 8.0 Hz, 1H), 2.59 (t, *J* = 8.0 Hz, 2H), 2.02 (q, *J* = 7.2 Hz, 2H), 1.60-1.72 (m, 3H), 1.50 (s, 3H), 0.91 (t, *J* = 8.0 Hz, 9H), 0.91 (d, *J* = 6.8 Hz, 3H), 0.69 (d, *J* = 6.8 Hz, 3H), 0.54 (q, *J* = 8.0 Hz, 6H).

^{13}C (125 MHz, $CDCl_3$) δ 142.6, 137.5, 128.3, 128.2, 126.4, 125.6, 85.0, 35.6, 31.9, 31.3, 27.0, 19.3, 19.2, 11.1, 6.9, 4.8.

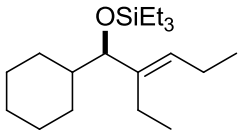

(*R,E*)-(1-Cyclohexyl-2-ethylpent-2-enyloxy)triethylsilane (Table 2.4, Entry 5)

Following the general procedure, $Ni(COD)_2$ (6 mg, 0.02 mmol), ligand (*S,S*), $\mathbf{I_{Me,Cy}}$**•HBF$_4$** (16 mg, 0.02 mmol), *t*BuOK (3 mg, 0.02 mmol), triethylsilane (64 µL, 0.40 mmol), 3-hexyne (20 mg, 0.24 mmol) and cyclohexane carboxaldehyde (24 µL, 0.2 mmol) were employed to give (*R,E*)-(1-cyclohexyl-2-ethylpent-2-enyloxy)triethylsilane (52 mg, 0.17 mmol 84% yield), after column chromatography (SiO_2, hexanes) as a colorless oil.

^{1}H NMR (400 MHz, $CDCl_3$) δ 5.05 (t, *J* = 7.2 Hz, 1H), 3.46 (d, *J* = 8.0 Hz, 1H), 1.79-1.96 (m, 5H), 1.46-1.64 (m, 3H), 1.32-1.40 (m, 1H), 1.18-1.28 (m, 1H), 0.95-1.10 (m, 3H), 0.78-0.88 (m, 15H), 0.60-0.76 (m, 2H), 0.43 (q, *J* = 8.0 Hz, 6H).

^{13}C (125 MHz, $CDCl_3$) δ 140.7, 129.1, 83.2, 41.5, 30.1, 29.0, 26.6, 26.15, 26.13, 20.5, 19.5, 14.3, 14.1, 6.8, 4.8.

HRMS (EI) *m*/*z* calculated for M^+ 310.2691, found 310.2677.

Following the general procedure, Mosher ester was synthesized (with *R*-MTPA-Cl) followed by ^{19}F NMR analysis which illustrated 85% ee.

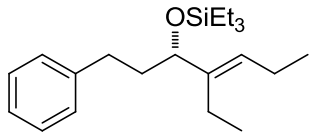

(*S*,*E*)-(4-Ethyl-1-phenylhept-4-en-3-yloxy)triethylsilane (Table 2.4, Entry 6)

Following the general procedure, Ni(COD)2 (2.7 mg, 0.01 mmol), ligand (*R*,*R*)-**$I_{Me,Cy}$•HBF_4** (8.2mg, 0.01 mmol), *t*BuOK (1.1 mg, 0.01 mmol), triethylsilane (32 μL, 0.2 mmol), 3-hexyne (17.3 mg, 0.21 mmol) and 3-phenylpropanal (13.4 mg, 0.1 mmol) were employed to give (*S*,*E*)-triethyl(4-ethyl-1-phenylhent-4-en-3-yloxy)silane (26 mg, 0.08 mmol, 75 % yield), after column chromatography (SiO2, hexanes) as a colorless oil.

1H NMR (CDCl3, 400 MHz) δ 7.21-7.23 (m, 2H), 7.13-7.15 (m, 3H), 5.27 (t, *J* = 7.2 Hz, 1H), 3.99 (t, *J* = 6.4 Hz, 1H), 2.61 (dt, *J* = 13.6, 8.2 Hz, 1H), 2.49 (dt, *J* = 14.4, 8.0 Hz, 1H), 1.98-2.03 (m, 4H), 1.78 (q, *J* = 7.8 Hz, 2H), 0.88-0.99 (m, 15H), 0.54 (q, *J* = 8.0 Hz, 6H).

13C NMR (CDCl3, 100 MHz) δ 142.7, 141.9, 128.3, 128.2, 128.1, 125.5, 77.2, 38.6, 29.7, 20.6, 19.7, 14.6, 14.3, 6.9, 4.9.

IR (thin film, KBr, cm-1) 3027, 2959, 2875, 1456, 1238, 1073, 1004, 742, 698.

HRMS (ES+) calculated for $C_{19}H_{27}Br$ $[M]^+$ 334.1296, found: 334.1287.

Following the general procedure, Mosher ester was synthesized with *S*-Mosher's acid followed by 19F NMR analysis which illustrated 78% ee (see S40 for characteristic diagnostic peaks at -70.05 and -71.36 ppm for enantioenriched and racemic spectra of ^{19}F-NMR).

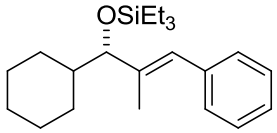

(*S*,*E*)-(1-Cyclohexyl-2-methyl-3-phenylallyloxy)triethylsilane (Table 2.4, Entry 7) Following the general procedure, $Ni(COD)_2$ (6 mg, 0.02 mmol), ligand (*R*,*R*)-**$I_{Me,Cy}$•HBF_4** (16 mg, 0.02 mmol), *t*BuOK (3 mg, 0.02 mmol), triethylsilane (64 µL, 0.4 mmol), 1-phenyl-1-propyne (28 mg, 0.24 mmol) and cyclohexane carboxaldehyde (24 µL, 0.2 mmol) were employed to give (*S*,*E*)-(1-cyclohexyl-2-methyl-3-phenylallyloxy)triethylsilane (54 mg, 0.157 mmol, 78% yield, 91:9 regioselectivity), after column chromatography (SiO_2, hexanes) as a colorless oil.

^{1}H NMR (500 MHz, $CDCl_3$) δ 7.32-7.37 (m, 2H), 7.25-7.31 (m, 2H), 7.19-7.24 (m, 1H), 6.34 (s, 1H), 3.75 (d, *J* = 8.0 Hz, 1H), 2.03-2.10 (m, 1H), 1.82 (d, *J* = 1.5 Hz, 3H), 1.64-1.80 (m, 3H), 1.46-1.50 (m, 2H), 1.10-1.30 (m, 3H), 0.97 (t, *J* = 8.0 Hz, 9H), 0.88-0.95 (m, 2H), 0.63 (q, *J* = 8.0 Hz, 6H).

^{13}C (125 MHz, $CDCl_3$) δ 140.1, 137.9, 128.8, 128.0, 126.4, 126.1, 84.1, 41.7, 29.8, 29.6, 26.4, 26.3, 26.2, 13.1, 6.9, 4.9.

HRMS (EI) *m*/*z* calculated for $C_{22}H_{36}OSiNa$ $[M+Na]^+$ 367.2433, found 367.2417. Following the general procedure, Mosher ester was synthesized (with *R*-MTPA-Cl) followed by ^{1}H NMR analysis which illustrated 81% ee.

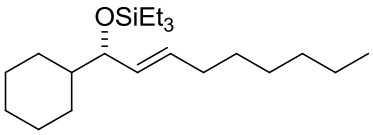

(*S*,*E*)-(1-Cyclohexylnon-2-enyloxy)triethylsilane (Table 2.4, Entry 8). Following the general procedure, $Ni(COD)_2$ (6 mg, 0.02 mmol), ligand (*R*,*R*)- **$I_{Me,Cy}$•HBF_4** (16 mg, 0.02 mmol), *t*-BuOK (3 mg, 0.02 mmol), triethylsilane (64 µL, 0.40 mmol), 1-octyne (26 mg, 0.24 mmol) and cyclohexane carboxaldehyde (24 µL, 0.20 mmol) were employed to give (*S*,*E*)-(1-cyclohexylnon-2-enyloxy)triethylsilane (43 mg, 0.13 mmol, 64% yield), after column chromatography (SiO_2, hexanes) as a colorless oil.

^{1}H NMR (500 MHz, $CDCl_3$) δ 5.47 (dt, *J* = 15.5, 6.5 Hz, 1H), 5.37 (dd, *J* = 15.0, 8.0 Hz, 1H), 3.70 (t, *J* = 7.5 Hz, 1H), 2.02 (q, *J* = 7.0 Hz, 2H), 1.84-1.90 (m, 1H), 1.68-1.77 (m,

2H), 1.61-1.68 (m, 2H), 1.01-1.42 (m, 12H), 0.95 (t, *J* = 7.5 Hz, 9H), 0.86-0.93 (m, 5H), 0.58 (m, 6H).

^{13}C (125 MHz, $CDCl_3$) δ 132.2, 131.4, 78.5, 44.4, 32.1, 31.6, 29.2, 29.0, 28.9, 28.8, 26.6, 26.2, 26.1, 22.6, 14.0, 6.8, 5.0.

HRMS (EI) *m*/*z* calculated for M^+ 338.3005, found 338.2992.

Following general procedure, Mosher's ester was synthesized (with *R*-MTPA-Cl) followed by ^{19}F NMR analysis which illustrated 65% ee.

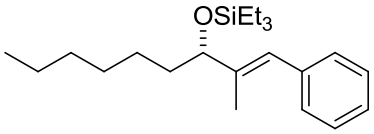

(*S*,*E*)-(2-Methyl-1-phenylnon-1-en-3-yloxy)triethylsilane (Table 2.4, Entry 9). Following the general procedure, $Ni(COD)_2$ (6 mg, 0.02 mmol), ligand (*R*,*R*)-**$I_{Me,Cy}$•HBF_4** (16 mg, 0.02 mmol), *t*-BuOK (3 mg, 0.02 mmol), triethylsilane (64 µL, 0.4 mmol), 1-phenyl-1-propyne (28 mg, 0.24 mmol) and heptaldehyde (28 µL, 0.2 mmol) were employed to give (*S*,*E*)-triethyl(2-methyl-1-phenylnon-1-en-3-yloxy)silane (49 mg, 0.14 mmol, 70% yield, 10:1 regioselectivity), after column chromatography (SiO_2, hexanes) as a colorless oil. Spectral data of the compound were identical with the previously reported compound.[3] Following the general procedure, Mosher ester was synthesized (with *R*-MTPA-Cl) followed by ^{1}H NMR analysis which illustrated 73% ee.

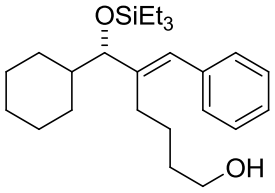

(*S*,*E*)-5-(Cyclohexyl(triethylsiloxy)methylhex-5-en-1-ol (Table 2.4, Entry 10). Following the general procedure, $Ni(COD)_2$ (6 mg, 0.02 mmol), ligand (*R*,*R*)-**$I_{Me,Cy}$•HBF_4** (16 mg, 0.02 mmol), *t*BuOK (3 mg, 0.02 mmol), triethylsilane (64 µL, 0.4 mmol), 6-phenylhex-5-yn-1-ol (42 mg, 0.24 mmol) and cyclohexane carboxaldehyde (24 µL, 0.2 mmol) were employed to give (*S*,*E*)-5-(cyclohexyl(triethylsiloxy)methylhex-5-

en-1-ol (79 mg, 0.196 mmol, 99% yield, 90:10 regioselectivity), after column chromatography (SiO_2, hexanes) as a colorless oil.

^{1}H NMR (400 MHz, $CDCl_3$) δ 7.11-7.32 (m, 5H), 6.34 (s, 0.9H, major isomer), 5.57 (t, *J* = 7.6 Hz, 0.10H, minor isomer), 4.00 (d, *J* = 5.2 Hz, 0.10H, minor isomer), 3.81 (d, *J* = 6.8 Hz, 0.90H, major isomer), 3.56 (bs, 2H), 2.20-2.30 (m, 1H), 2.08-2.18 (m, 1H), 1.30-1.96 (m, 11H), 1.02-1.30 (m, 4H), 0.93 (t, *J* = 8.0 Hz, 9H), 0.64 (q, *J* = 8.0, 6H).

^{13}C (125 MHz, $CDCl_3$) (major isomer) δ 143.6, 138.1, 128.4, 128.2, 126.8, 126.2, 82.4, 62.4, 41.9, 33.1, 30.4, 28.3, 27.6, 26.5, 26.3, 26.2, 25.0, 7.0, 4.9.

HRMS (EI) *m*/*z* calculated for $[M+Na]^+$ 425.2852, found 425.2850.

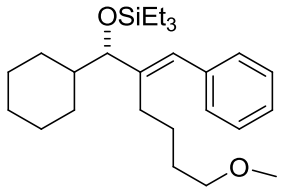

(*S*,*E*)-(2-Benzylidene-1-cyclohexyl-6-methoxyhexyloxy)triethylsilane.

To a suspension of NaH (6 mg, 0.22 mmol) in 0.5 mL DMF under nitrogen, a solution of (*S*,*E*)-(2-benzylidene-1-cyclohexyl-6-methoxyhexyloxy)triethylsilane (80 mg, 0.20 mmol) in DMF (1 mL) was added at 0 ^{o}C and stirred for 30 min. MeI (14 μL, 0.21 mmol) was the added to the reaction mixture which gave the product (*S*,*E*)-(2-benzylidene-1-cyclohexyl-6-methoxyhexyloxy)triethylsilane (75 mg, 0.18 mmol, 89% yield), after column chromatography (SiO_2, 20:1 hexanes/ethyl acetate) as a colorless oil.

^{1}H NMR (300 MHz, $CDCl_3$) δ 7.14-7.36 (m, 5H), 6.38 (s, 0.9H, major isomer), 5.60 (t, *J* = 7.5 Hz, 0.10H, minor isomer), 4.03 (d, *J* = 4.8 Hz, 0.1H, minor isomer), 3.86 (d, *J* = 6.3 Hz, 0.9H, major isomer), 3.27-3.36 (m, 5H), 1.02-2.40 (m, 17H), 0.97 (t, *J* = 7.5 Hz, 9H), 0.64 (t, *J* = 7.5 Hz, 6H).

^{13}C (125 MHz, $CDCl_3$) (major isomer) δ 143.7, 138.1, 128.5, 128.1, 126.7, 126.1, 82.2, 72.3, 58.5, 41.9, 30.5, 30.1, 28.1, 28.0, 26.6, 26.4, 26.3, 25.4, 7.0, 5.0.

Following the general procedure, Mosher ester was synthesized (with *R*-MTPA-Cl) followed by ^{1}H NMR analysis which illustrated 79% ee.

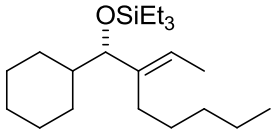

(*S*,*E*)-(1-Cyclohexyl-2-ethylideneheptyloxy)triethylsilane (Scheme 2.11, Product B). Following the general procedure, $Ni(COD)_2$ (6 mg, 0.02 mmol), ligand (*R*,*R*)-**$I_{Me,Cy}$•HBF_4** (16 mg, 0.02 mmol), *t*BuOK (3 mg, 0.02 mmol), triethylsilane (64 µL, 0.40 mmol), 2-octyne (26 mg, 0.24 mmol) and cyclohexane carboxaldehyde (24 µL, 0.20 mmol) were employed to give a 3 : 1 mixture of the regioisomers (*S*,*E*)-(1-cyclohexyl-2-ethylideneheptyloxy)triethylsilane and (*S*,*E*)-(1-cyclohexyl-2-methyloct-2-enyloxy)triethylsilane (54 mg, 0.16 mmol, 79% yield, 75:25 regioselectivity), after column chromatography (SiO_2, hexanes) as a colorless oil.

^{1}H NMR (400 MHz, $CDCl_3$) δ 5.25 (q, *J* = 6.8 Hz, 1H), 3.56 (d, *J* = 7.6 Hz, 1H), 1.86-1.98 (m, 3H), 1.60-1.74 (m, 3H), 1.56 (d, *J* = 6.8 Hz, 3H), 1.00-1.46 (m, 11H), 0.74-0.93 (m, 14H), 0.52 (q, *J* = 8.0 Hz, 6H).

^{13}C (125 MHz, $CDCl_3$) δ 141.5, 121.4, 83.1, 41.7, 32.7, 30.2, 29.0, 26.8, 26.6, 26.2, 22.5, 14.0, 12.9, 6.9, 4.9.

IR (Thin film, KBr, cm^{-1}) 2953, 2929, 2875, 1457, 1067, 1006, 724.

HRMS (EI) *m*/*z* calculated for M^+ 338.3005, found 338.3015.

Following the general procedure, Mosher ester was synthesized (with *R*-MTPA-Cl) followed by ^{19}F NMR analysis which illustrated 76% ee. The Mosher ester of the minor isomer was also synthesized (with *R*-MTPA-Cl) followed by ^{19}F NMR analysis which illustrated 76% ee.

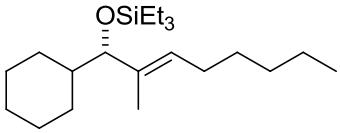

(*S*,*E*)-(1-Cyclohexyl-2-methyloct-2-enyloxy)triethylsilane (Scheme 2.11. Product A). Following the general procedure, $Ni(COD)_2$ (6 mg, 0.02 mmol), ligand (*R*,*R*)-**L4•HBF_4** (12 mg, 0.02 mmol), *t*BuOK (5 mg, 0.04 mmol), triethylsilane (64 µL, 0.40 mmol), 2-octyne (26 mg, 0.24 mmol) and cyclohexane carboxaldehyde (24 µL, 0.2 mmol) were employed to give 6 : 1 mixture of the regioisomers (*S*,*E*)-(1-cyclohexyl-2-methyloct-2-enyloxy)triethylsilane and (*S*,*E*)-(1-cyclohexyl-2-ethylideneheptyloxy)triethylsilane (32

mg, 0.095 mmol, 47% yield, 6:1 regioselectivity), after column chromatography (SiO_2, hexanes) as a colorless oil.

^{1}H NMR (400 MHz, $CDCl_3$) δ 5.17 (td, *J* = 7.2, 0.8 Hz, 1H), 3.49 (d, *J* = 8.4 Hz, 1H), 1.88-2.04 (m, 3H), 1.54-1.74 (m, 3H), 1.48 (s, 3H), 1.00-1.38 (m, 11H), 0.64-0.92 (m, 14H), 0.52 (q, *J* = 8.0 Hz, 6H).

^{13}C (125 MHz, $CDCl_3$) δ 136.2, 127.2, 84.1, 41.2, 31.5, 29.9, 29.5, 29.1, 27.3, 26.6, 26.2, 26.1, 22.5, 14.0, 10.9, 6.8, 4.8.

Following the general procedure, Mosher ester was synthesized (with *R*-Mosher acid) followed by ^{19}F NMR analysis which illustrated 79% ee.

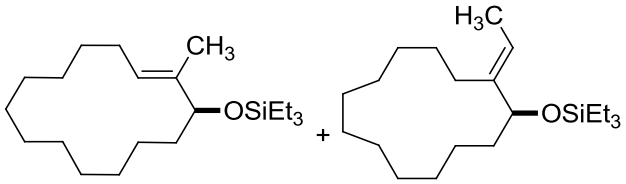

(*S*,*E*)-(2-methylcyclotetradec-2-enyloxy)triethylsilane (Scheme 2.12, regioisomer 1) and (*S*,*E*)-(2-ethylidenecyclotridecyloxy)triethylsilane (Scheme 2.12, regioisomer 2). $Ni(COD)_2$ (5 mg, 0.017 mmol), ligand (*R*,*R*)-**$I_{Me,Cy}$•HBF_4** (14 mg, 0.017 mmol), *t*BuOK (2 mg, 0.017 mmol) were weighed in an oxygen free inert atmosphere glove box in a flame-dried 50 mL round-bottomed flask with a stir bar and sealed with a septum. 5 mL toluene is added to the mixture under nitrogen atmosphere at rt and stirred for 10 min, followed by dilution with 20 mL toluene. Triethylsilane (60 µL, 0.340 mmol) was added, followed by syringe drive addition of pentadec-13-enal (50 mg, 0.167 mmol) in 10 mL toluene over 2h. The reaction was quenched by stirring the mixture in air for 30 min. and concentrated by rotary evaporation. The crude mixture was purified by column chromatography (SiO_2, 1:20 ethyl acetate/hexanes) to afford an 86:14 mixture of the regioisomers (*S*,*E*)-(2-methylcyclotetradec-2-enyloxy)triethylsilane (**regioisomer 1**) and (*S*,*E*)-(2-ethylidenecyclotridecyloxy)triethylsilane (**regioisomer 2**) (42 mg, 0.124 mmol, 76% yield) after column chromatography (SiO_2, 1:20 ethyl acetate/hexanes) as a colorless oil.

^{1}H NMR (400 MHz, $CDCl_3$) δ 5.40 (q, *J* = 6.8 Hz, 0.15H, minor isomer), 5.16-5.24 (dd, J= 9.6, 5.2 Hz, 0.85H, major isomer), 3.95 (dd, *J* = 10.4, 4.0 Hz, 0.85H, major isomer),

3.90 (t, *J* = 5.6 Hz, 0.15H, minor isomer), 2.05-2.20 (m, 1H), 1.82-2.00 (m, 1H), 1.57 (d, *J* = 6.8 Hz, 0.45H, minor isomer), 0.51 (s, 2.55H, major isomer), 0.98-1.48 (m, 20H), 0.88(t, *J* = 8.0 Hz, 9H), 0.52 (q, *J* = 8.0 Hz, 6H).

^{13}C (125 MHz, $CDCl_3$); (major and minor) δ 142.3, 137.1, 127.1, 120.0, 78.5, 77.5, 35.5, 34.8, 27.9, 27.6, 26.9, 26.8, 26.7, 26.5, 26.4, 26.0, 25.9, 25.7, 25.3, 25.0, 24.4, 24.3, 24.2, 23.5, 23.4, 23.1, 22.7, 13.2, 10.5, 6.9, 6.8, 4.8, 4.7.

IR (Thin film, KBr, cm^{-1}) 2931, 1457, 1062, 1006, 742.

HRMS (EI) *m*/*z* calculated for M^+ 338.3005, found 338.2994.

Following the general procedure, silyl deprotection gave the alcohols which were separated by column chromatography (6:1/ethyl acetate:hexanes). Following the general procedure, Mosher ester of the major regioisomer was synthesized (with *R*-Mosher acid) followed by ^{19}F NMR analysis which illustrated 79% ee. Mosher ester of the minor isomer was also synthesized (with *R*-Mosher acid) followed by ^{1}H NMR analysis which illustrated 42% ee.

5.2.3 Determination of Absolute Configuration of Allylic Alcohol Products

5.2.3.1 Measured Optical rotations

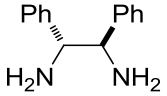

(1*R*,2*R*)-1,2-diphenylethane-1,2-diamine

Literature Value:

$[\alpha]_D$ = +102 (23 ˚C, 589 nm, 1.00 g/100 mL, MeOH)

Measured:

$[\alpha]_D$ = +48.3 (23 ˚C, 589 nm, 0.50 g/100 mL, MeOH)

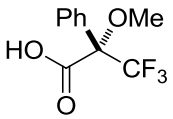

(*S*)-Mosher's acid

$[\alpha]_D$ = -63.0 (23 ˚C, 589 nm, 1.6 g/100 mL, MeOH)

Measured:

$[\alpha]_D$ = -30.6 (23 ˚C, 589 nm, 0.50 g/100 mL, MeOH)

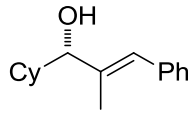

(*S*,*E*)-1-cyclohexyl-2-methyl-3-phenylprop-2-en-1-ol

Literature Value (*R* enantiomer)[55]:

$[\alpha]_D$ = -19.05 (25 ˚C, 589 nm, 1.0 g/100 mL, $CHCl_3$)

Measured:

$[\alpha]_D$ = +11.0 (23 ˚C, 589 nm, 1.0 g/100 mL, $CHCl_3$)

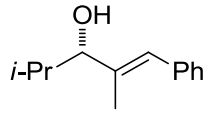

(*S*,*E*)-2,4-dimethyl-1-phenylpent-1-en-3-ol

Literature Value (*R* enantiomer)[55]:

$[\alpha]_D$ = -47.27 (25 ˚C, 589 nm, 1.05 g/100 mL, $CHCl_3$)

Measured:

$[\alpha]_D$ = +10.4 (23 ˚C, 589 nm, 0.50 g/100 mL, $CHCl_3$)

5.2.3.2 Mosher's Ester Analysis

All Mosher's esters synthesized from Mosher's acid choride where synthesized as follows:

A solution of (*R*)-(-)-α-methoxy- α-trifluoromethylphenylacetyl chloride (*R*-MTPA-Cl) (2 equiv) (weighed in glove box in a vial) in 1mL/mmol CH_2Cl_2, was added to a solution of alcohol (1 equiv) in CH_2Cl_2 (1 mL/mmol) at 0 °C under nitrogen followed by the addition of pyridine (1 mL/mmol). The mixture was stirred until all the starting alcohol is consumed as judged by TLC analysis. The reaction mixture was filtered through a small silica plug and washed with CH_2Cl_2.

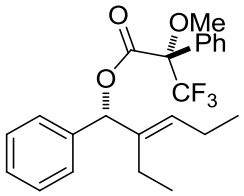

(*S*)-(*R*,*E*)-2-ethyl-1-phenylpent-2-en-1-yl 3,3,3-trifluoro-2-methoxy-2-phenylpropanoate

Characteristic alkenyl protons were observed at 5.39 ppm (triplet, minor diastereomer) and 5.58 ppm (triplet, major diastereomer).

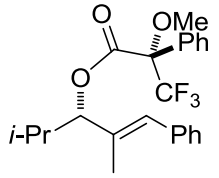

(*S*)-(*S*,*E*)-2,4-dimethyl-1-phenylpent-1-en-3-yl 3,3,3-trifluoro-2-methoxy-2-phenylpropanoate

Characteristic alkenyl protons were observed at 5.04 ppm (doublet, 1H, minor diastereomer) and 5.18 ppm (doublet, 1H, major diastereomer). Characteristic methylether protons were observed at 3.43 ppm (singlet, 3H, major diastereomer) and 3.51 ppm (singlet, 3H, minor diastereomer).

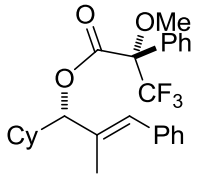

(*S*)-(*S*,*E*)-1-cyclohexyl-2-methyl-3-phenylallyl 3,3,3-trifluoro-2-methoxy-2-phenylpropanoate

Characteristic alkenyl protons were observed at 5.10 ppm (doublet, 1H, minor diastereomer) and 5.20 ppm (doublet, 1H, major diastereomer). Characteristic methylether protons were observed at 3.45 ppm (singlet, 3H, major diastereomer) and 3.53 ppm (singlet, 3H, minor diastereomer).

(*S*)-(*S*,*E*)-1-cyclohexyl-2-methyl-3-phenylallyl 3,3,3-trifluoro-2-methoxy-2-phenylpropanoate was also prepared from (*S*)-Mosher's acid as follows:

To a vial was added (*S*)-(-)-α-methoxy- α-trifluoromethylphenylacetic acid (*S*-MTPA) (7.3 mg, 0.031 mmol), Dicyclohexylcarbodiimide (DCC) (4.34 mg, 0.031 mmol) and CH_2Cl_2 (0.5 mL) followed by a solution of alcohol (4.0 mg, 0.021 mmol) in CH_2Cl_2 (0.5 mL) under nitrogen, followed by 4-Dimethylaminopyridine (DMAP) (5.0 mg, 0.42 mmol). The mixture was stirred until all the starting alcohol was consumed as judged by TLC analysis. The reaction mixture was filtered through a small silica plug and washed with CH_2Cl_2. Proton NMR indicated that the same major diastereomer was formed as when (*R*)-Mosher's acid chloride was used to form the ester.

5.2.4 Carbon Fused Ligands

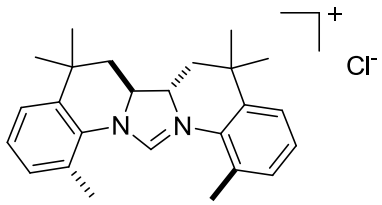

L12

racemic

(+/-)-(6a*S*,6b*S*)-1,5,5,8,8,12-hexamethyl-5,6,6a,6b,7,8-hexahydroimidazo[1,5-a:3,4-a']diquinolin-13-ium chloride (L12)

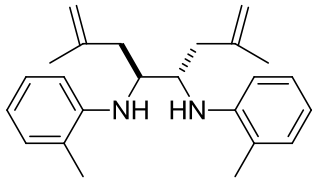

racemic

2,7-dimethyl-N^4,N^5-di-*o*-tolylocta-1,7-diene-4,5-diamine

N,*N'*-(ethane-1,2-diylidene)bis(2-methylaniline) (0.630 g, 2.67 mmol) was dissolved in diethyl ether (10 mL) and cooled to -78 ˚C. (2-methylallyl)magnesium chloride (0.5 M in Et_2O, 16 mL, 8.0 mmol) was added over 30 min. The reaction was then allowed to warm to rt and stir over 12 h. Water and diethyl ether was then added to quench the reaction, followed by saturated aqueous ammonium chloride. The aqueous layer was extracted with diethyl ether, and the combined organics were dried with Na_2SO_4 and concentrated.

By crude ^{1}H NMR the product was formed in a 6:1 ratio of meso:racemic. (+/-)-(4*S*,5*S*)-2,7-dimethyl-N^4,N^5-di-*o*-tolylocta-1,7-diene-4,5-diamine (260 mg, 78%) was isolated as a single disastereometer after column chromatography (SiO_2, 1:20 ethyl acetate/hexanes, rf = 0.7 in 1:4 ethyl acetate/hexanes).

^{1}H (500 MHz, $CDCl_3$) δ 7.14 (t, *J* = 7.5 Hz, 2H), 7.07 (d, *J* = 7.5 Hz, 2H), 6.76 (d, *J* = 7.5 Hz, 2H), 4.83 (d, *J* = 21 Hz, 4H), 3.95 (q, *J* = 7.5 Hz, 2H), 3.50 (d, *J* = 8.5 Hz, 2H), 2.44 (dd, *J* = 9.0, 6.5 Hz, 2H), 2.30 (dd, *J* = 9.0, 6.5 Hz, 2H), 2.15 (s, 3H), 1.67 (s, 3H).

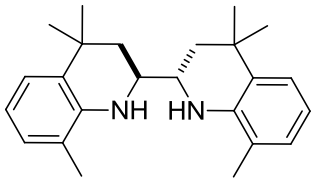

racemic

(+/-)-(2*S*,2'*S*)-4,4,4',4',8,8'-hexamethyl-1,1',2,2',3,3',4,4'-octahydro-2,2'-biquinoline

(+/-)-(4*S*,5*S*)-2,7-dimethyl-N^4,N^5-di-*o*-tolylocta-1,7-diene-4,5-diamine (260 mg, 0.75 mmol) was dissolved in concentrated sulfuric acid (6 mL) and heated to 50 ˚C for 4 h. The reaction was cooled to rt, then poored on ice. $NaHCO_3$ was slowly added until the pH was neutral, followed by extraction with diethyl ether, drying with Na_2SO_4 and concentration. (+/-)-(2*S*,2'*S*)-4,4,4',4',8,8'-hexamethyl-1,1',2,2',3,3',4,4'-octahydro-2,2'-biquinoline (230 mg, 88%) was isolated as a white solid after column chromatography (SiO_2, 1:20 ethyl acetate/hexanes, rf = 0.3 in 1:9 ethyl acetate/hexanes).

^{1}H (500 MHz, $CDCl_3$) δ 7.15 (d, *J* = 7.5 Hz, 2H), 6.94 (d, *J* = 7.0 Hz, 2H), 6.68 (t, *J* = 7.5 Hz, 2H), 3.80 (s, 1H), 3.51-3.47 (m, 2H), 2.15 (s, 3H), 1.78-175 (m, 4H), 1.42 (s, 3H), 1.32 (s, 3H).

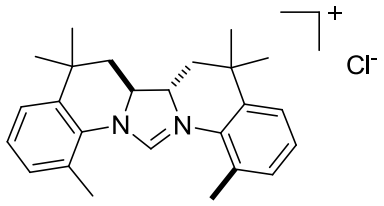

L12

racemic

(+/-)-(6a*S*,6b*S*)-1,5,5,8,8,12-hexamethyl-5,6,6a,6b,7,8-hexahydroimidazo[1,5-a:3,4-a']diquinolin-13-ium chloride (L12)

(+/-)-(2*S*,2'*S*)-4,4,4',4',8,8'-hexamethyl-1,1',2,2',3,3',4,4'-octahydro-2,2'-biquinoline (920 mg, 2.64 mmol) was heated to 120 ˚C for 16 h with triethyl orthoformate (511 mg, 3.45 mmol) and aqueous concentrated hydrochloric acid (440 μL, 5.28 mmol). The resulting crude mixture was cooled to rt, then ethyl acetate (75 mL) was added and the result precipitate was collected by filtration. The imidazolium salt **L12** (910 mg, 87% yield) was then dried under vacuum at 50 ˚C for 12 h.

^{1}H (500 MHz, $CDCl_3$) δ 9.99 (s, 1H), 7.30-7.20 (m, 6H), 4.29 (d, *J* =13 Hz, 2H), 2.76 (s, 6H), 2.41 (t, *J* =12.5 Hz, 2H), 2.13 (d, *J* = 13.5 Hz, 2H), 1.59 (s, 3H), 1.52 (s, 3H), 1.43 (s, 3H).

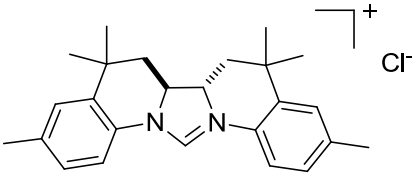

(+/-)-(6a*S*,6b*S*)-3,5,5,8,8,10-hexamethyl-5,6,6a,6b,7,8-hexahydroimidazo[1,5-a:3,4-a']diquinolin-13-ium chloride ((+/-)-L13)

The same procedures were followed to produce **L13** as **L12**, only substituting *N*,*N*'-(ethane-1,2-diylidene)bis(4-methylaniline) for *N*,*N*'-(ethane-1,2-diylidene)bis(2-methylaniline).

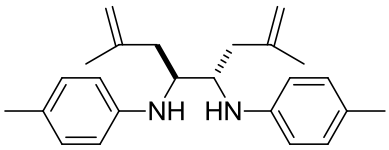

(+/-)-(4*S*,5*S*)-2,7-dimethyl-*N*^{4},*N*^{5}-di-*p*-tolylocta-1,7-diene-4,5-diamine.

^{1}H (400 MHz, $CDCl_3$) δ 7.00 (d, *J* = 8.0 Hz, 2H), 6.60 (d, *J* = 8.4 Hz, 2H), 4.85 (s, 1H), 4.79 (s, 1H), 3.77-3.73 (m, 1H), 3.38 (s, 1H), 2.37 (dd, *J* = 14.4, 7.6 Hz, 1 H). 2.56-2.50 (m, 7H), 1.69 (s, 6H).

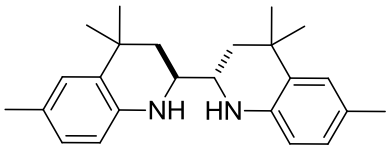

(+/-)-(2*S*,2'*S*)-4,4,4',4',6,6'-hexamethyl-1,1',2,2',3,3',4,4'-octahydro-2,2'-biquinoline

^{1}H (500 MHz, $CDCl_3$) δ 7.02 (d, *J* = 0.8 Hz, 2H), 6.82 (dd, *J* = 6.4, 1.2 Hz, 2 H), 6.5 (d, *J* = 6.4 Hz, 2H), 3.82 (s, 2H), 3.41-3.39 (m, 2H), 2.25 (s, 6H), 1.39 (s, 6H), 1.26 (s, 6H).

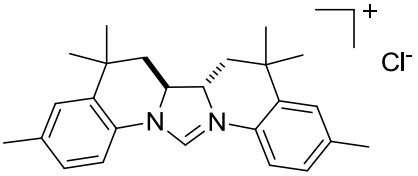

(+/-)-(6a*S*,6b*S*)-3,5,5,8,8,10-hexamethyl-5,6,6a,6b,7,8-hexahydroimidazo[1,5-a:3,4-a']diquinolin-13-ium chloride ((+/-)-L13)

^{1}H (500 MHz, $CDCl_3$) δ 12.18 (s, 1H), 8.68 (d, *J* = 8.5 Hz, 2H), 7.26 (d, *J* = 8.5 Hz, 2H), 7.15 (s, 2H), 4.28-4.25 (m, 2H), 2.35 (s, 6H), 2.20-2.14 (m, 2H), 1.48 (s, 6H), 1.39 (s, 6H).

5.3 Chapter 3 Experimental

5.3.1 Chapter 3 Ligands

L14 synthesis will be discussed in section 5.4.1.

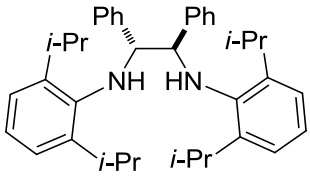

racemic

(+/-)-(1*R*,2*R*)-N^1,N^2-bis(2,6-diisopropylphenyl)-1,2-diphenylethane-1,2-diamine

N-Benzylidene-2,6-diisopropylaniline (reference 60) (10.0 g, 37.7 mmol), magnesium powder (Aldrich reagent plus 99.5% purity, 2.75 g, 113 mmol) and 120 mL of benzene was placed in 1 L flame dried round bottom flask with a stir bar under nitrogen. Triflouroacetic acid (17.4 mL, 226 mmol) was then added over 1 hour via syringe drive. The reaction was allowed to stir at rt, under nitrogen overnight. 250 mL of saturated $NaHCO_{3(aq)}$ was added to the reaction, and it was allowed to stir for 1 hour. The layers were separated, and the aqueous layer was extracted with 3 x 100 mL of EtOAc. The organic layers were combined, dried with Na_2SO_4, filtered and concentrated yielding a crude oil. The oil was treated with 40 mL of methanol and placed in a -20 ˚C freezer overnight. The solvent was decanted from the resulting precipitate, yielding 7.0 g of a mixture of racemic and meso product. The 7.0 grams of the mixture of meso and racemic

isomers was dissolved in 250 mL of refluxing methanol. Some material did not dissolve after 1 h, and the solution was filtered hot to remove this solid. The hot methanol solution was removed from heat and allowed to slowly cool to rt. The flask was allowed to sit overnight producing a white crystalline solid. The solvent was then decanted leaving 2.5 g of the meso isomer. The resulting solvent was concentrated to 125 mL, then heated to reflux until all material redissolved. The solution was then cooled to RT, then placed in a -20 ˚C freezer overnight. The solvent was decanted to produce 3.2 g of solid with material in a with a ratio of 94:6 racemic:meso.

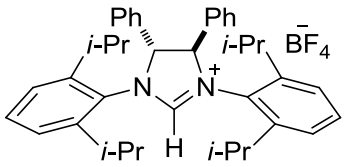

(±)-(4*R*,5*R*)-1,3-Bis(2,6-diisopropylphenyl)-4,5-diphenyl-4,5-dihydro-1H-imidazol-3-ium tetrafluoroborate (DP-IPr)

(±)-(1*R*, 2*R*)-N^1,N^2-Bis(2,6-diisopropylphenyl)-1,2-diphenylethane-1,2-diamine[2] (0.580 g, 0.940 mmol), ammonium tetrafluoroborate (98 mg, 0.94 mmol), triethylorthoformate (1.11 g, 7.52 mmol), and formic acid (1 drop) were placed in a dry 25 mL round-bottom flask with a reflux condenser under nitrogen. The reaction was then heated to 120 ˚C with stirring for 24 h. The reaction was allowed to cool to rt and then concentrated under high vacuum. The reaction mixture was then purified by column chromatography (SiO_2, 0.5% methanol/99.5% dichloromethane) followed by washing with EtOAc to afford **5c** (0.530 g, 0.84 mmol, 89% yield) as a pale yellow solid.

^{1}H NMR (400 MHz, $(D_3C)_2SO$): δ 9.79 (s, 1H), 7.51–7.39 (m, 14H), 7.19–7.14 (m, 2H), 6.25 (s, 2H), 3.29 (sept, *J* = 6.8 Hz, 2H), 2.74 (sept, *J* = 7.2 Hz, 2H), 1.66 (d, *J* = 6.8 Hz, 6H), 1.31 (d, *J* = 6.4 Hz, 6H), 1.04 (d, *J* = 6.8 Hz, 6H), 0.50 (d, *J* = 6.4 Hz, 6H).

^{13}C NMR (100 MHz, $(D_3C)_2SO$): δ 159.0, 147.1, 146.2, 131.5, 130.6, 129.7, 129.3, 129.1, 127.8, 125.1, 124.6, 72.8, 29.3, 29.0, 25.38, 25.34, 23.5, 21.7.

IR (thin film): ν 3064, 3035, 2966, 2931, 2872, 1614, 1583 cm^{-1}.

HRMS Electrospray (*m*/*z*): $[M–BF_4]^+$ calcd for $C_{39}H_{47}N_2$, 543.3839; found 543.3743.

5.3.2 Chapter 3 Reductive Coupling Products

General Procedure A for the Ni(COD)$_2$/*i*-Pr-BAC-Promoted Reductive Coupling of Alkynes, Aldehydes, and Di-*tert*-butylsilane:

To a solid mixture of Ni(COD)$_2$ (22 mol %), *i*-Pr-BAC·HBF$_4$ salt (20 mol %) was added THF (0.25 M). To the resulting solution was added *n*-BuLi (2.5 M in hexanes) (20 mol %). The resulting solution was stirred for 5 min at rt until the solution turned dark red in appearance. The alkyne (1.0 equiv), aldehyde (1.0 equiv), di-*tert*-butylsilane (1.2 equiv), and THF (0.25 M) were added via syringe pump addition over 60 minutes and the reaction mixture was allowed to stir until starting materials were consumed. The reaction mixture was filtered through silica gel eluting with 50% EtOAc/hexanes. The solvent was removed *in vacuo*, and the crude residue was purified via flash chromatography on silica gel to afford the desired product.

General Procedure B for the Ni(COD)$_2$/SIPr-Promoted Reductive Coupling of Alkynes, Aldehydes, and Triisoproylsilane:

To a solid mixture of Ni(COD)$_2$ (12 mol %), SIPr·HCl salt (10 mol %), and *t*-BuOK (10 mol %) was added THF (0.125 M). The resulting solution was stirred for 5 min at rt until the solution turned dark brown in appearance. The alkyne (1.0 equiv), aldehyde (1.0 equiv), and triisopropylsilane (2.0 equiv) were added sequentially, and the reaction mixture was allowed to stir until starting materials were consumed. The reaction mixture was filtered through silica gel eluting with 50% EtOAc/hexanes. The solvent was removed *in vacuo*, and the crude residue was purified via flash chromatography on silica gel to afford the desired product.

General Procedure C for the Ni(COD)$_2$/IMes-Promoted Reductive Coupling of Alkynes, Aldehydes, and Triisoproylsilane:

To a solid mixture of Ni(COD)$_2$ (12 mol %), IMes·HCl salt (10 mol %), and *t*-BuOK (10 mol %) was added THF (0.125 M). The resulting solution was stirred for 5 min at rt until the solution turned dark blue in appearance. The alkyne derivative (1.0 equiv), aldehyde (1.0 equiv), and triisopropylsilane (2.0 equiv) were added sequentially, and the reaction mixture was allowed to stir until starting materials were consumed. The reaction mixture

was filtered through silica gel eluting with 50% EtOAc/hexanes. The solvent was removed *in vacuo*, and the crude residue was purified via flash chromatography on silica gel to afford the desired product.

General Procedure D for the Ni(COD)$_2$/5c-Promoted Reductive Coupling of Alkynes, Aldehydes, and Triethylsilane:

To a solid mixture of Ni(COD)$_2$ (12 mol %), (+/-)-DP-IPr·HBF$_4$ salt (10 mol %) was added THF (0.2 M). To the resulting solution was added *n*-BuLi (2.5 M in hexanes) (10 mol %). The resulting solution was stirred for 5 min at rt until the solution turned dark red in appearance. Triethylsilane (2.0 equiv) was then added to the reaction mixture. The alkyne (1.2 equiv), aldehyde (1.0 equiv), and THF (0.2 M) were added via syringe pump addition over 30 minutes and the reaction mixture was allowed to stir until starting materials were consumed. The reaction mixture was filtered through silica gel eluting with 50% EtOAc/hexanes. The solvent was removed *in vacuo*, and the crude residue was purified via flash chromatography on silica gel to afford the desired product.

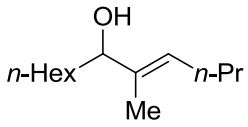

(*E*)-5-Methyldodec-4-en-6-ol (Table 3.3, Entry 1, Regioisomer 1)

Following Procedure A, Ni(COD)$_2$ (37 mg, 0.14 mmol), *i*-Pr-BAC·HBF$_4$ salt (39 mg, 0.12 mmol), *n*-BuLi (2.5 M in hexanes) (49 μL, 0.12 mmol), di-*tert*-butylsilane (105 mg, 0.73 mmol), 2-hexyne (50 mg, 0.59 mmol), 1-heptanal (68 mg, 0.59 mmol) gave a crude residue which was purified via flash chromatography (100 % hexanes) to afford a single regioisomer in a 88:12 isolated regioselectivity (156 mg, 0.46 mmol, 78% yield). This compound was subsequently subjected to *n*-tetrabutylammonium fluoride deprotection for characterization purposes.

Spectral data as previously reported.[66]

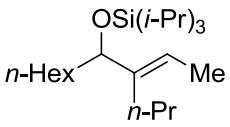

(*E*)-[(4-Ethylideneundecan-5-yl)oxy]triisopropylsilane (Table 3.3, Entry 1, Regioisomer 2)

Following Procedure B, $Ni(COD)_2$ (20 mg, 0.073 mmol), SIPr·HCl salt (25 mg, 0.059 mmol), *t*-BuOK (6.7 mg, 0.059 mmol), triisopropylsilane (0.24 mL, 1.18 mmol), 2-hexyne (50 mg, 0.59 mmol), 1-heptanal (68 mg, 0.59 mmol) gave a crude residue which was purified via flash chromatography (100% hexanes) to afford a single regioisomer in a >98:2 isolated regioselectivity (93:7 crude regioselectivity) (179 mg, 0.51 mmol, 85% yield).

Spectral data as previously reported.[66]

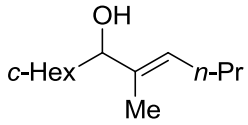

(*E*)-1-Cyclohexyl-2-methylhex-2-en-1-ol (Table 3.3, Entry 2, Regioisomer 1)

Following Procedure A, $Ni(COD)_2$ (37 mg, 0.14 mmol), *i*-Pr-BAC·HBF_4 salt (39 mg, 0.12 mmol), *n*-BuLi (2.5 M in hexanes) (49 μL, 0.12 mmol), di-*tert*-butylsilane (105 mg, 0.73 mmol), 2-hexyne (50 mg, 0.59 mmol), cyclohexylcarboxaldehyde (68 mg, 0.59 mmol) gave a crude residue which was purified via flash chromatography (100 % hexanes) in a 82:18 isolated regioselectivity (150 mg, 0.44 mmol, 75% yield). This compound was subsequently subjected to *n*-tetrabutylammonium fluoride deprotection for characterization purposes.

^{1}H NMR (400 MHz, $CDCl_3$): δ 5.30 (t, *J* = 7.2 Hz, 1H), 5.59 (d, *J* = 8.0 Hz, 1H), 197 (app q, *J* = 7.2 Hz, 2H), 1.76–1.60 (m, 3H), 1.55 (s, 3H), 1.45–1.31 (m, 4H), 1.25–1.08 (m, 4H), 1.02 (s, 1H), 0.96–0.79 (m, 2H), 0.87 (t, *J* = 7.2 Hz, 3H).

^{13}C NMR (100 MHz, $CDCl_3$): δ 136.1, 128.1, 83.3, 40.5, 29.56, 29.55, 29.3, 26.5, 26.2, 26.0, 22.7, 13.8, 11.1.

IR (thin film): ν cm^{-1}. ν 3430, 2944, 2867, 1461 cm^{-1}.

HRMS Electron Ionization (*m*/*z*): $[M]^+$ calcd for $C_{13}H_{24}O$, 219.2; found 219.2.

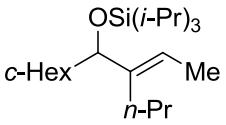

(*E*)-[(1-Cyclohexyl-2-ethylidenepentyl)oxy]triisopropylsilane (Table 3.3, Entry 2, Regioisomer 2)

Following Procedure B, $Ni(COD)_2$ (20 mg, 0.073 mmol), SIPr·HCl salt (25 mg, 0.059 mmol), *t*-BuOK (6.7 mg, 0.059 mmol), triisopropylsilane (0.24 mL, 1.18 mmol), 2-hexyne (50 mg, 0.59 mmol), cyclohexylcarboxaldehyde (68 mg, 0.59 mmol) gave a crude residue which was purified via flash chromatography (100% hexanes) to afford a single regioisomer in a >98:2 isolated regioselectivity (95:5 crude regioselectivity) (191 mg, 0.54 mmol, 91% yield).

^{1}H NMR (400 MHz, $CDCl_3$): δ 5.28 (q, *J* = 7.2 Hz, 1H), 3.78 (d, *J* = 7.2 Hz, 1H), 2.01–1.88 (m, 2H), 1.74–1.53 (m, 6H), 1.41–1.27 (m, 3H), 1.22–1.09 (m, 4H), 1.05–1.02 (m, 21H), 0.92 (t, *J* = 7.2 Hz, 3H), 0.88–0.81 (m, 3H).

^{13}C NMR (100 MHz, $CDCl_3$): δ 141.5, 121.7, 83.2, 42.7, 30.3, 29.8, 29.1, 26.8, 26.5, 26.4, 22.6, 19.4, 18.30, 18.27, 15.1, 12.8.

IR (thin film): ν 2925, 2864, 1464 cm^{-1}.

HRMS Electron Ionization (*m*/*z*): $[M]^+$ calcd for $C_{22}H_{44}OSi$, 352.3161; found 352.3160.

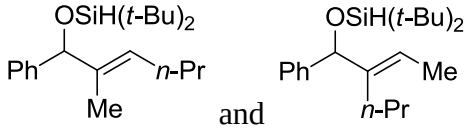

(*E*)-Di-*tert*-butyl[(2-methyl-1-phenylhex-2-en-1-yl)oxy]silane (Table 3.3, Entry 3, Regioisomer 1 Major), **(*E*)-Di-*tert*-butyl[(2-ethylidene-1-phenylpentyl)oxy]silane. (Table 3.3, Entry 3, Regioisomer 2)**

Following Procedure A, $Ni(COD)_2$ (37 mg, 0.14 mmol), *i*-Pr-BAC·HBF_4 salt (39 mg, 0.12 mmol), *n*-BuLi (2.5 M in hexanes) (49 μL, 0.12 mmol), di-*tert*-butylsilane (105 mg, 0.73 mmol), 2-hexyne (50 mg, 0.59 mmol), benzaldehyde (63 mg, 0.59 mmol) gave a crude residue which was purified via flash chromatography (100 % hexanes) to afford a mixture of regioisomers in a 85:15 isolated regioselectivity (84:16 crude regioselectivity) (143 mg, 0.43 mmol, 72% yield).

^{1}H NMR (400 MHz, $CDCl_3$): δ 7.39–7.34 (m, 2H), 7.32–7.27 (m, 2H), 7.23–7.19 (m, 1H), 5.77 (q, *J* = 6.8 Hz, 0.15H), 5.64 (t, *J* = 7.2 Hz, 0.85H), 5.19 (s, 0.85H), 5.15 (s, 0.15

H), 4.07 (s, 0.85H), 4.02 (s, 0.15H), 2.03 (m, 2H), 1.88–1.62 (m, 1H), 1.46–1.39 (m, 4H), 1.08–1.01 (m, 10H), 0.94–0.93 (m, 9H), 0.91–0.88 (m, 2H).

^{13}C NMR (100 MHz, $CDCl_3$): δ 143.39, 143.33, 141.9, 136.8, 128.8, 127.2, 126.8, 126.7, 126.6, 126.1, 120.6, 83.5, 82.2, 29.6, 29.1, 27.40, 27.36, 27.29, 27.25, 22.7, 22.1, 20.3, 20.1, 20.0, 19.9, 14.5, 13.9, 13.1, 11.3.

IR (thin film): ν 3087, 3063, 3028, 2962, 2930, 1891, 1858, 2090, 1493, 1470 cm^{-1}.

HRMS Electron Ionization (*m*/*z*): $[M]^+$ calcd for $C_{21}H_{36}OSi$, 332.2535; found 332.2522.

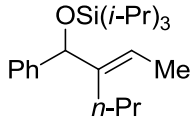

(*E*)-[(2-Ethylidene-1-phenylpentyl)oxy]triisopropylsilane (Table 3.3, Entry 3, Regioisomer 2)

Following Procedure B, $Ni(COD)_2$ (20 mg, 0.073 mmol), SIPr·HCl salt (25 mg, 0.059 mmol), *t*-BuOK (6.7 mg, 0.059 mmol), triisopropylsilane (0.24 mL, 1.18 mmol), 2-hexyne (50 mg, 0.59 mmol), benzaldehyde (63 mg, 0.59 mmol) gave a crude residue which was purified via flash chromatography (100 % hexanes) to afford a single regioisomer in a >98:2 isolated regioselectivity (95:5 crude regioselectivity) (191 mg, 0.54 mmol, 91% yield).

^{1}H NMR (400 MHz, $CDCl_3$): δ 7.45–7.41 (m, 2H), 7.34–7.29 (m, 2H), 7.25–7.21 (m, 1H), 5.80 (q, *J* = 6.8 Hz, 1H), 5.24 (s, 1H), 2.00–1.86 (m, 2H), 1.69 (d, *J* = 7.2 Hz, 3H), 1.20–1.04 (m, 23H), 0.83 (t, *J* = 7.6 Hz, 3H).

^{13}C NMR (100 MHz, $CDCl_3$): δ 144.5, 143.1, 127.7, 126.6, 126.3, 120.0, 79.4, 28.7, 22.3, 19.4, 18.07, 18.04, 14.6, 12.4.

IR (thin film): ν 3085, 3061, 3026, 2958, 2891, 2866, 1492, 1464 cm^{-1}.

HRMS Electron Ionization (*m*/*z*): $[M]^+$ calcd for $C_{22}H_{38}OSi$, 346.2692; found 346.2683.

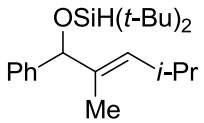

(*E*)-Di-*tert*-butyl[(2,4-dimethyl-1-phenylpent-2-en-1-yl)oxy]silane (Table 3.3, Entry 4, Regioisomer 1)

Following Procedure A, $Ni(COD)_2$ (37 mg, 0.14 mmol), *i*-Pr-BAC·HBF_4 salt (39 mg, 0.12 mmol), *n*-BuLi (2.5 M in hexanes) (49 μL, 0.12 mmol), di-*tert*-butylsilane (105 mg, 0.73 mmol), 4-methylpent-2-yne (50 mg, 0.59 mmol), benzaldehyde (63 mg, 0.59 mmol) gave a crude residue which was purified via flash chromatography (100 % hexanes) to afford a single regioisomer in a >98:2 isolated regioselectivity (97:3 crude regioselectivity) (168 mg, 0.51 mmol, 85% yield).

^{1}H NMR (400 MHz, $CDCl_3$): δ 7.35 (m, 2H), 7.28 (m, 2H), 7.19 (m, 1H), 5.43 (d, *J* = 9.2 Hz, 1H), 5.12 (s, 1H), 4.04 (s, 1H), 2.49 (septd, *J* = 9.2 Hz, 6.8 Hz, 1H), 1.37 (d, *J* = 1.6 Hz, 3H), 1.02 (s, 9H), 0.98 (d, *J* = 6.8 Hz, 3H), 0.96 (d, *J* = 6.8 Hz, 3H), 0.92 (s, 9H).

^{13}C NMR (100 MHz, $CDCl_3$): δ 143.3, 135.1, 134.2, 127.7, 126.5, 126.0, 83.5, 27.4, 27.3, 26.9, 22.87, 22.84, 20.4, 19.8, 11.1.

IR (thin film): ν 3087, 3064, 3028, 1962, 2930, 2892, 2858, 2091, 1493, 1470 cm^{-1}.

HRMS Electron Ionization (*m*/*z*): $[M]^+$ calcd for $C_{21}H_{36}OSi$, 332.2535; found 332.2528.

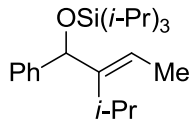

(*E*)-Triisopropyl[(2-isopropyl-1-phenylbut-2-en-1-yl)oxy]silane (Table 3.3, Entry 4, Regioisomer 2)

Following Procedure C, $Ni(COD)_2$ (20 mg, 0.073 mmol), SIPr·HCl salt (25 mg, 0.059 mmol), *t*-BuOK (6.7 mg, 0.059 mmol), triisopropylsilane (0.24 mL, 1.18 mmol), 4-methylpent-2-yne (50 mg, 0.59 mmol), benzaldehyde (63 mg, 0.59 mmol) gave a crude residue which was purified via flash chromatography (100 % hexanes) to afford a single regioisomer in a >98:2 isolated regioselectivity (90:10 crude regioselectivity) (183 mg, 0.53 mmol, 89% yield).

^{1}H NMR (400 MHz, $CDCl_3$): δ 7.39–7.37 (m, 2H), 7.29–7.24 (m, 2H), 7.21–7.17 (m, 1H), 5.74 (q, *J* = 7.2 Hz, 1H), 5.18 (s, 1H), 2.52 (sept, *J* = 7.2 Hz, 1H), 1.75 (d, *J* = 7.2 Hz, 3H), 1.16–1.00 (m, 24H), 0.70 (d, *J* = 7.2 Hz, 3H).

^{13}C NMR (100 MHz, $CDCl_3$): δ 147.4, 144.4, 127.60, 126.55, 119.89, 79.6, 27.2, 21.5, 21.2, 19.4, 18.1, 18.0, 12.4.

IR (thin film): ν 3085, 2062, 3026,2959, 2942, 289, 2866, 1493, 1463 cm^{-1}.

HRMS Electron Ionization (*m*/*z*): $[M]^+$ calcd for $C_{22}H_{38}OSi$, 346.2692; found 346.2696.

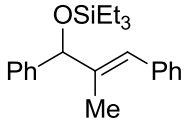

(*E*)-Triethyl[(2-methyl-1,3-diphenylallyl)oxy]silane (Table 3.3, Entry 5, Regioisomer 1)

The following compound was previously reported.[66]

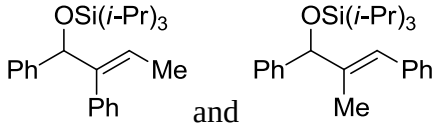

(*E*)-[(1,2-Diphenylbut-2-en-1-yl)oxy]triisopropylsilane (**Table 3.3, Entry 5, Regioisomer 1)** and **(*E*)-Triisopropyl[(2-methyl-1,3-diphenylallyl)oxy]silane** (**Table 3.3, Entry 5, Regioisomer 2)**

Following Procedure B, $Ni(COD)_2$ (20 mg, 0.073 mmol), SIPr·HCl salt (26 mg, 0.059 mmol), *t*-BuOK (6.7 mg, 0.059 mmol), triisopropylsilane (0.24 mL, 1.18 mmol), prop-1-yn-1-ylbenzene (71 mg, 0.61 mmol), benzaldehyde (65 mg, 0.61 mmol) gave a crude residue which was purified via flash chromatography (100 % hexanes) to afford a mixture of regioisomers in a 80:20 isolated regioselectivity (81:19 crude regioselectivity) (233 mg, 0.61 mmol, 99% yield).

^{1}H NMR (400 MHz, $CDCl_3$): δ 7.52–7.29 (m, 2H), 7.24–7.17 (m, 6H), 6.89 (m, 2H), 6.82 (s, 0.2H), 6.13 (q, *J* = 6.0 Hz, 0.8H), 5.48 (s, 0.8H), 5.40 (s, 0.2H), 1.75 (d, *J* = 1.2 Hz, 1H), 1.57 (d, *J* = 6.8 Hz, 2H), 1.26–1.05 (m, 21H).

^{13}C NMR (100 MHz, $CDCl_3$): δ 145.0, 143.7, 143.6, 141.2, 138.2, 137.8, 129.7, 129.0, 128.1, 127.9, 127.47, 127.46, 126.8, 126.60, 126.56, 126.4, 126.3, 126.1, 125.0, 80.4, 79.4, 19.4, 18.07, 18.05, 18.0, 14.1, 12.9, 12.3, 10.2.

IR (thin film): ν 3080, 3058, 3026, 2942, 2890, 2865, 1491, 1463, 1451, 1441 cm^{-1}.

HRMS Electron Ionization (*m*/*z*): $[M]^+$ calcd for $C_{25}H_{36}OSi$, 380.2535; found 380.2525.

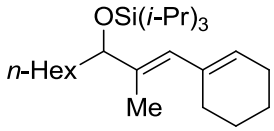

(*E*)-{[1-(Cyclohex-1-en-1-yl)-2-methylnon-1-en-3-yl]oxy}triisopropylsilane (Table 3.3, Entry 6, Regioisomer 1)

Following Procedure C, $Ni(COD)_2$ (20 mg, 0.073 mmol), IMes·HCl salt (20 mg, 0.059 mmol), *t*-BuOK (6.7 mg, 0.059 mmol), triisopropylsilane (0.24 mL, 1.18 mmol), 1-(prop-1-yn-1-yl)cyclohex-1-ene (72 mg, 0.59 mmol), 1-heptanal (68 mg, 0.59 mmol) gave a crude residue which was purified via flash chromatography (100 % hexanes) to afford a single regioisomer in a >98:2 isolated regioselectivity (97:3 crude regioselectivity) (225 mg, 0.59 mmol, 85% yield).

^{1}H NMR (400 MHz, $CDCl_3$): δ 5.65 (s, 1H), 5.54 (m, 1H), 4.05 (t, *J* = 6.4 Hz, 1H), 2.09–2.05 (m, 4H), 1.71 (s, 3H), 1.66–1.51 (m, 4H), 1.30–1.14 (m, 10H), 1.06–1.01 (m, 21H), 0.87 (t, *J* = 6.8 Hz, 3H).

^{13}C NMR (100 MHz, $CDCl_3$): δ 137.0, 135.1, 128.4, 126.0, 79.0, 36.3, 31.9, 29.4, 29.3, 25.6, 25.4, 23.0, 22.7, 22.3, 18.14, 18.10, 14.1, 12.7, 12.4.

IR (thin film): ν 2931, 2865, 1464 cm^{-1}.

HRMS Electron Ionization (*m*/*z*): $[M]^+$ calcd for $C_{25}H_{48}OSi$, 392.3474; found 392.3468.

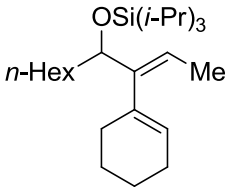

(*E*)-{[3-(Cyclohex-1-en-1-yl)dec-2-en-4-yl]oxy}triisopropylsilane (Table 3.3, Entry 6, Regioisomer 2)

Following Procedure B, $Ni(COD)_2$ (20 mg, 0.073 mmol), SIPr·HCl salt (25 mg, 0.059 mmol), *t*-BuOK (6.7 mg, 0.059 mmol), triisopropylsilane (0.24 mL, 1.18 mmol), 1-(prop-1-yn-1-yl)cyclohex-1-ene (72 mg, 0.59 mmol), 1-heptanal (68 mg, 0.59 mmol) gave a crude residue which was purified via flash chromatography (100 % hexanes) to afford a single regioisomer in a >98:2 isolated regioselectivity (91:9 crude regioselectivity) (175 mg, 0.46 mmol, 77% yield).

^{1}H NMR (400 MHz, $CDCl_3$): δ 5.42 (qd, *J* = 6.8 Hz, 1.2 Hz, 1H), 5.33 (td, *J* = 3.6 Hz, 1.6 Hz, 1H), 4.21 (m, 1H), 2.07–1.98 (m, 4H), 1.65–1.39 (m, 7H), 1.28–1.11 (m, 10H), 1.09–0.94 (m, 21H), 0.85 (t, *J* = 6.8 Hz, 3H).

^{13}C NMR (100 MHz, $CDCl_3$): δ 145.5, 135.5, 125.5, 119.7, 75.7, 36.0, 31.9, 29.5, 29.0, 25.4, 23.8, 23.1, 22.7, 22.4, 18.20, 18.17, 14.1, 14.0, 12.5.

IR (thin film): ν 2928, 2865, 1464 cm^{-1}.

HRMS E Electron Ionization (*m*/*z*): $[M–i\text{-}Pr]^+$ calcd for $C_{22}H_{41}OSi$, 349.2927; found 349.2928.

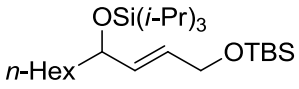

(E)-8-hexyl-10,10-diisopropyl-2,2,3,3,11-pentamethyl-4,9-dioxa-3,10-disiladodec-6-ene (Table 3.4, Entry 1, Regioisomer 1)

Following Procedure C, $Ni(COD)_2$ (20 mg, 0.073 mmol), IMes·HCl salt (20 mg, 0.059 mmol), *t*-BuOK (6.7 mg, 0.059 mmol), triisopropylsilane (0.24 mL, 1.18 mmol), *tert*-butyldimethyl(prop-2-yn-1-yloxy)silane (101 mg, 0.59 mmol), heptaldehyde (75 mg, 0.66 mmol) gave a crude residue which was purified via flash chromatography (100 % hexanes) to afford >98:2 isolated regioselectivity (220 mg, 0.52 mmol, 86% yield).

^{1}H NMR (400 MHz, $CDCl_3$): δ 5.62-5.61 (m, 2H), 4.21-4.17 (m, 1H), 4.14 (d, *J* = 2.4 Hz, 2H), 1.56-1.41 (m, 2H), 1.29-1.20 (m, 8H), 1.06-1.01 (m, 21H), 0.91-0.82 (m, 12H), 0.04 (s, 6H).

^{13}C NMR (100 MHz, $CDCl_3$): δ 133.7, 128.9, 73.2, 63.3, 38.6, 31.9, 29.4, 25.9, 24.7, 22.6, 18.4, 18.14, 18.12, 14.1, 12.4, -5.2.

IR (thin film): ν 2929, 2893, 2863,1462, 1255, 1094, 836, 775, 678 cm^{-1}.

HRMS Electrospray (*m*/*z*): $[M+Na]^+$ calcd for $C_{25}H_{54}O_2Si_2$, 465.3560, found 465.3559.

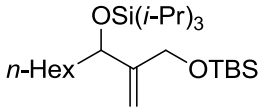

7-hexyl-9,9-diisopropyl-2,2,3,3,10-pentamethyl-6-methylene-4,8-dioxa-3,9-disilaundecane (Table 3.4, Entry 1, Regioisomer 2)

Following Procedure C, $Ni(COD)_2$ (5.1 mg, 0.024 mmol), DP-IPR·BF_4 salt (12 mg, 0.020 mmol), *t*-BuOK (2.2 mg, 0.020 mmol), triethylsilane (46.4 mg, 0.40 mmol), *tert*-butyldimethyl(prop-2-yn-1-yloxy)silane (40.8 mg, 0.20 mmol), heptaldehyde (22.8 mg, 0.20 mmol) gave a crude residue which was purified via flash chromatography (100 % hexanes) to afford a mixture of regioisomers in 28:72 regioselectivity (40 mg, 0.10 mmol, 50% yield).

Product was not cleanly isolated.

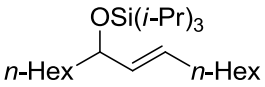

(*E*)-Triisopropyl[(1-hexylnon-2-en-1-yl)oxy]silane (Table 3.4, Entry 2, Regioisomer 1),

Following Procedure C, $Ni(COD)_2$ (20 mg, 0.073 mmol), IMes·HCl salt (20 mg, 0.059 mmol), *t*-BuOK (6.7 mg, 0.059 mmol), triisopropylsilane (0.24 mL, 1.18 mmol), 1-octyne (67 mg, 0.59 mmol), heptaldehyde (69 mg, 0.59 mmol) gave a crude residue which was purified via flash chromatography (100 % hexanes) to afford >98:2 isolated regioselectivity (98:2 crude regioselectivity) (177 mg, 0.46 mmol, 82% yield).

^{1}H NMR (400 MHz, $CDCl_3$): δ 5.47 (dt, *J* = 15.6 Hz, 6.4 Hz, 1H), 5.36 (dd, *J* = 15.2 Hz, 6.8 Hz, 1H), 4.10 (td, *J* = 7.2 Hz, 5.2 Hz, 1H), 1.99 (dt, *J* = 7.6, 6.4, 2H), 1.57-1.37 (m, 2H), 1.35-1.20 (m, 16H), 1.03 (app S, 21 H), 0.87 (t, *J* = 7.2 Hz, 3H), 0.86 (t, *J* = 7.2 Hz, 3H).

^{13}C NMR (100 MHz, $CDCl_3$): δ 133.9, 130.4, 74.1, 38.8, 32.2, 31.9, 31.8, 29.4, 29.3, 28.9, 25.0, 22.68, 22.65, 18.16, 18.12, 14.1, 12.4.

IR (thin film): ν 2956, 2926, 2864, 2464, 2087, 2063, 882 cm^{-1}.

HRMS EI (*m*/*z*): $[M\text{-iPr}]^+$ calcd for $C_{24}H_{50}OSi$, 339.3083; found 339.3080.

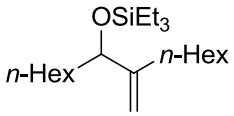

Triethyl[(2-methylene-1-hexyloctyl)oxy]silane (Table 3.4, Entry 2, Regioisomer 2)

Following Procedure D, $Ni(COD)_2$ (7.7 mg, 0.036 mmol), **DP-IPR** ·BF_4 salt (19 mg, 0.030 mmol), *n*-BuLi (2.5 M in hexanes) (12 μL, 0.030 mmol), triethylsilane (0.96 mL,

0.60 mmol), 1-octyne (39.6 mg, 0.30 mmol), heptaldehyde (37 mg, 0.32 mmol) gave a crude residue which was purified via flash chromatography (100 % hexanes) to afford a mixture of regioisomers in a 24:76 isolated regioselectivity (28:72 crude regioselectivity) (20 mg regioisomer 1, 65 mg regioisomer 2, 84% yield).

Full characterization will be included in the final version.

^{1}H NMR (400 MHz, $CDCl_3$): δ 4.93 (m, 1H), 4.75 (m, 1H), 4.03 (t, *J* = 6.4 Hz, 1H), 2.05 (dt, *J* = 15.6 Hz, 8.0 Hz, 1H), 1.92 (dt, *J* = 15.6 Hz, 7.6 Hz, 1H), 1.50-1.42 (m, 4H), 1.34-1.24 (m, 14H), 0.94 (t, *J* = 8.0 Hz, 9H), 0.91-0.85 (m, 6H), 0.58 (q, *J* = 8.0 Hz, 6H).

^{13}C NMR (100 MHz, $CDCl_3$): δ 152.15, 108.68, 76.53, 36.64, 31.83, 31.77, 30.30, 29.32, 29.26, 27.78, 25.55, 22.61, 14.04, 6.86, 4.80.

IR (thin film): ν 2954, 2928, 2874, 2856, 1458, 1079, 742, 724 cm^{-1}.

HRMS EI (*m*/*z*): $[M]^+$ calcd for $C_{21}H_{44}OSi$, 340.3161; found 340.3163.

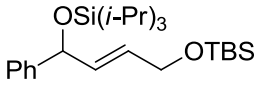

(*E*)-10,10-Diisopropyl-2,2,3,3,11-pentamethyl-8-phenyl-4,9-dioxa-3,10-disiladodec-6-ene. (**Table 3.4, Entry 3, Regioisomer 1)**

Following Procedure C, $Ni(COD)_2$ (20 mg, 0.073 mmol), IMes·HCl salt (20 mg, 0.059 mmol), *t*-BuOK (6.7 mg, 0.059 mmol), triisopropylsilane (0.24 mL, 1.18 mmol), *tert*-butyldimethyl(prop-2-yn-1-yloxy)silane (101 mg, 0.59 mmol), benzaldehyde (63 mg, 0.59 mmol) gave a crude residue which was purified via flash chromatography (100 % hexanes) to afford a single regioisomer in a >98:2 isolated regioselectivity (227 mg, 0.52 mmol, 88% yield).

^{1}H NMR (400 MHz, $CDCl_3$): δ 7.33–7.25 (m, 4H), 7.20–7.16 (m, 1H), 5.75–5.73 (m, 2H), 5.25 (d, *J* = 4.0 Hz, 1H), 4.13 (dd, *J* = 3.2 Hz, 0.8 Hz, 2H), 1.13–1.04 (m, 3H), 1.02 (d, *J* = 6.8 Hz, 9K), 0.98 (d, *J* = 6.8 Hz, 9H), 0.86 (s, 9H), 0.02 (d, *J* = 1.2 Hz, 6H).

^{13}C NMR (100 MHz, $CDCl_3$): δ 144.4, 134.1, 128.3, 128.1, 126.9, 126.0, 75.2, 63.2, 25.9, 18.3, 18.05, 18.01, 12.3, -5.2.

IR (thin film): ν 3085, 3062, 3026, 2944, 2891, 2865, 1471, 1463 cm^{-1}.

HRMS Electrospray (*m*/*z*): $[M+Na]^+$ calcd for $C_{25}H_{46}O_2Si_2Na$, 475.2934; found 457.2926.

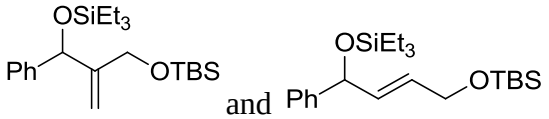

9,9-Diethyl-2,2,3,3-tetramethyl-6-methylene-7-phenyl-4,8-dioxa-3,9-disilaundecane. (**Table 3.4, Entry 3, Regioisomer 1)** and **(*E*)-10,10-diethyl-2,2,3,3-tetramethyl-8-phenyl-4,9-dioxa-3,10-disiladodec-6-ene** (**Table 3.4, Entry 3, Regioisomer 2)**.

Following Procedure D, $Ni(COD)_2$ (7.7 mg, 0.036 mmol), (+/-)-DP-IPr·BF_4 salt (19 mg, 0.030 mmol), *n*-BuLi (2.5 M in hexanes) (12 μL, 0.030 mmol), triethylsilane (0.96 mL, 0.60 mmol), *tert*-butyldimethyl(prop-2-yn-1-yloxy)silane (61 mg, 0.36 mmol), benzaldehyde (31 mg, 0.29 mmol) gave a crude residue which was purified via flash chromatography (100 % hexanes) to afford a mixture of regioisomers in a 84:16 isolated regioselectivity (85:15 crude regioselectivity) (99 mg, 25 mmol, 86% yield).

^{1}H NMR (400 MHz, $CDCl_3$): δ 7.33–7.17 (m, 5H), 5.75 (app t, *J* = 4.4 Hz, 0.15H), 5.26 (s, 0.85H), 5.21 (d, *J* = 0.8 Hz, 0.85H), 5.18 (d, *J* = 4.0 Hz, 0.15H), 5.14 (d, *J* = 1.2 Hz, 0.85H), 4.72 (s, 0.15H), 4.15 (d, *J* = 0.8 Hz, 0.3H), 4.10 (d, *J* = 14.8 Hz, 0.85H), 3.87 (d, *J* = 14.8 Hz, 0.85), 0.98 (t, *J* = 8.0 Hz, 1.35H), 0.92–0.85 (m, 16.65H), 0.63 (q, *J* = 8.0 Hz, 0.9H), 0.56 (q, *J* = 7.6 Hz, 5.1H), 0.02 (s, 0.9H), -0.04 (s, 2.55H), -0.05 (s, 2.55H)

^{13}C NMR (100 MHz, $CDCl_3$): δ 151.0, 144.0, 143.0, 133.5, 128.9, 128.0, 127.9, 127.0, 126.2, 126.0, 109.1, 75.6, 74.8, 63.2, 62.3, 25.8, 18.3, 6.8, 4.9, 4.8, 4.5, -5.3, -5.5.

IR (thin film): ν 3087, 3063, 3028, 2954, 2929, 2876, 2856, 1492, 1471, 1462 cm^{-1}.

HRMS Electrospray (*m*/*z*): $[M+Na]^+$ calcd for $C_{22}H_{40}O_2Si_2Na$, 415.2465; found 15.2458.

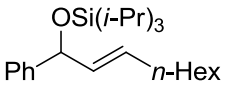

(*E*)-Triisopropyl[(1-phenylnon-2-en-1-yl)oxy]silane (Table 3.4, Entry 4, Regioisomer 1)

Following Procedure C, $Ni(COD)_2$ (20 mg, 0.073 mmol), IMes·HCl salt (20 mg, 0.059 mmol), *t*-BuOK (6.7 mg, 0.059 mmol), triisopropylsilane (0.24 mL, 1.18 mmol), 1-

octyne (67 mg, 0.59 mmol), benzaldehyde (63 mg, 0.59 mmol) gave a crude residue which was purified via flash chromatography (100 % hexanes) to afford a single regioisomer in a >98:2 isolated regioselectivity (97:3 crude regioselectivity) (191 mg, 0.50 mmol, 82% yield).

^{1}H NMR (400 MHz, $CDCl_3$): δ 7.35–7.33 (m, 2H), 7.30–7.26 (m, 2H), 7.21–7.17 (m, 1H), 5.64 (dt, *J* = 15.2 Hz, 6.8 Hz, 1H), 5.51 (dd, *J* = 15.2 Hz, 6.4 Hz, 1H), 5.19 (d, *J* = 6.8 Hz, 1H), 1.98 (app q, *J* = 6.8 Hz, 2H), 1.36–1.20 (m, 8H), 1.14–1.06 (m, 3H), 1.03 (d, *J* = 6.8 Hz, 9H), 1.00 (d, *J* = 6.8 Hz, 9H), 0.86 (t, *J* = 6.8 Hz, 3H).

^{13}C NMR (100 MHz, $CDCl_3$): δ 145.0, 134.2, 130.0, 128.0, 126.7, 125.9, 75.9, 32.1, 32.7, 29.2, 28.9, 22.6, 18.05, 18.04, 14.1, 12.3.

IR (thin film): ν 3085, 3062, 2956, 2940, 2926, 2865, 1491, 1463 cm^{-1}.

HRMS Electron Ionization (*m*/*z*): $[M]^+$ calcd for $C_{24}H_{42}OSi$, 374.3005; found 374.3007.

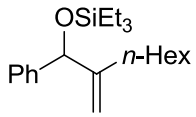

Triethyl[(2-methylene-1-phenyloctyl)oxy]silane (Table 3.4, Entry 4, Regioisomer 2)

Following Procedure D, $Ni(COD)_2$ (7.7 mg, 0.036 mmol), (+/-)-DP-IPr·BF_4 salt (19 mg, 0.030 mmol), *n*-BuLi (2.5 M in hexanes) (12 μL, 0.030 mmol), triethylsilane (0.96 mL, 0.60 mmol), 1-octyne (39.6 mg, 0.30 mmol), benzaldehyde (32 mg, 0.30 mmol) gave a crude residue which was purified via flash chromatography (100 % hexanes) to afford a mixture of regioisomers in a 93:7 isolated regioselectivity (88:22 crude regioselectivity) (71 mg, 0.21 mmol, 71% yield).

^{1}H NMR (400 MHz, $CDCl_3$): δ 7.36 (m, 2H), 7.31 (m, 2H), 7.23 (m, 1H), 5.22 (s, 1H), 5.14 (s, 1H), 4.87 (s, 1H), 1.95 (dt, *J* = 16.0 Hz, 7.5 Hz, 1H), 1.76 (dt, *J* = 16.0 Hz, 7.5 Hz, 1H), 1.39–1.20 (m, 8H), 0.93 (t, *J* = 7.5 Hz, 9H), 0.86 (t, *J* = 7.0 Hz, 3H), 0.59 (q, *J* = 8.0 Hz, 6H).

^{13}C NMR (100 MHz, $CDCl_3$): δ 152.0, 143.5, 127.8, 126.3, 109.2, 78.0, 31.7, 30.5, 29.1, 27.6, 22.5, 14.0, 6.77, 4.78.

IR (thin film): ν 3063, 3023, 2954, 2929, 2874, 2857, 1491, 1456 cm^{-1}.

HRMS Electrospray (*m*/*z*): $[M]^+$ calcd for $C_{21}H_{36}OSi$, 332.2535; found 332.2532.

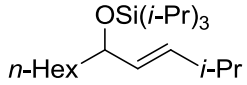

(*E*)-Triisopropyl[(2-methylundec-3-en-5-yl)oxy]silane (Table 3.4, Entry 5, Regioisomer 1)

Following Procedure C, $Ni(COD)_2$ (20 mg, 0.073 mmol), IMes·HCl salt (20 mg, 0.059 mmol), *t*-BuOK (6.7 mg, 0.059 mmol), triisopropylsilane (0.24 mL, 1.18 mmol), 3-methylbut-1-yne (41 mg, 0.59 mmol), 1-heptanal (68 mg, 0.59 mmol) gave a crude residue which was purified via flash chromatography (100 % hexanes) to afford a single regioisomer in a >98:2 isolated regioselectivity (97:3 crude regioselectivity) (155 mg, 0.46 mmol, 74% yield).

^{1}H NMR (400 MHz, $CDCl_3$): δ 5.44 (dd, J = 16.0 Hz, 6.8 Hz, 1H), 5.31 (ddd, *J* = 15.6 Hz, 7.6 Hz, 1.2 Hz, 1H), 4.08 (td, *J* = 6.8 Hz, 5.6 Hz, 1H), 2.24 (dsept, *J* = 7.6 Hz, 6.8 Hz, 1H), 1.58–1.35 (m, 2H), 1.31–1.17 (m, 8H), 1.06–1.00 (m, 21H), 0.95 (dd, *J* = 7.2 Hz, 2.8 Hz, 6H), 0.86 (t, *J* = 7.2 Hz).

^{13}C NMR (100 MHz, $CDCl_3$): δ 137.4, 130.8, 74.2, 38.8, 31.9, 30.6, 29.4, 25.0, 22.6, 22.4, 22.2, 18.16, 18.12, 14.1, 12.4.

IR (thin film): ν 2958, 2929, 2865, 1464 cm^{-1}.

HRMS Electron Ionization (*m*/*z*): $[M–i\text{-}Pr]^+$ calcd for $C_{18}H_{37}OSi$, 297.2614; found 297.2622.

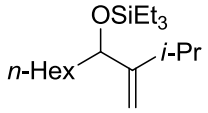

Triethyl[(2-methyl-3-methylenedecan-4-yl)oxy]silane (**Table 3.4, Entry 5, Regioisomer 2**)

Following Procedure D, $Ni(COD)_2$ (7.7 mg, 0.036 mmol), (+/-)-DP-IPr·BF_4 salt (19 mg, 0.030 mmol), *n*-BuLi (2.5 M in hexanes) (12 μL, 0.030 mmol), triethylsilane (0.96 mL, 0.60 mmol), 3-methylbut-1-yne (26 mg, 38 mmol), 1-heptanal (34 mg, 0.30 mmol) gave a crude residue which was purified via flash chromatography (100 % hexanes) to afford a

single regioisomer in a >98:2 isolated regioselectivity (95:5 crude regioselectivity) (68 mg, 23 mmol, 76% yield).

^{1}H NMR (400 MHz, $CDCl_3$): δ 4.94 (s, 1H), 4.78 (s, 1H), 4.01 (t, *J* = 5.6 Hz, 1H), 2.20 (sept, *J* = 6.8 Hz, 1H), 1.50–1.34 (m, 2H), 1.30–1.14 (m, 8H), 1.02 (d, *J* = 7.2 Hz, 3H), 0.99 (d, *J* = 6.8 Hz, 3H), 0.91 (t, *J* = 8.0 Hz, 9H), 0.84 (t, *J* = 6.8 Hz, 3H), 0.54 (q, *J* = 7.6 Hz, 6H).

^{13}C NMR (100 MHz, $CDCl_3$): δ 158.6, 106.8, 75.7, 37.2, 31.8, 29.3, 29.0, 25.6, 23.8, 23.0, 22.6, 14.0, 6.9, 4.9.

IR (thin film): ν 2957, 2923, 2875, 1459 cm^{-1}.

HRMS Electrospray (*m*/*z*): $[M]^+$ calcd for $C_{18}H_{38}OSi$, 298.2692; found 298.2684.

5.4 Chapter 4 Experimental

5.4.1 Chapter 4 Ligand Synthesis

Ligand **L15** was prepared following the preparation as described in reference 72.

Ligands **L19-L22** are described in Hasnain Malik's thesis.

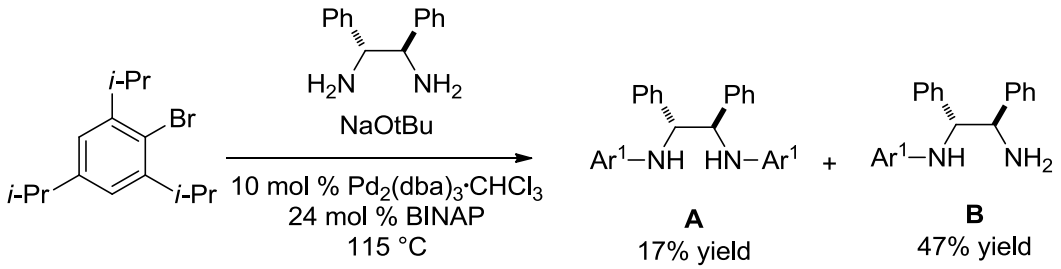

(1*R*,2*R*)-1,2-diphenyl-N1,N2-bis(2,4,6-triisopropylphenyl)ethane-1,2-diamine and **(1*R*,2*R*)-1,2-diphenyl-N1-(2,4,6-triisopropylphenyl)ethane-1,2-diamine:**

(1*R*,2*R*)-1,2-diphenylethane-1,2-diamine (250 mg, 1.18 mmol), $Pd_2(dba)_3CHCl_3$ (122 mg, 0.118 mmol), BINAP (178 mg, 0.283 mmol), and NaO*t*-Bu (340 mg, 3.54 mmol) were placed in a vial followed by 2-bromo-1,3,5-triisopropylbenzene (1.33 g, 4.71 mmol). The vial was sealed then heated to 115 ˚C for 20 h. The reaction was then allowed to cool to rt, dissolved in ethyl acetate and ran through a plug of silica, flushing with 1:1 ethyl acetate/hexane. Column chromatography (SiO_2) at 1:99 ethyl acetate/hexanes until product **A** was removed (rf 0.6 in 8% ethyl acetate/hexanes), followed by a ramp to 1:9 ethyl acetate/hexanes until the column no longer had impurities being removed, followed

by 1:4 ethyl acetate/hexanes at which time product **B** eluted from the column. Repeated chromatography may be required to isolate product **A**, small amounts of impurities were carried forward.

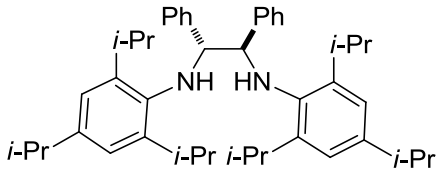

(1*R*,2*R*)-1,2-diphenyl-*N*^{1},*N*^{2}-bis(2,4,6-triisopropylphenyl)ethane-1,2-diamine

^{1}H (500 MHz, $CDCl_3$) δ 7.2-7.0 (m, 10 H), 6.89 (s, 4 H), 4.57 (s, 2 H), 4.2 (s, 2 H), 3.18 (sept, *J* = 6.5 Hz, 2 H), 2.92 (sept, *J* = 6.5 Hz, 1 H). 1.26 (m, 24 H), 0.90, (d, *J* = 7.0 Hz, 12 H).

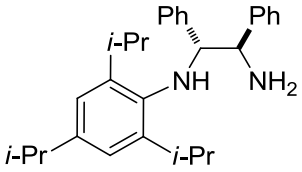

(1*R*,2*R*)-1,2-diphenyl-*N*^{1}-(2,4,6-triisopropylphenyl)ethane-1,2-diamine

^{1}H (500 MHz, $CDCl_3$) δ 7.28-7.00 (m, 10 H), 6.81 (s, 2 H), 4.50 (d, *J* = 8 Hz, 1 H), 4.16 (d, *J* = 8 Hz, 1 H), 3.16 (sept, *J* = 6.5 Hz, 2 H), 2.88 (sept, *J* = 6.5 Hz, 1 H), 2.32 (bs, 2 H), 1.2 (d, *J* = 7 Hz, 12 H), 0.89 (d, *J* = 7 Hz, 6 H).

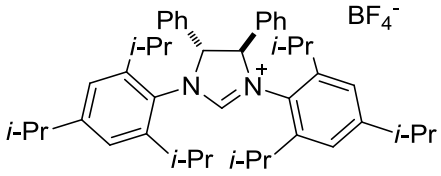

(*4R*,*5R*)-4,5-diphenyl-1,3-bis(2,4,6-triisopropylphenyl)-4,5-dihydro-1*H*-imidazol-3-ium tetrafluoroborate (L14•HBF$_4$)

(1*R*,2*R*)-1,2-diphenyl-*N*^{1},*N*^{2}-bis(2,4,6-triisopropylphenyl)ethane-1,2-diamine (110 mg, 0.18 mmol) was heated to 120 ˚C for 16 h with formic acid (1 drop), triethyl orthoformate (267 mg, 1.8 mmol) and ammonium tetrafluoroborate (18.6 mg, 0.18 mmol). The resulting crude mixture was then concentrated, followed by column chromatography (SiO_2, 1:66 methanol/CH_2Cl_2, rf = 0.2 at 1:20 methanol/ethyl acetate). The imidazolium salt (72 mg, 56% yield) was then dried under vacuum at 50 ˚C for 12 h.

^{1}H (500 MHz, $CDCl_3$) δ 8.68 (s, 1H), 7.43-7.41 (m, 4H), 7.30-7.27 (m, 6H), 7.00 (s, 2H), 6.82 (s, 2H), 5.86 (s, 2H), 3.23 (sept, *J* = 6.5 Hz, 2H), 2.90 (sept, *J* = 7.0 Hz, 2H), 2.65 (sept, *J* = 7.0 Hz, 2H), 1.73 (d, *J* = 7.0 Hz, 6H), 1.47 (d, *J* = 6.5 Hz, 6H), 1.25 (ap. dd, *J* = 6.5 Hz, 2.0 Hz, 12H) , 1.23 (d, *J* = 7.0 Hz, 6H), 0.40 (d, *J* = 6.4 Hz, 6H).

^{13}C NMR (125 MHz, $CDCl_3$): δ 158.56, 152.23, 146.99, 145.31, 130.87, 130.19, 129.74, 129.06, 125.39, 122.99, 122.80, 74.37, 34.16, 29.98, 29.67, 25.48, 25.02, 24.76, 23.73, 23.69, 22.12.

IR (thin film): 2960, 2927, 2868, 2614, 1460, 697 cm-1.

HRMS Electrospray (*m*/*z*): $[M-BF4]^+$ calcd for $C_{45}H_{59}N_2^+$, 627.4673; found 627.4676.

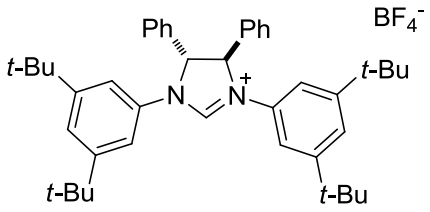

(4*R*,5*R*)-1,3-bis(3,5-di-tert-butylphenyl)-4,5-diphenyl-4,5-dihydro-1H-imidazol-3-ium tetrafluoroborate (L16•HBF_4)

(1*R*,2*R*)-1,2-diphenylethane-1,2-diamine (150 mg, 0.71 mmol), $Pd_2(dba)_3CHCl_3$ (36.6 mg, 0.035 mmol), BINAP (53.3 mg, 0.0848 mmol), and NaO*t*-Bu (203.5 mg, 2.12 mmol) were placed in a round bottom followed by 1-bromo-3,5-di-tert-butylbenzene (152 mg, 1.77 mmol) and toluene (2 mL). The reaction was heated to 90 ˚C for 48 h (only 20 h required). The reaction was then allowed to cool to rt, dissolved in 1:1 ethyl acetate/hexane and ran through a plug of silica, flushing with 1:1 ethyl acetate/hexane, and concentrated. The *N*-arylated intermediate (170 mg, 80%) was isolated after column chromatography (SiO_2, 1:99 ethyl acetate/hexanes). The *N*-arylated intermediate (95 mg, 0.154 mmol) was then heated to 120 ˚C for 16 h with formic acid (1 drop), triethyl orthoformate (228 mg, 1.54 mmol) and ammonium tetrafluoroborate (16 mg, 0.154 mmol). The resulting crude mixture was then concentrated, followed by column chromatography (SiO_2, 1:66 methanol/CH_2Cl_2, rf = 0.2 in 1:20 methanol/ CH_2Cl_2). **L16•HBF_4** (115 mg, 96% yield) was then dried under vacuum at 50 ˚C for 12 h.

^{1}H (500 MHz, $CDCl_3$) δ 9.41 (s, 1H), 7.45-7.39 (m, 5H), 7.32 (s, 2H), 7.18 (s, 4H), 5.72 (s, 2H), 1.24 (s, 36H).

^{13}C NMR (100 MHz, $CDCl_3$): δ 153.28, 134.84, 133.93, 130.00, 129.89, 127.31, 122.679, 115.953, 75.23, 35.09, 31.06.

IR (thin film): 2958, 2868, 1622, 1584, 1059, 701 cm^{-1}.

HRMS Electrospray (*m*/*z*): $[M-BF4]^+$ calcd for $C_{43}H_{55}N_2^+$, 599.4360; found 599.4372.

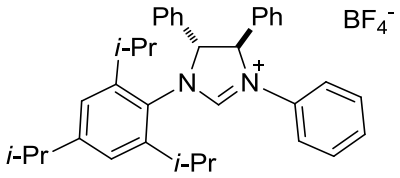

(4*R*,5*R*)-3,4,5-triphenyl-1-(2,4,6-triisopropylphenyl)-4,5-dihydro-1H-imidazol-3-ium tetrafluoroborate (**L17•HBF_4**)

(1*R*,2*R*)-1,2-diphenyl-N^1-(2,4,6-triisopropylphenyl)ethane-1,2-diamine (180 mg, 0.44 mmol), $Pd_2(dba)_3CHCl_3$ (22.5 mg, 0.022 mmol), BINAP (32.8 mg, 0.0522 mmol), and NaO*t*-Bu (62.6 mg, 0.65 mmol) were placed in a round bottom followed by bromobenzene (152 mg, 1.77 mmol) and toluene (2 mL). The reaction was heated to 90 ˚C for 48 h (only 20 h required). The reaction was then allowed to cool to rt, dissolved in 1:1 ethyl acetate/hexane and ran through a plug of silica, flushing with 1:1 ethyl acetate/hexane, and concentrated. The *N*-arylated intermediate (325 mg, 78%) was isolated after column chromatography (SiO_2, 1:99 ethyl acetate/hexanes, rf = 0.4 in 1:20 ethyl acetate/hexanes). The *N*-arylated intermediate (135 mg, 0.276 mmol) was then heated to 120 ˚C for 16 h with formic acid (1 drop), triethyl orthoformate (408 mg, 2.76 mmol) and ammonium tetrafluoroborate (29 mg, 0.276 mmol). The resulting crude mixture was then concentrated, followed by column chromatography (SiO_2, 1:66 methanol/CH_2Cl_2, rf = 0.25 in 1:20 methanol/ CH_2Cl_2, UV active, streaking appearance on TLC). The imidazolium salt **L17•HBF_4** (140 mg, 86% yield) was then dried under vacuum at 50 ˚C for 12 h.

^{1}H (400 MHz, $CDCl_3$) δ 9.16 (s, 1H), 7.53 (d, *J* = 8.0 Hz, 2H), 7.43-7.38 (m, 10H), 7.28-7.24 (m, 3H), 7.02 (d, *J* = 1.6 Hz, 1H), 6.81 (d, *J* = 1.6 Hz, 1H), 6.35 (d, *J* = 6.8 Hz, 1H),

5.11 (d, *J* = 7.2 Hz), 2.90-2.78 (m, 2H), 2.45 (sept, *J* = 6.8 Hz, 1H), 1.35 (d, *J* = 6.8 Hz, 3H), 1.20-1.15 (m, 9H), 1.10 (d, *J* = 6.8 Hz, 3H), 0.27 (d, *J* = 6.8 Hz, 3H).

^{13}C NMR (100 MHz, $CDCl_3$): δ 155.10, 151.85, 146.47, 145.32, 135.40, 134.27, 132.49, 130.82, 130.34, 130.04, 129.96, 129.77, 128.81, 128.35, 125.97, 125.41, 122.95, 122.74, 120.32,78.57, 70.91, 34.07, 29.02, 28.90, 25.64, 24.71, 23.98, 23.67, 23.63, 22.51.

IR (thin film): 2964, 2932, 2869, 1617, 1593, 1457, 1059, 757, 699, 665 cm^{-1}.

HRMS Electrospray (*m*/*z*): $[M-BF4]^+$ calcd for $C_{36}H_{41}N_2^+$, 501.3264, 501.3268.

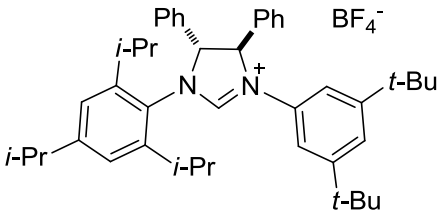

(4*R*,5*R*)-3-(3,5-di-tert-butylphenyl)-4,5-diphenyl-1-(2,4,6-triisopropylphenyl)-4,5-dihydro-1H-imidazol-3-ium tetrafluoroborate (L18•HBF$_4$)

(1*R*,2*R*)-1,2-diphenyl-*N*^{1}-(2,4,6-triisopropylphenyl)ethane-1,2-diamine (125 mg, 0.453 mmol), $Pd_2(dba)_3CHCl_3$ (15.6 mg, 0.015 mmol), BINAP (22.8 mg, 0.0363 mmol), and NaO*t*-Bu (43.5 mg, 0.453 mmol) were placed in a round bottom followed by 1-bromo-3,5-di-tert-butylbenzene (152 mg, 1.77 mmol) and toluene (2 mL). The reaction was heated to 90 ˚C for 48 h (only 20 h required). The reaction was then allowed to cool to rt, dissolved in 1:1 ethyl acetate/hexane and ran through a plug of silica, flushing with 1:1 ethyl acetate/hexane, and concentrated. The *N*-arylated intermediate (115 mg, 63%) was isolated by column chromatography (SiO_2, 1:66 ethyl acetate/hexanes, rf = 0.45 in 1:20 ethyl acetate/hexanes). [1H (500 MHz, $CDCl_3$) δ] The *N*-arylated intermediate (90 mg, 0.149 mmol) was then heated to 120 ˚C for 20 h with formic acid (1 drop), triethyl orthoformate (220 mg, 1.49 mmol) and ammonium tetrafluoroborate (16 mg, 0.15 mmol). The resulting crude mixture was then concentrated, followed by column chromatography (SiO_2, 1:66 methanol/CH_2Cl_2, rf = 0.25 in 1:20 methanol/ CH_2Cl_2). The imidazolium salt **L18•HBF$_4$** (70 mg, 67% yield) was then dried under vacuum at 50 ˚C for 12 h. Compound contained an impurity that prevented publication quality characterization, and seemed to be produced by additional chromatography.

^{1}H (400 MHz, $CDCl_3$) δ 9.03 (s, 1H), 7.45-6.80 (m, 15H), 6.31 (d, *J* = 8.0 Hz, 1H), 5.18 (d, *J* = 8.0 Hz, 1H), 2.98 (sept, *J* = 6.8 Hz, 1H), 2.81 (sept, *J* = 6.8 Hz, 1H), 2.55 (sept, *J* = 6.8 Hz, 1H), 1.38 (d, *J* = 6.8 Hz, 3H), 1.24-1.11 (m, 30H), 0.31 (d, *J* = 6.8 Hz, 3H).

5.4.2 Reductive Coupling Products

General Procedure (A) for the Ni(COD)$_2$/Ligand-Promoted Reductive Coupling of Alkynes, Aldehydes, and Triethylsilane using Butyl Lithium as a Base:

To a solid mixture of $Ni(COD)_2$ (12 mol %), **L•HBF$_4$** salt (10 mol %) was added THF (0.2 M). To the resulting solution was added *n*-BuLi (1.6 M in hexanes) (10 mol %). The resulting solution was stirred for 5 min at rt until the solution turned dark red in appearance. Silane (2.0 equiv) was then added to the reaction mixture. The alkyne (1.2 equiv), aldehyde (1.0 equiv), and THF (0.2 M) were added via syringe pump addition over 30 minutes and the reaction mixture was allowed to stir until starting materials were consumed. The reaction mixture was filtered through silica gel eluting with 50% EtOAc/hexanes. The solvent was removed *in vacuo*, and the crude residue was purified via flash chromatography on silica gel to afford the desired product.

General Procedure (B) for the Ni(COD)$_2$/Ligand-Promoted Reductive Coupling of Alkynes, Aldehydes, and Triethylsilane using *t*-BuOK as a Base:

To a solid mixture of $Ni(COD)_2$ (12 mol %), **L•HBF$_4$** salt (10 mol %), *t*-BuOK (10 mol %) was added THF (0.2 M). The resulting solution was stirred for 5 min at rt until the solution turned dark red in appearance. Silane (2.0 equiv) was then added to the reaction mixture. The alkyne (1.2 equiv), aldehyde (1.0 equiv), and THF (0.2 M) were added via syringe pump addition over 30 minutes and the reaction mixture was allowed to stir until starting materials were consumed. The reaction mixture was filtered through silica gel eluting with 50% EtOAc/hexanes. The solvent was removed *in vacuo*, and the crude residue was purified via flash chromatography on silica gel to afford the desired product.

TBAF desilylation to produce free alcohols:

Allylic silyl ether was stirred for 2 hours at rt with THF (1 mL/0.1 mmol) and 1 M TBAF in THF (3 equiv). Aqueous workup with sat. $NaHCO_3$,followed by extractions with ethyl

acetate. Organic layer was dried with $MgSO_4$ and concentrated, followed by column chromatography.

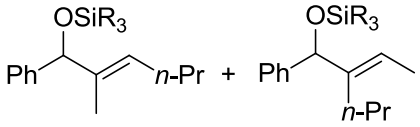

(*E*)-trialkyl((2-methyl-1-phenylhex-2-en-1-yl)oxy)silane (**Table 4.2, regioisomer 1**) and **(*E*)-trialkyl((2-ethylidene-1-phenylpentyl)oxy)silane** (**Table 4.2, regioisomer 2**) Characterization of the (t-Bu)$_2$SiH- adduct is described in reference 68. Chiral HPLC conditions were optimal at 2% *i*PrOH in Hexanes, 1 mL/min on the chiralcel OD-H.

Reaction with **L14**:

General Conditions B. $Ni(COD)_2$ (6.6 mg, 0.024 mmol), **L14**-HBF_4 (14.3 mg, 0.02 mmol), *t*-BuOK (2.24 mg, 0.02 mmol), benzaldehyde (20 mg, 0.19 mmol), 2-hexyne (19.7 mg, 0.24 mmol), Et_3SiH (46.4 mg, 0.40 mmol), THF (2 mL). Isolated product with 2:>98 regioselectivity (5:95 crude regioselectivity)(45 mg, 0.15 mmol, 79% yield). Chiral HPLC analysis of the free alcohol indicated 75% *ee*, and 36% *ee* respectively.

Reaction with **L15**:

General Conditions A. $Ni(COD)_2$ (9.86 mg, 0.036 mmol), **L15**-HBF_4 (20.6 mg, 0.03 mmol), BuLi (19 uL, 0.03 mmol), benzaldehyde (31.8 mg, 0.3 mmol), 2-hexyne (29.5 mg, 0.36 mmol), (t-Bu)$_2SiH_2$ (86.4 mg, 0.60 mmol), THF (3 mL). Isolated products as a 89:11 mixture of regioisomers (88:12 crude regioselectivity)(12 mg, 0.03 mmol, 10% yield). Chiral HPLC analysis of the free alcohol indicated 79% *ee*, and 73% *ee* respectively.

Reaction with **L16**:

General Conditions A. $Ni(COD)_2$ (9.86 mg, 0.036 mmol), **L16**-HBF_4 (18.9 mg, 0.03 mmol), BuLi (19 uL, 0.03 mmol), benzaldehyde (31.8 mg, 0.3 mmol), 2-hexyne (29.5 mg, 0.36 mmol), (i-Pr)$_3SiH$ (94.8 mg, 0.60 mmol), THF (3 mL). Isolated trace product

(80:20 crude regioselectivity). Chiral HPLC analysis of the free alcohol indicated 42% *ee*, and 46% *ee* respectively.

Reaction with **L17**:

General Conditions B. $Ni(COD)_2$ (6.6 mg, 0.024 mmol), **L17**-HBF_4 (12 mg, 0.02 mmol), *t*-BuOK (2.24 mg, 0.02 mmol), benzaldehyde (21.2 mg, 0.20 mmol), 2-hexyne (19.7 mg, 0.24 mmol), Et_3SiH (46.4 mg, 0.40 mmol), THF (2 mL). Isolated a 32:68 mixture of regioisomers (34:66 crude regioselectivity)(7 mg, 0.024 mmol, 12% yield). Chiral HPLC analysis of the free alcohol indicated 34% *ee*, and 32% *ee* respectively.

Reaction with **L18**:

General Conditions B. $Ni(COD)_2$ (6.6 mg, 0.024 mmol), **L18**-HBF_4 (14 mg, 0.02 mmol), *t*-BuOK (2.24 mg, 0.02 mmol), benzaldehyde (21.2 mg, 0.20 mmol), 2-hexyne (19.7 mg, 0.24 mmol), Et_3SiH (46.4 mg, 0.40 mmol), THF (2 mL). Isolated a 55:45 mixture of regioisomers (55:45 crude regioselectivity)(10 mg, 0.032 mmol, 16% yield). Chiral HPLC analysis of the free alcohol indicated 31% *ee*, and 16% *ee* respectively.

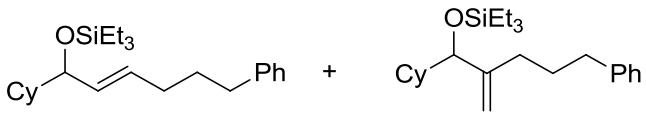

(E)-((1-cyclohexyl-6-phenylhex-2-en-1-yl)oxy)triethylsilane (**Scheme 4.6, regioisomer 1**) and **((1-cyclohexyl-2-methylene-5-phenylpentyl)oxy)triethylsilane** (**Scheme 4.6, regioisomer 2**)

Chiral HPLC conditions were optimal at 1% *i*PrOH in Hexanes, 0.5 mL/min on the chiralcel OD-H. Solvent system should be premixed, as the HPLC's pumps are not accurate at or below 1%. Previous HPLC separation of the linear product is described in reference 73. Regioisomer 1 was characterized as the free alcohol.

(E)-((1-cyclohexyl-6-phenylhex-2-en-1-yl)oxy)triethylsilane (**Scheme 4.6, regioisomer 1**)

The free alcohol matched the literature reference 73.

1-cyclohexyl-2-methylene-5-phenylpentan-1-ol (Scheme 4.6, regioisomer 2)

^{1}H (500 MHz, $CDCl_3$) δ 7.30 (t, *J* = 7.5 Hz, 4H), 7.22-7.18 (m, 6H), 4.89 (s, 1H), 4.83 (d, *J* = 2.0 Hz, 1H), 3.71 (d, *J* = 7.5 Hz, 1H), 2.67 (t, *J* = 7.5 Hz, 2H), 2.20-2.16 (m, 1H), 1.99-1.62 (m, 8H), 1.48-1.42 (m, 1H), 1.4-1.1 (m, 4H), 0.94 (t, *J* = 8 Hz, 9H), 0.92-0.85 (m, 2H), 0.57 (q, *J* = 8 Hz, 6H).

^{13}C NMR (100 MHz, $CDCl_3$): δ 150.386, 142.59, 128.38, 128.25, 125.65, 110.29, 82.12, 41.35, 36.03, 29.92, 29.47, 29.36, 28.93, 26.60, 26.31, 26.18, 6.96, 4.88.

IR (thin film): 2929, 2870, 2847, 2641, 1448, 1057, 665 cm^{-1}.

HRMS EI (*m*/*z*): $[M]^+$ calcd for $C_{24}H_{40}OSi$, 372.2848, observed 372.2842.

Reaction with **(+/-)-DP-IPr**:

General Conditions B. $Ni(COD)_2$ (9.9 mg, 0.036 mmol), **(+/-)-DP-IPr** -HBF_4 (18.9 mg, 0.03 mmol), *t*-BuOK (3.36 mg, 0.03 mmol), cyclohexylcarboxaldehyde (51.9 mg, 0.30 mmol), pent-4-yn-1-ylbenzene (51.9 mg, 0.36 mmol), Et_3SiH (69.9 mg, 0.60 mmol), THF (3 mL). Isolated a 36:64 mixture of regioisomers (37:63 crude regioselectivity)(83 mg, 0.25 mmol, 83% yield).

Reaction with **L14**:

General Conditions B. $Ni(COD)_2$ (6.6 mg, 0.024 mmol), **L14**-HBF_4 (14.3 mg, 0.02 mmol), *t*-BuOK (2.24 mg, 0.02 mmol), cyclohexylcarboxaldehyde (33.6 mg, 0.30 mmol), pent-4-yn-1-ylbenzene (51.9 mg, 0.36 mmol), Et_3SiH (69.9 mg, 0.60 mmol), THF (3 mL). Isolated a 50:50 mixutre of regioisomers (50:50 crude regioselectivity) (51 mg, 0.21 mmol, 69% yield). Chiral HPLC analysis of the free alcohol indicated 11% *ee*, and 47% *ee* respectively.

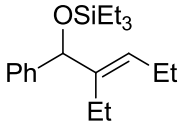

(E)-triethyl((2-ethyl-1-phenylpent-2-en-1-yl)oxy)silane.

Characterization of this product is described in reference 58.

Chiral HPLC conditions were optimal at 0.5% *i*PrOH/ Hexanes, 1 mL/min on the chiralcel OD-H. Solvent system should be premixed, as the HPLC's pumps are not accurate at or below 1%. Previous HPLC separation is described in reference 73.

Reaction with **L14**:

General Conditions B. $Ni(COD)_2$ (6.6 mg, 0.024 mmol), **L14**-HBF_4 (14 mg, 0.02 mmol), *t*-BuOK (2.2 mg, 0.02 mmol), benzaldehyde (21.2 mg, 0.20 mmol), 3-hexyne (19.7 mg, 0.24 mmol), Et_3SiH (46.4 mg, 0.40 mmol), THF (2 mL). Isolated product (50 mg, 0.16 mmol, 82% yield). Chiral HPLC analysis of the free alcohol indicated 72% *ee*.

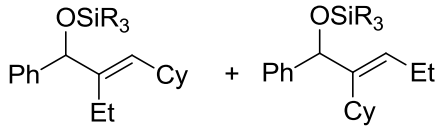

(E)-(2-(cyclohexylmethylene)-1-phenylbutoxy)triethylsilane (Table 4.3, Regioisomer 1) and **(E)-((2-cyclohexyl-1-phenylpent-2-en-1-yl)oxy)triisopropylsilane** (Table 4.3, Regioisomer 2)

Chiral HPLC conditions were optimal at 0.05% *i*PrOH/ Hexanes, 1 mL/min on the chiralcel OD-H. Such low concentrations must be made as a solution as the HPLC pumps are not accurate at or below 1%.

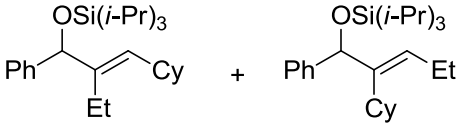

(E)-((2-cyclohexyl-1-phenylpent-2-en-1-yl)oxy)triisopropylsilane (major) and (E)-(2-(cyclohexylmethylene)-1-phenylbutoxy)triisopropylsilane (minor)

Characterized as a mixture of 3:1 regioisomers.

^1H (500 MHz, $CDCl_3$) δ 7.37 (d, *J* = 7.0 Hz, 2H), 7.29-7.25 (m, 2H), 7.21-7.17 (m, 1H), 5.60 (t, *J* = 7.5 Hz, 0.25H, minor), 5.46 (d, *J* = 10.0 Hz, 0.75H, major), 5.16 (s, 0.75H, major), 5.15 (s, 0.25H, minor), 2.23-2.06 (m, 1.5H), 1.98-1.85 (m, 1.5H), 1.78-1.40 (m, 5H), 1.34-0.99 (m, 29.75H), 0.71 (t, *J* = 7.5 Hz, 2.25H).

^{13}C NMR (100 MHz, $CDCl_3$): δ 144.55, 141.37, 132.11, 128.10, 127.58, 127.44, 126.52, 126.43, 126.19, 79.686, 79.36, 38.59, 36.61, 33.47, 33.20, 31.95, 31.53, 27.28, 27.22, 26.23, 26.13, 25.96, 21.71, 19.62, 18.08, 18.03, 14.82, 14.62, 12.31, 12.27.

IR (thin film): 2925, 2865, 1465, 1448, 1060, 882, 700, 665 cm^{-1}.

HRMS EI (*m*/*z*): $[M]^+$ predicted for $C_{26}H_{44}OSi$, 400.3161, observed 400.3162.

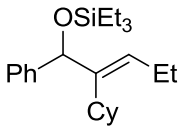

(E)-(2-(cyclohexylmethylene)-1-phenylbutoxy)triethylsilane

^{1}H (400 MHz, $CDCl_3$) δ 7.33 (d, *J* = 7.6 Hz, 2H), 7.25 (t, *J* = 7.6 Hz, 2H), 7.20 (t, *J* = 7.6 Hz, 1H), 5.51 (t, *J* = 7.2 Hz, 1H), 5.05 (s, 1H), 2.21-2.05 (m, 3H), 1.92-0.85 (m 22H), 0.60 (q, *J* = 7.5 Hz, 6H).

^{13}C NMR (100 MHz, $CDCl_3$): δ 144.59, 144.19, 128.59, 127.54, 126.63, 126.48, 78.83, 38.99, 32.07, 31.71, 27.21, 26.22, 21.54, 14.62, 6.87, 4.90.

IR (thin film): 2921, 2866, 2849, 1651, 1444, 694 cm^{-1}.

HRMS EI (*m*/*z*): $[M]^+$ predicted for $C_{23}H_{38}OSi$, 358.2692, observed 358.2688.

Reaction with **(+/-)-DP-IPr**:

General Conditions B. $Ni(COD)_2$ (6.6 mg, 0.024 mmol), **(+/-)-DP-IPr** -HBF_4 (14 mg, 0.02 mmol), *t*-BuOK (2.2 mg, 0.02 mmol), benzaldehyde (21.2 mg, 0.20 mmol), but-1-yn-1-ylcyclohexane (32.7 mg, 0.24 mmol), Et_3SiH (46.4 mg, 0.40 mmol), THF (2 mL). Isolated a 2:>98 mixture of regioisomers (5:95 crude regioselectivity) (42 mg, 0.11 mmol, 56% yield).

Reaction with **L14**:

Note: Lower catalyst loading was used.

General Conditions B. $Ni(COD)_2$ (6.6 mg, 0.024 mmol), **L14**-HBF_4 (7 mg, 0.01 mmol), *t*-BuOK (2.2 mg, 0.02 mmol), benzaldehyde (21.2 mg, 0.20 mmol), but-1-yn-1-ylcyclohexane (32.7 mg, 0.24 mmol), Et_3SiH (46.4 mg, 0.40 mmol), THF (2 mL). Isolated a 90:10 mixture of regioisomers (92:8 crude regioselectivity)(20 mg, 0.056

mmol, 28% yield). Chiral HPLC analysis of the free alcohol indicated 82% *ee* for the major product.

Reaction with **IMes**:

General Conditions B. $Ni(COD)_2$ (3.3 mg, 0.012 mmol), **IMes**-HBF_4 (3.4 mg, 0.01 mmol), *t*-BuOK (1.1 mg, 0.01 mmol), benzaldehyde (10.6 mg, 0.10 mmol), but-1-yn-1-ylcyclohexane (15.2 mg, 0.12 mmol), Et_3SiH (23.2 mg, 0.20 mmol), THF (1 mL). Isolated products as a 78:22 mixture of regioisomers (78:22 crude regioseletctivity) (32 mg, 0.075 mmol, 75%).

Reaction with **L15**:

General Conditions B. $Ni(COD)_2$ (13.2 mg, 0.048 mmol), **L15**-HBF_4 (27.5 mg, 0.04 mmol), *t*-BuOK (4.5 mg, 0.04 mmol), benzaldehyde (21.2 mg, 0.20 mmol), but-1-yn-1-ylcyclohexane (32.7 mg, 0.24 mmol), Et_3SiH (46.4 mg, 0.40 mmol), THF (2 mL). Isolated trace product (>97:3 crude regiochemistry). Chiral HPLC analysis of the free alcohol indicated 90% *ee* for the major product.

References

1. Chrovian, C. C.; Knapp-Reed, B.; Montgomery, J. *Org. Lett.* **2008**; *10*, 811.
2. Tang, X. Q.; Montgomery, J. *J. Am. Chem. Soc.* **2000**, *122*, 6950.
3. Godleski, S. A. In *Comprehensive Organic Synthesis*; Trost, B. M.; Fleming, I., Ed.; Pergamon: Oxford 1991; Vol. 4, p 585.
4. Johnson, R. A.; Sharpless, K. B. In *Comprehensive Organic Synthesis*; Trost, B. M.; Fleming, I., Ed.; Pergamon: Oxford 1991; Vol. 7, p 389.
5. Denmark, S. E.; O'Conner, S. P. *J. Org. Chem.* **1997**, *62*, 584.
6. Charette, A. B.; Marcoux, J. F. *Synlett*, **1995**, 1197.
7. Overman, L. E.; *Acc. Chem. Res.* **1992**, *25*, 352.
8. Lipshutz, B. H.; Sengupta, S. In *Organic Reactions*; Paquette, L. A. Ed.; Wiley: New York 1992; Vol. 41, p 135.
9. Wipf, P. In *Comprehensive Organic Synthesis*; Trost, B. M. Ed.; Pergamon: Oxford 1991; Vol 5, p 827.
10. Jin, H.; Uenishi, J.; Christ, W. J.; Kishi, Y. *J. Am. Chem. Soc.* **1986**, *108*, 5644.
11. Takai, K.; Tagashira, M.; Kuroda, T.; Oshima, K.; Utimoto, K.; Nozaki, H. *J. Am. Chem. Soc.* **1986**, *108*, 6048.
12. Hargaden, G. C.; Guiry, P. J. *Adv. Synth. Catal.* **2007**, *349*, 2407.
13. Furstner, N.; Shi, J. *J. Am. Chem. Soc.* **1996**, *118*, 12349.
14. Montgomery, J.; Sormunen, G. J. In *Topics in Current Chemistry*; Krische, M. J. Ed.; Springer: Berlin 2007; Vol. 279, p 1.
15. Oppolzer, W.; Radinov, R. N. *Helv. Chim. Acta.* **1992**, *75*, 170.
16. Oppolzer, W.; Radinov, R. N. *J. Am. Chem. Soc.* **1993**, *115*, 1593.
17. Wipf, P.; Xu, W. *Tetrahedron Lett.* **1994**, *35*, 5197.
18. Wipf P.; Xu, W. *Org. Synth. Coll.* **1998**, *9*, 143.
19. Okukado, N.; Negishi, E. *Tetrahedron Lett.* **1978**, *19*, 2357.
20. Bahadoor, A. B.; Micalizio G. C. *J. Am. Chem. Soc.* **2005**, *127*, 3694.
21. Shimp, H. L.; Micalizio G. C. *Org. Lett.* **2005**, *7*, 5111.
22. Bahadoor, A. B.; Micalizio G. C. *Org. Lett.* **2006**, *8*, 1181.
23. Crowe, W. E.; Rachita, M. J. *J. Am. Chem. Soc.* **1995**, *117*, 6787.

24. Kablaoui, N. M.; Buchwald, S. L. *J. Am. Chem. Soc.* **1996**, *118*, 3182.

25. Komanduri, V.; Krische, M. J. *J. Am. Chem. Soc.* **2006**, *128*, 16448.

26. Rhee, J. U.; Krische, M. J. *J. Am. Chem. Soc.* **2006**, *128*, 10674.

27. Oblinger, E; Montgomery, J. *J. Am. Chem. Soc.* **1997**, *119*, 9065.

28. Huang, W.; Chan, J.; Jamison, T. F. *Org. Lett.* **2000**, *2*, 4221.

29. Colby, E. A.; O'Brien, K. C.; Jamison, T. F. *J. Am. Chem. Soc.* **2003**, *125*, 11514.

30. Colby, E. A.; O'Brien, K. C.; Jamison, T. F. *J. Am. Chem. Soc.* **2004**, *126*, 10682.

31. Tang, X. Q.; Montgomery, J. *J. Am. Chem. Soc.* **1999**, *121*, 6098.

32. Takai, K.; Sakamoto, S.; Isshiki, T. *Org. Lett.* **2003**, *5*, 653.

33. Takai, K.; Sakamoto, S.; Isshiki, T.; Kokumai, T. *Tetrahedron.* **2006**, *62*, 7534.

34. Mahandru, G.M.; Liu, G.; Montgomery, J. *J. Am. Chem. Soc.* **2004**, *126*, 3698.

35. Irrgang, T.; Schareina, T.; Kempe, R. *J. Mol. Catal. A* **2006**, *257*, 48.

36. Kong, Y. K.; Kim, J.; Choi, S.; Choi, S.-B. *Tetrahedron Lett.* **2007**, *48*, 2033.

37. Chaulagain, M. R.; Mahandru, G., M. .; Montgomery, J. *Tetrahedron* **2006**, *62*, 7560.

38. Bourissou, D.; Guerret, O.; Gabbaï, F. P.; Bertrand, G. *Chem. Rev.*, **2000**, *100*, 39.

39. W.; Bucher, G.; Wierlacher, S. *Chem. Rev.* **1993**, *93*, 1583.

40. Heinemann, C.; Müller, T.; Apeloig, Y.; Schwarz, H. *J. Am. Chem. Soc.* **1996**, *118*, 2023.

41. Boehme, C.; Frenking, G. *J. Am. Chem. Soc.* **1996**, *118*, 2039.

42. Crabtree, R. H. In *The Organometallic Chemistry of the Transition Metals (4th ed.)*. Wiley-Interscience: New Jersey 2005.

43. Wanzlick, H. W.; Kleiner, H. J. *Angew. Chem.* **1961**, *73*, 493.

44. Arduengo, A. J.; Harlow, R. L.; Kline, M. *J. Am. Chem. Soc.* **1991**, *113*, 361.

45. Dorta, R.; Stevens, E. D.; Scott, N. M.; Costabile, C.; Cavallo, L.; Hoff, C. D.; Nolan, S. P. *J. Am. Chem. Soc.* **2005**, *127*, 2485.

46. Perry, M. C.; Burgess, K. *Tetrahedron: Asymmetry* **2003**, *14*, 951.

47. Garrison, J. C.; Youngs, W. J. *Chem. Rev.* **2005**, *105*, 3978.

48. Arduengo, A. J.; Gamper, S. F.; Calabrese, J. C.; Davidson, F. *J. Am. Chem. Soc.* **1994**, *116*, 4391.

49. Colby, E. A.; O'Brien, K. C.; Jamison, T. F. *J. Am. Chem. Soc.* **2005**, *127*, 4297-4307.

50. Knapp-Reed, B.; Mahandru, M. G.; Montgomery, J. *J. Am. Chem. Soc.* **2005**, *127*, 13157.

51. Sa-ei, K.; Montgomery, J. *Org. Lett.* **2006**, *8*, 4441.

52. Sa-ei, K.; Montgomery, J. *Tetrahedron*, **2009**, 65, 6707.

53. Moser, R.; Boskovic, Z. V.; Crowe, C. S.; Lipshutz, B. H. *J. Am. Chem. Soc.* **2010**, *132*, 7852.

54. Guo, H.; Dong, C.; Kim, D.; Urabe, D.; Wang, J.; Kim, J. T.; Liu, X.; Sasaki T.; Kishi, Y. *J. Am. Chem. Soc.*, **2009**, *131*, 15387.

55. Miller, K. M.; Huang, W.; Jamison, T. F. *J. Am. Chem. Soc.* **2003**, *125*, 3442.

56. Huang, J.; Stevens, E. D.; Nolan, S. P.; Petersen, J. L. *J. Am. Chem. Soc.* **1999**, *121*, 2674.

57. Seiders, J. T.; Ward, D. W.; Grubbs, R. H. *Org. Lett*. **2001**, *3*, 3225.

58. Chaulagain, M. R.; Sormunen, G.; Montgomery, J. *J. Am. Chem. Soc.* **2007**, *129*, 9568.

59. Olah, G. A.; Lin, H. C.; Olah, J. A,; Narang, S. C. *Proc. Natl. Acad. Sci. U.S.A.* **1978**, *75*, 545-548.

60. Mercer, G. J.; Sturdy, M.; Jensen, D. R.; Sigman, M. S. *Tetrahedron*, **2005**, *61*, 6418-6424.

61. Hoye, T. R.; Jeffrey, C. S.; Shao, F. *Nature Protocols* **2007**, *2*, 2451.

62. Baxter, R.; Montgomery, J. *J. Am. Chem. Soc.* **2008**, *130*, 9662.

63. J. J. Van Veldhuizen, J. E. Campbell, R. E. Guidici, A. H. Hoveyda *J. Am. Chem. Soc.* **2005**, *127*, 6877.

64. Zinner, S. C.; Herrmann, W. A.; Kühn, F. E. *Tet. Asymm.* **2008**, *19*, 1532.

65. Reichard, H. A.; McLaughlin, M.; Chen, M. Z.; Micalizio, G. C. *Eur. J. Org. Chem.* **2010**, 391.

66. Miller, K. M.; Jamison, T. F. *J. Am. Chem. Soc.* **2004**, *126*, 15342.

67. Malik, H. A.; Chaulagain, M.; Montgomery, J. *Org. Lett.* **2009**, *11* , 5734.

68. Malik, H. A.; Sormunen, G. J.;Montgomery, J. *J. Am. Chem. Soc.* **2010**, *132*, 6304.

69. McCarren, P. R. Liu, P.; Cheong, P. H.-Y.; Jamison, T. F.; Houk, K. N. *J. Am. Chem. Soc.* **2009**, *131*, 6654-6655.

70. Evenson, D. A.; Shrestha, R.; Weix, D. J. *J. Am. Chem. Soc.* **2010**, *132*, 920.

71. Peris, E. *Top. Organomet. Chem.* **2007**, *21*, 83.

72. Funk, T. W.; Berlin, J. M.; Grubbs, R. H. *J. Am. Chem. Soc.* **2006**, *128*, 1840.

73. Wu, H.-L.; Wu, P.-Y.; Uang, B.-J. *J. Org. Chem.* **2007**, *72*, 5935.